Defining parameters for multi-colour flow cytometry and molecular identification of human T cell subsets

Nicoleen Gasparillo

Department of Clinical Medicine, Faculty of Medicine and Health Sciences,
Macquarie University

A thesis submitted for the partial fulfilment of the requirements for the degree of Master of Research in Medicine and Health Sciences

October 2015

Nicoleen Gasparillo
SID 43898505

Supervisors
Dr. Lisa Sedger[1]
Dr. Seray Adams[2]
[1]Department of Clinical Medicine and [2]Department of Biomedical Science,
Faculty of Medicine and Health Sciences, Macquarie University, NSW Australia

Keywords: Multi-colour flow cytometry, intracellular staining, T lymphocytes, Naïve T cells, lymphoedema, stromal vasculature fraction

Main text word count: 19177
Abstract: 249
Number of figures: 15
Number of tables: 2

Declaration of originality:

I certify that the work in this thesis entitled 'Defining parameters for multi-colour flow cytometry and molecular identification of human T cell subsets' has not previously been submitted for a degree nor has it been submitted as part of a requirement for a degree to any other university or institution other than Macquarie University.

I also certify that the thesis is an original piece of research and it has been written by me. Any help and assistance that I have received in my research work and the preparation of the thesis itself have been appropriately acknowledged.

In addition, I certify that all information sources and literature used are indicated in the thesis. The research in this thesis was approved by the Macquarie University Research Ethics Committee, reference number 5201300315

Signature

Nicoleen Gasparillo

Abstract

Flow cytometry is widely used to define cell populations in immunology. Here, we describe an optimised multi-parameter flow cytometry protocol that enables T cell subset identification in human blood and tissue, using a comprehensive panel of surface and intracellular markers. Antibody selection, cell membrane permeabilisation, T cell stimulation, controls and surrogate markers were considerations taken in establishing the methodology. With the optimised method, CD4 T helper cell subsets, Th1 (T-bet$^+$, IFNγ$^+$,) Th2 (GATA3$^+$, IL-4$^+$, IL-13$^+$), Th17 (RORγt$^+$, IL-17A$^+$) and regulatory T cells (FoxP3$^+$CD25$^+$TNFR2$^+$, IL-10$^+$, TGFβ$^+$), as well as CD8 T cell subsets Tc1 (IFNγ$^+$) and Tc2 (IL-4$^+$), are detectable at varying frequencies in healthy human blood and in blood and stromal vasculature fractions from lymphoedema patients. Suggested surrogate markers for Th1 (CD183 [CXCR3]), and Th2 (CD194 [CCR4]), are evaluated as well. Furthermore, naïve and memory T cells are comprehensively assessed using a combination of antibodies to CD45RA/RO, CD27, CD62L, CCR7 and CD31. CCR7 expression further distinguishes the central and effector memory subsets, while CD31 expression differentiates the recent thymic emigrants from peripherally expanded CD4 naïve T cells. These two naïve T cell subsets can be further investigated for T cell receptor diversity by way of next-gen sequencing, to confirm if clonality decreases due to homeostatic expansion, especially as thymic output is said to decrease with age.

A thorough definition of these T cell subsets will be valuable to a wide range of human immunology studies where the T cells play a role in exacerbating or in alleviating a condition.

Conflict of interest statement

We declare that there are no conflicts of interest and that this research was conducted in the absence of any commercial or financial relationship that could be construed as a potential conflict of interest.

List of figures

List of tables

List of abbreviations

AF	Alexa Fluor
AP-1	Activator protein-1
AT	Adipose tissue
APC-Cy7	Allophycocyanin-cyanine 7
APC	Allophycocyanin
APC	Antigen presenting cell
BUV	Brilliant Ultraviolet
BV	Brilliant Violet
CD	Cluster of differentiation
CDR3	Complementarity determining region 3
DN	Double negative
DP	Double positive
FITC	Fluorescein isothiocyanate
FMO	Fluorescence minus one
FoxP3	Fork-head box protein 3
FSC	Forward scatter
GATA	GATA binding protein 3
Ig	Immunoglobulin
ICOS/L	Inducible co-stimulator/ligand
IP3	Inositol triphosphate
IFNγ	Interferon gamma
IL	Interleukin
LE	Lymphoedema
MHC	Major histocompatibility complex
NK	Natural killer
NGS	Next-generation sequencing
NF-κB	Nuclear factor kappa-B
NFAT	Nuclear factor of activated T cells
PFA	Paraformaldehyde
PerCP	Peridinin chlorophyll protein
PBMC	Peripheral blood mononuclear cells
PMA	Phorbol-12-myristate 13-acetate
PBS	Phosphate buffer saline
PIP2	Phosphatidylinositol biphosphate
PE	Phycoerythrin
PE-Cy7	Phycoerythrin-cyanine 7
CD31/PECAM-1	Platelet endothelial cell adhesion molecule-1
PCR	Polymerase chain reaction
PKC	Protein kinase C
Rorγt	RAR-related orphan receptor gamma
RTE	Recent thymic emigrants
Treg	Regulatory T cell
SSC	Side scatter
SVF	Stromal vascular fraction
TCR	T cell receptor
TREC	T cell receptor excision circle
Th	T helper cell
T-bet	T-box transcription factor
TGFβ	Transforming growth factor beta

1. Introduction

The adaptive immune system has the unique ability to recognize a range of foreign threats, and establish short- or long-term defense against future attacks. Crucial to this are the T lymphocytes (T cells), which bear a diverse T cell receptor (TCR) set that can theoretically recognise all potential pathogens in an individual's lifetime (Harding and Unanue, 1990; Janeway CA Jr et al., 2008). To generate a diverse TCR repertoire that can recognise various antigens, a developing lymphocyte in the thymus undergoes somatic DNA recombination of the TCR gene locus, composed of variable (V), joining (J) and diversity (D) [in β and γ chains] genes (**Figure 1**) (Calis and Rosenberg, 2014). Along the V(D)J joints, junctional diversity, generated through the template-independent/random insertion and deletion of nucleotides, increases sequence variation. This region spanning the V(D)J segment that confers TCR specificity and provides the peptide-binding site of the T cell is called the complementarity determining region 3 (CDR3), and serves as a 'molecular fingerprint' unique to each T cell and its clonal descendants, or clonotype (Woodsworth et al., 2013). The somatic V(D)J gene rearrangement, coupled with junctional diversity and the pairing of the αβ and γδ chains, generates an estimated 10^{18} different TCRs (Janeway et al., 2008). More than 90% of TCRs in peripheral blood (the most accessible source of T cells) are comprised of αβ chains, with γδ TCRs found mostly in other tissue compartments. During the TCR V(D)J gene rearrangement, T cell receptor excision circles (TRECs) are simultaneously produced from the deleted intervening DNA sequences in the TCR loci that have circularised and formed DNA episomes . TRECs are stable nucleic acid products with no known function and are not duplicated during mitosis (Douek et al., 1998). Consequently, T cell receptor excision circles are highly abundant in thymocytes, but they are also present in recent thymic emigrants (RTE), while low or absent in proliferating progeny T cells (Kimmig, 2002).

Double positive (DP, $CD4^+CD8^+$), double negative (DN, $CD4^-CD8^-$), or self-reactive cells are initially selected against in the thymus. Mature, single positive (SP, $CD4^+$ or $CD8^+$), and immunologically naïve T cells are then released into the bloodstream for immunosurveillance (Janeway et al., 2008). With the aid of homing receptors such as CD62L and CCR7, these cells travel from the blood, enter secondary lymphoid organs through specialised high endothelial venules, and recirculates back into blood via the afferent lymph (Appay et al., 2008; Campbell et al., 2001). When a TCR recognises a peptide on an antigen presenting cell (APC) within the lymphoid organ, the TCR-CD3 complex binds with the peptide-major histocompatibility complex (MHC) of the APC, generating the first signal required for T cell activation. Further verification signals are then required, which are created by the binding between co-stimulatory receptors CD28 and CD80/B7, and/or the inducible co-stimulator (ICOS) and its ICOS ligand on the APC **(Figure 2)** (Hutloff et al., 1999). Upon sufficient activation, a signalling cascade induces expression of interleukin-2 (IL-2), a cytokine that drives T cell proliferation and expansion into specialised effector cells. CD8 T cells recognize MHC I molecules and kill infected cells. CD4 T cells are activated by peptide presentation of MHC II, and differentiate to so-called 'helper' or regulatory T cells, which serve various functions (Janeway et al., 2008). Unstimulated naïve T cells remain in the cycle, proliferating slowly via homeostatic signals from cytokines IL-2 and IL-15, to maintain the naïve pool (Zhu et al., 2010).

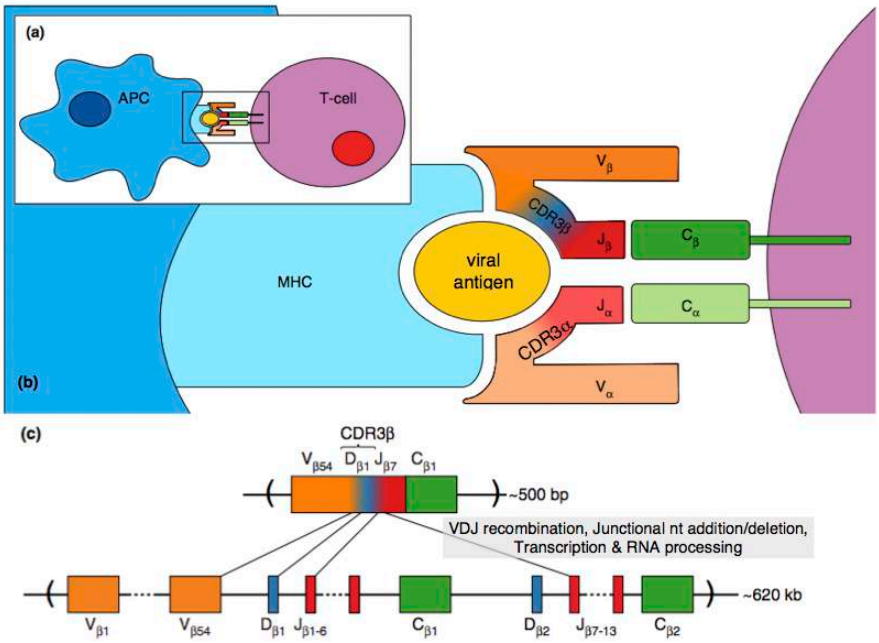

Figure 1. TCR-peptide-MHC interaction and TCR diversification. (a) An APC (blue), via the MHC (turquoise), presents a viral peptide (yellow) to a T cell (purple). If binding avidity is sufficient, the lymphocyte is activated. (b) A closer look into peptide-MHC engaging TCR. The TCR heterodimer is composed of V (orange/light pink), D (blue), J (red/pink) regions, with CDR3 spanning the V(D)J junctions, defining the antigen-binding site. Constant regions (green) anchor TCR to T-cells. (c) The TCRβ locus is ~620 kilobases long, containing all V,D,J segments available for somatic recombination. Gene rearrangement and nucleotide addition/deletion generates a ~500 base pair segment. Colour gradients indicate junctional diversity. Adapted from: (Woodsworth et al., 2013).

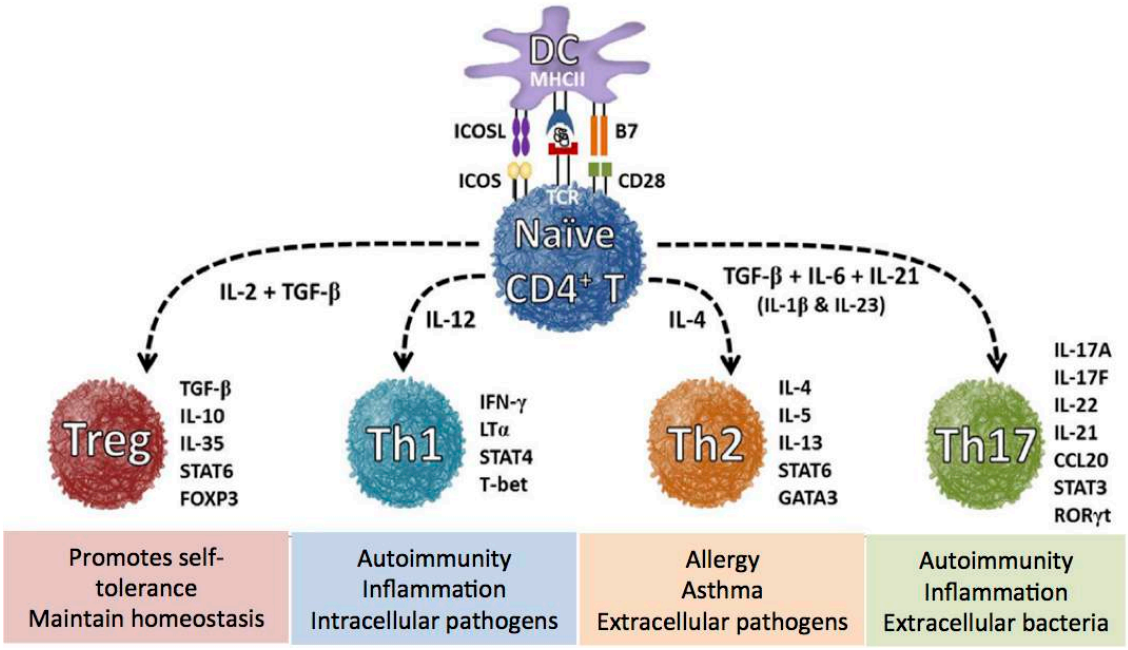

Figure 2. Activation and differentiation of CD4 T cells. Upon TCR and co-stimulatory activation, T cells differentiate according to cytokine signals in the milieu. Th1, Th2, Th17 and Treg cells are controlled by different transcriptions factors and produce characteristic cytokines, working in concert to regulate immune responses. Source: (Bailey et al., 2014).

Lymphocytes differentiate into various phenotypically and functionally distinct populations, distinguished by a combination of cluster of differentiation (CD) surface markers, and cytokine and transcription factor profiles. The major subsets and their characteristic transcription factor expression and cytokine profiles investigated in this project focus on CD4 Thelper-1 (Th1) (T-bet, IFNγ), Th2 (GATA3, IL-4, IL-13), Th17 (RORγt, IL-17) and regulatory T (Treg) (FoxP3, IL-10, TGFβ) cells **(Figure 2)**. Other effector T cell subsets/sub-populations, outside the scope of this project, include IL-22-producing Th22 cells and IL-9-producing Th9 cells (reviewed in Zhu et al., 2010).

Th1 cells, regulated by T-bet (T-box transcription factor), secrete high levels of pro-inflammatory interferon-γ (IFNγ), and are important in combating intracellular pathogens; they are also in important tumour immune rejection (Mosmann and Coffman, 1989; Szabo et al., 2000; Zhu and Paul, 2010). T-bet binds to the DNA *IFNG* gene promoter to induce IFNγ expression. IFNγ secretion further induces transcription of the T-bet gene *TBX21*, thus stimulating increased T-bet-induced IFNγ production (Szabo et al., 2000). Th1 is associated with several autoimmune diseases due to its pro-inflammatory properties, including type 1 diabetes, multiple sclerosis and rheumatoid arthritis (Raphael et al., 2014). It may also have a role in the pathogenesis of acute allograft rejection, contact dermatitis, and other chronic inflammatory disorders (reviewed in Romagnani, 2000).

While Th1 cells promote cell-mediated immunity and pathogen-dependent inflammation, Th2 cells promote and support B cell antibody production and eosinophil cell responses, and induce inflammation that is mainly phagocyte-independent (Romagnani, 2000). Th2 cells, controlled by GATA3 (GATA binding protein 3), mainly produce IL-4, as well as IL-5, IL-6, IL-9 and IL-13, are often predominantly found in epithelial tissues, particularly in the lungs and intestinal tract (Mosmann and Coffman, 1989; Zheng and Flavell, 1997). IL-4 mediates Immunoglobulin E class switching in B cells, leading to histamine secretion that in turn initiates an allergic responses; IL-4 receptors on monocytes and macrophages are also activated by IL-4 binding, allowing these phagocytic cells to respond to pathogens (reviewed in Raphael et al., 2014; Zhu et al., 2010). Moreover, IL-9 and IL-13 induces mucin production in epithelial cells (Annunziato and Romagnani, 2009) and this contributes to airway hyperresponsiveness in situations such as asthma (O'Garra and Arai, 2000).

Th17 lymphocytes, regulated by RORγt (retinoid-related orphan receptor γ t), produce IL-17A, IL-17F, IL-21, IL-22 (Bailey et al., 2014; Ivanov et al., 2007). They develop in the presence of transforming growth factor beta (TGFβ), IL-6 and IL-1β, and are maintained by STAT3-activating cytokines IL-21 and IL-23 (Raphael et al., 2014). Secretion of IL-17 recruits neutrophils, activates innate immune cells, and promotes the release of additional pro-inflammatory cytokines such as TNF and IL-1β. These further increase IL-17 production, enabling the immune response to control extracellular pathogens, but they may also lead to, or be involved in, autoimmunity (Korn et al., 2009; Lovett-Racke et al., 2011). Th17 overexpression is also associated in inflammatory and autoimmune conditions including multiple sclerosis, rheumatoid arthritis and airway inflammatory diseases (reviewed in Raphael et al., 2014). In addition, Th17 cells have been found to accumulate in tumour tissue

in a wide range of malignancies, suggesting that tumours produce factors that encourage Th17 migration to the diseased site (Bailey et al., 2014; Tosolini et al., 2011).

The fourth major CD4 T cell subset is the suppressive or regulatory T cell that highly express the T cell activation marker CD25 (IL-2-receptor α-chain), the Foxp3 (fork-head box protein 3) transcription factor, and produce suppressive cytokines, particularly IL-10 and TGFβ (Fontenot et al., 2003; Yssel et al., 1992). Tregs maintain self-tolerance and immune homeostasis by regulating conventional T cells. They can do this via several mechanisms, including, (1) high expression of IL-2Rα - the high affinity IL-2 receptor – thereby acting as a competitive sink for IL-2 (and thus effectively starving conventional T cells of IL-2), (2) by producing inhibitory cytokines such as IL-10 and TGFβ, or (iii) acting in a directly cytolytic manner through the expression of death molecules such as Fas Ligand, granzymes/perforin etc, that suppress and/or kill conventional CD4 and CD8 T cells (reviewed in Grant et al., 2015; Sakaguchi et al., 2008). Tregs can also supress APCs, dampen B-cell antibody production, among others functions (Brusko et al., 2008). A loss of Tregs is therefore clearly associated with inflammatory diseases in humans, including autoimmune diseases, and targeting these cells for immunotherapy has facilitated the accurate identification of these cells (Baecher-Allan et al., 2005).

In addition to the effector T cell subsets, T cells can be further characterised by their naïve and memory status. Expression of CD45RA was traditionally associated with naïve T cell status, and CD45RO as memory T cells status (Akbar et al., 1988; Sallusto et al., 1999). However, several studies have revealed this simple designation to be inadequate; multiple markers are now required when isolating bona fide naïve and memory T cells (Berard and Tough, 2002; De Rosa et al., 2001). In addition, other issues such as phenotypic reversion, i.e. the CD45RA re-expression of previously CD45RO T cells, has been observed to occur in CD4 and CD8 cells (Wills et al., 1999). The reversion is suggested to mark recent activation of a T cell rather than memory conversion, or to represent a return to a resting state due to insufficient contact with antigen (Berard and Tough, 2002). Thus, identification of naïve cells by multiple markers (such as CD62L, CCR7) is required in order to improve the specificity of naïve T cell identification and isolation (De Rosa et al., 2001), especially because, unlike specific-pathogen free mice, humans are essentially never completely 'antigen naïve'.

Furthermore, naïve CD4 T cells can be divided into two subsets based on their proliferative history. Recent thymic emigrants (RTE) are naïve cells that have recently left the thymus and have not undergone further peripheral proliferation; they are identified to have a high expression of CD31, and a higher TREC content (Kimmig, 2002). On the other hand, peripherally expanded naive T cells are lymphocytes that have undergone homeostatic proliferation, maintaining the absolute naïve T cell count in humans, not only to ensure that sufficient lymphocytes are available at any given time, but to compensate for the progressive decline of thymic output associated with aging as well (Kilpatrick et al., 2008).

An assumption of homeostatic expansion is that all naïve T cell progenitor specificities are preserved; that is, an extensive TCR diversity that enables efficient immune response is retained throughout adulthood without reliance on thymic production of new TCRs (Kohler

and Thiel, 2009). However, TCR diversity studies by CDR3 spectratyping have been inconclusive so far. More oligoclonal expansions in peripherally proliferated naïve CD4 T cells than in RTEs were found, indicating a preferential selection for certain clonotypes during homeostatic cell turnover (Kohler et al., 2005). On the other hand, another study reported repertoire diversity to be maintained in both RTE and proliferated naïve cells, indicating that naïve T cell proliferation is mostly non-selective (Kilpatrick et al., 2008). The discrepancy between the two studies was hypothesised to be due to the age groups of the participants in the studies (Kilpatrick et al., 2008), but more than that, the method of CDR3 spectratyping used only provided an overview of TCR diversity, as it is limited in resolution and is not reflective of actual diversity.

TCR repertoire analysis evaluates the diversity of the TCRs available in the immune system, and identifies the expanded clonotypes that have dominated the repertoire in the immune response. While flow cytometry enables phenotypic and functional characterisation of lymphocyte populations at the single-cell level, it falls short in TCR analysis. Flow cytometry methods, which are limited by the availability of TCRVβ-specific monoclonal antibodies (**Figure 3. A**), and the aforementioned CDR3 spectratyping, which uses PCR primers to amplify Vβ-specific regions, have only provided a general view into diversity **(Figure 3. B);** both techniques assume that CDR3s with the specific Vβ represent a single clonotype only, without acknowledging heterogeneity of nucleotide content along the entire CDR3 length (Calis and Rosenberg, 2014; Kedzierska et al., 2008).

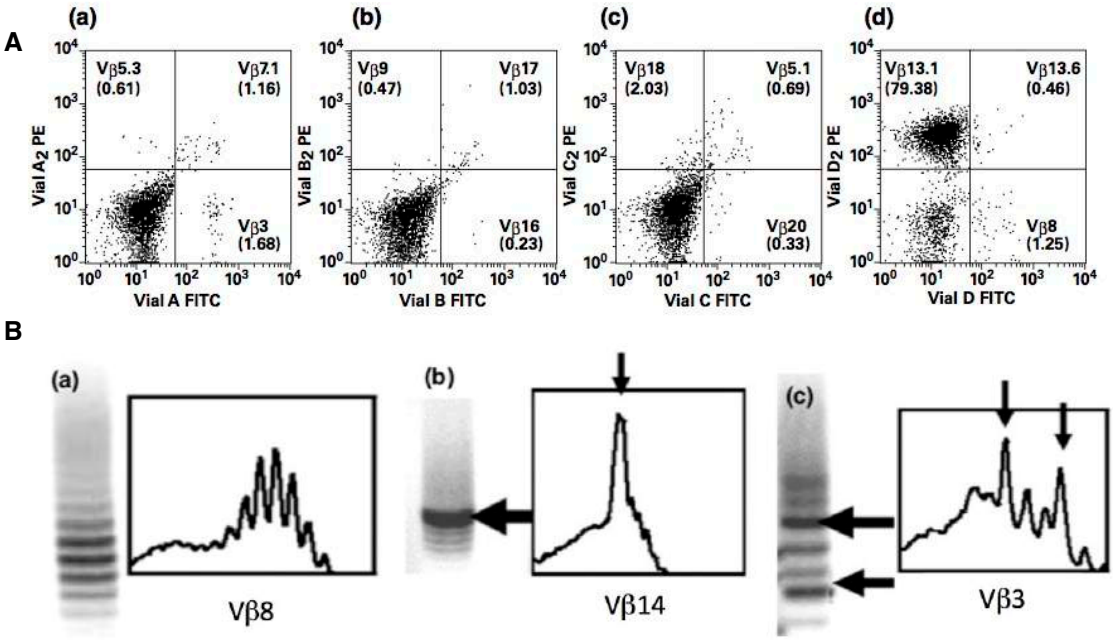

Figure 1. **A. Flow cytometric TCR analysis of a patient with lymphoid malignancy.** Cells are characterised by TCRVβ-specific mAbs. (a-c) Non-expansion of the specified TCRs. (d) The upper left quadrant shows clonal expansion of TCRVβ13.1. Each test used three mAbs conjugated to: PE, FITC or PE and FITC. Source: (Beck et al., 2003)**. B. Representative CDR3 spectratypes using Vβ-specific primers**. Band intensity patterns on the left, and corresponding peak profiles on the right. (a) In a healthy individual, a bell-shaped distribution indicates restriction of clonal expansions. (b-c) In a myasthenia gravis patient, dominant bands and peaks (arrows) signify monoclonal and oligoclonal expansions. Adapted from (Matsumoto et al., 2006).

In recent years, next-generation sequencing (NGS) has allowed for a more informative TCR analysis at the nucleotide level, enabling a higher resolution assessment of clonotype identification, quantitation and diversity (Robins et al., 2009; Warren et al., 2011). Deep sequencing is done in conjunction with the amplification of the highly specific CDR3 sequence, using an adaptor-mediated or a multiplex PCR approach targeting the V and J segment (Calis and Rosenberg, 2014). When performed in parallel with spectratyping, it has been revealed that identical-length CDR3 (a spectratype 'peak') are actually comprised of different clonotypes and at varying frequencies, and has allowed increased detection of ubiquitous but low-frequency or rare clones **(Figure 4)** (Krell et al., 2013)

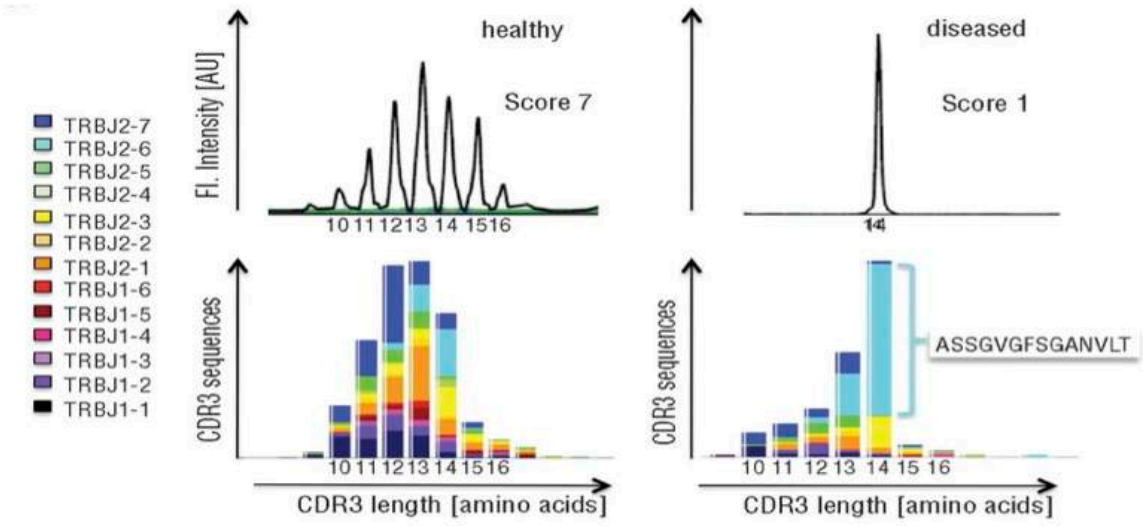

Figure 2. Representative CDR3 spectratypes (top) compared with 'virtual' spectratypes derived from NGS data (bottom) of a TCRVβ segment in healthy and diseased individuals. NGS reveals that different TCRs constitute identical-length CDR3s, using various TCRJb reverse primers (coloured bars). In a healthy person (left), both spectratypes confirm polyclonality. In a diseased state (right), a monoclonal expansion shown by conventional spectratyping (upper right) was confirmed by NGS and its amino acid sequence identified (lower right). Additional TCRs that represent rare or low-frequency clonotypes were also revealed. Source: (Krell et al., 2013).

This technique is gaining ground and its contribution to immunology studies is growing. It has enabled exact TCR quantitation, giving a baseline of 3-4x10^6 unique TCRβ sequences in human blood (Robins et al., 2009). It facilitates diagnosing and tracking of low-frequency cancer cells in malignancies such as cutaneous T cell lymphomas, where NGS can identify a malignant clonotype in 50,000 cells, compared to conventional spectratyping that had a specificity of only 1 in 100 cells (Weng et al., 2013; Wu et al., 2012). In addition, NGS has provided further insight to the potential implications of a diverse TCR profile. A study observing the correlation between aging and TCR diversity has found that a significant decrease in diversity was found in the elderly, while absolute T-cell counts had no significant differences (Britanova et al., 2014). The T cell repertoire after haematopoietic stem cell transplantation was also investigated in patients with multiple sclerosis (Muraro et al., 2014) and with different cancer diagnoses (Van Heijst et al., 2013). The importance of a diverse repertoire for successful immune reconstitution was highlighted, as patients who failed to

respond to treatment (Muraro et al., 2014), or who was more prone to infections and cancer relapse (Van Heijst et al., 2013), had limited TCR diversity.

Having a precise definition of the TCR diversity between the two naïve populations may contribute to the current knowledge of naïve cells and their relation to disease and therapeutic approaches. In HIV, where there is a decline in $CD4^+$ naïve T cells and decreased TCR diversity as the disease progresses (Connors et al., 1997), accurate naïve diversity assessments may influence immune-based therapeutics, not only in HIV therapies, but in cancers or other diseases where there is a need to focus on the cells that will confer a more robust immune reconstitution (Calis and Rosenberg, 2014; De Rosa et al., 2001). Likewise, the exact mechanisms behind the decreased effectiveness of vaccines and the increased susceptibility to infectious diseases due to aging remain unclear (Kilpatrick et al., 2008) – this may provide better vaccines and treatments in immuno-compromised individuals that will target the more responsive cells. By combining the abilities of flow cytometry and next-gen sequencing to enhance the current knowledge of T cell response in the immune system, having the ability to target specific TCRs may one day take personalised medicine one step further (Woodsworth et al., 2013).

There remains much to be learned in the immune system, especially with classic definitions of subsets using a single marker becoming inadequate, and the characterisation of 'new' T cell populations remaining incomplete e.g. Th9, Th22 cells, etc. (Zhu and Paul, 2010). Flow cytometry has been extensively used since the 1960s (Hulett et al., 1969) to examine various leukocyte subsets, by using cell surface and intracellular staining markers in the form of fluorochome-conjugated monoclonal antibodies. Cell populations can then be distinguished and characterised in order to understand an individual's immune response to infections, diseases, or treatments. Technological improvements such as the increasing number of detection channels available, brought by the capacity to add more lasers and filters to machines, and of analysis platforms that allow automatic compensations for overlapping spectra, have advanced multi-parametric flow cytometry studies. More antibodies, in a wider variety of colours, and other reagents are also now available that enables efficient multicolour analyses. In the current four-laser BD LSRFortessa X-20 analytical flow cytometer, it is theoretically possible to study as many as 20 parameters simultaneously. Thus, key to a multi-colour approach is designing a staining panel that acknowledges the inherent intensities of dyes used, the expression levels of targeted markers, and the spectral overlaps due to excitation/emission bleed-throughs (Baumgarth and Roederer, 2000; De Rosa et al., 2003).

These advancements, especially in the context of the highly complex human immune system, has recognised that analysing merely 'bulk' lymphocyte populations such as 'naïve' CD4 T cells are now inadequate, and that more discriminating parameters are needed to characterise 'fine' lymphocyte subsets (e.g. CD4 T cell subsets) (Peine et al., 2013; De Rosa et al., 2001, 2003). More markers are needed for a comprehensive survey of lymphocyte subsets that better reflects their functions, e.g. by way of measuring cytokine production and transcription factor expression, and perhaps by observing their proliferation and/or apoptotic potential – apoptosis or necrosis, etc. (Roederer et al., 1997).

Scope of this thesis

This project is aimed to establish a methodology for surveying human T cell populations in peripheral blood, using a multi-colour flow cytometry panel, and to present the potential of using next-generation sequencing to better elucidate TCR diversity in sorted cells. These techniques can be used in studies that want to look at T cell responses in a myriad of conditions, diseases, and treatments. Samples are not limited to blood draws, but can be applied to examination of tumour biopsies and other lymphocyte-containing tissues. For this reason, this research also represents an initial investigation into the T cell subsets present within disease tissue – specifically, the abnormal deposition of adipose tissue that accumulates in advanced cancer-related lymphoedema (a condition of tissue swelling associated with the loss of lymph nodes or lymphatic function). Thus, this study specifically aims to:

1. Establish a multi-colour flow cytometry staining panel to identify and distinguish select populations of human T cells, including CD4 Th1, Th2, Th17 and Tregs, and CD8 T cells.

2. To identify naïve versus antigen-experienced memory T cells.

3. To establish the methods for cell sorting of specific T cell subsets, and analyse sorted cells for TCR clonotype by next-generation sequencing.

Finally, although these aims are somewhat technical, it should be noted that these methods are all new to our research group, and in fact, they are not yet functionally established at any research laboratories present within the Macquarie University Faculty of Medicine and Health Science. This study therefore represents the initial establishment of these technological capabilities at Macquarie University.

2. Materials and methods

2.1. Ethics

This project has Macquarie University Human Research Ethics approval: Protocol "Lymphoedema Medical Research" Reference: 5201300315.

2.2. Cell culture media and supplementary reagents

Cells were cultured in RPMI-1640 media (Life Technologies) supplemented with 2 nM L-glutamine, 100 U/μg per ml penicillin/streptomycin, 0.5 mM sodium pyruvate, 0.05 mM MEM non-essential amino acid solution and 5 mM HEPES (all from Life Technologies). When used in culture, RPMI media was additionally supplemented with 10% heat-inactivated Human group O serum (Australian Red Cross) – here forth referred to as $RPMI_{10}HOS$. Peripheral blood mononuclear cells (PBMC) were cultured in $RPMI_{10}HOS$ containing 10 ng recombinant Human IL-2 (R&D Systems) in Tissue-culture treated 10 cm culture dishes (Sigma), at 37°C in 5% CO_2.

2.3. Human tissue sample preparation

2.3.1. Blood preparation

With written informed consent, peripheral blood samples (~20 mL in total) were collected by venepuncture into two K_2EDTA Vacutainer tubes (Becton, Dickinson Biosciences, BD). Alternatively, blood was purchased from the Australian Red Cross. PBMCs were isolated by density gradient centrifugation as follows. Blood was diluted 1:1 in 1X Phosphate Buffer Saline (PBS, Life Technologies) and gently layered over an equal amount of Ficoll-Paque Plus (Sigma) in 50 ml Falcon tubes. Tubes were centrifuged at 400 x g with 0 deceleration for 60 minutes at 20°C. The serum-containing top layer was aspirated and discarded. The PBMC-containing 'buffy coat' in the middle layer was carefully harvested into a new tube and washed with RPMI, and the remaining bottom layer containing the Ficoll and erythrocytes were safely disposed. For washing, the buffy coat was resuspended in serum-free RPMI media and centrifuged at 200 x g with 0 deceleration for 10 minutes, at 20°C. Cell pellets were washed at least twice or until the supernatant is clear in order to remove platelets and residual Ficoll. PMBCs for staining were resuspended in $RPMI_{10}HOS$ culture media and plated (20 ml/ plate) with recombinant human IL-2, and 'rested' (cultured) overnight.

Cells for freezing were pelleted and resuspended in cold freezing media composed of 50% serum-free RPMI media, 40% foetal calf serum and 10% dimethyl sulfoxide (both from Sigma), and aliquoted into Corning cryogenic storage vials (Sigma) placed on ice. The cryovials were set in a chilled 'Mr. Frosty' (Thermo Scientific) freezing container filled with isopropyl alcohol, and the container placed in -80°C overnight. The cryovials were then transferred to liquid nitrogen until needed. To thaw frozen cells, the frozen cryovials were immediately placed into a 37°C water bath for <1 minute until only a small amount of ice remained. Warm (37°C), complete media was added and the tubes centrifuged at 180 x g for 5 min at 5°C. The cells were then resuspended in culture media with IL-2, and rested overnight.

2.3.2. Stromal vasculature fraction (SVF) preparation

Aliquots of adipose tissue (AT) were randomly taken from freshly collected liposuction collection bags and digested with 0.1% collagenase type II in PBS containing calcium and magnesium (Sigma) at 37°C with gentle shaking for 60-90 mins. The cell suspensions were filtered through a 100-μm gauze (Sefar) diluted 1:1 in $RPMI_{10}HOS$ and centrifuged at 200 x g for 5 mins to separate the floating adipocytes and the stromal vasculature fraction cell pellet rich in adipose tissue immune cells plus blood and lymphatic endothelial cells. The SVF pellet was resuspended in NH_4CL erythrocyte lysis buffer and washed. The recovered cells were resuspended in culture media, and rested overnight, as described previously (Brestoff et al., 2015). Where possible, subsequent steps (stimulation, staining, etc.) were performed simultaneously with PBMC samples obtained from the same patient.

2.4. Cell stimulation

To observe intracellular cytokine production the SVF and PBMCs were cultured with 10 ng/ml PMA (phorbol 12-myristate 13-acetate) and 1 μg/ml ionomycin for six hours, with the addition of 2μl Brefeldin A (all from Sigma) added in the final 3 hours. Alternatively, a T Cell Activation kit (Miltenyi Biotec), containing anti-CD3 and anti-CD28 beads was used on PBMCs, exactly according to the manufacturer's instructions. Briefly, cells were counted by diluting a small cell suspension in 0.4% Trypan Blue Solution (Life Technologies) to differentiate live and dead cells. Live cells were counted using the Countess automated cell counter (Invitrogen). Cell suspension volumes were adjusted by adding culture media to obtain 5 x 10^6 cells/ml. Anti-biotin antibody conjugated bead particles were then added to PBMCs in a 1:2 bead-to-cell ratio, and incubated overnight. In all experiments that used stimulated cells, an unstimulated control was maintained in the humidified chamber until ready for staining.

2.5. Flow cytometry

2.5.1. Cell preparation

Prior to staining, cultured cells were harvested by scraping from the culture dish and cell suspensions were filtered through 100-μm gauze (Sefar) to create a single-cell suspension and to remove particles that may block the flow cytometer. Human FcReceptor blocking antibody (Fc Block; Beckton Dickinson [BD] Biosciences) was added to the cell suspensions to prevent antigen non-specific antibody binding to Fc Receptors, at approximately 2.5 μg per 1 x 10^6 cells, for 1 hour at 4°C. Cell suspensions were transferred onto a 96-well round bottom plate in 100 μL aliquots (containing ~10^5 cells/ well) filling up wells as needed by the staining panel.

2.5.2. Surface staining

Fluorescent antibody cocktails for surface marker staining were prepared in 50 μL Brilliant Stain Buffer (BD) per test, and the antibodies added as per the manufacturer's recommended volumes. The BD Brilliant Stain Buffer was recommended when two or more BD Brilliant Violet staining reagents are used, to reduce fluorescence shifts that may occur due to interactions between BV dyes (Beckton Dickinson). Cells were incubated with the staining cocktail for 45 minutes at 4°C in the dark. For washing, 150-200 μL $RPMI_{10}HOS$ media was

added per well, and the plate was centrifuged at 180 x g for 5 minutes at 4°C (for the rest of the staining washes, this will be the centrifuge settings).

In one experiment, the live/dead fixable aqua dead cell stain (Life Technologies) was used to verify the percentage viability of cells. Following the last wash for surface marker staining, the pellets were resuspended in PBS and 1 μl of freshly prepared live/dead stain was added per well and incubated for 30 minutes at 4°C in the dark, and washed with PBS. As a positive control, an aliquot of the same cells were incubated with 1M hydrogen peroxide for one hour, then mixed 1:1 with untreated live cells.

Cells requiring only surface staining and the single-colour control cells were resuspended in ~300 μl 2% paraformaldehyde (PFA) in PBS. The cells were transferred to titertube micro test tubes (Bio-Rad), and set aside at 4°C in the dark, ready for analysis.

2.5.3. Intracellular staining

Two commercial buffers were tested in this project. After surface staining, cells were either permeabilised with: Protocol A, using the eBioscience permeabilisation buffer, and Protocol B, using the BD Transcription Factor buffer set, composed of Fix/Perm and Perm/Wash solutions. In protocol A, cells were fixed in 2% PFA/PBS for at least 15 minutes, washed with $RPMI_{10}HOS$ and resuspended in 150 μl/ well of 1 x permeabilisation buffer (eBioscience) for 20 minutes. Cells were then spun down, aspirated and resuspended in a cocktail of intracellular markers prepared in the permeabilisation buffer, for 1 hour at 4°C in the dark. The cells were washed twice with the permeabilisation buffer, with the final wash set for 30 mins to ensure removal of unbound antibodies. In protocol B, cells were incubated in 150 μl BD Fix/Perm buffer for 45 mins at 4°C. Cells were pelleted, resuspended in Perm/Wash, pelleted again and resuspended in a cocktail of intracellular markers prepared in Perm/Wash, for 1 hour at 4°C in the dark. Similarly, the cells were washed twice with the Perm/Wash buffer, with the final wash set at 30 mins to ensure removal of excess antibodies. Following either protocol, the cells were centrifuged for a final time, and the pellets resuspended in 300 μL of 2% PFA/PBS and transferred to titertube micro test tubes (Bio-Rad) for analysis. The fixed cells may be analysed immediately or stored in 4°C for analysis the next day.

The antibodies used in this study were conjugated to one of the following fluorochromes: fluorescein isothiocyanate (FITC), (Alexa Fluor) AF488, allophycocyanin (APC), APC-Cy7, (Brilliant UltraViolet) BUV395, BUV737, (Brilliant Violet) BV421, BV605, BV711, BV786, phycoerythrin (PE), PE-Cy7, or peridinin chlorophyll protein (PerCp). Antibodies for surface markers include: CD3 (clone SK7), CD4 (RPA-T4), CD8 (RPA-T8), CD183/CXCR3 (1C6), CD194/CCR4 (1G1), CD25 (2A3), CD27 (L128), CD197/CCR7 (3D12), CD120b/TNFR1 (hTNFR-M1), CD62L (SK11), CD45RA (HI100), CD45RO (UCHL1), CD31 (WM59), CD56 (B159), IL-7R/CD127 (HIL-7R-M21), all from BD Biosciences, and live/dead fixable Aqua 400 dead cell stain (Life Technologies). For intracellular markers the following antibodies were used, specific to, T-bet (clone O4-46), GATA3 (L50-823), RORγt (Q21-559), FoxP3 (259D/C7), IL-4 (8D4-8), IL-10 (JES3-9D7), IL-13 (JES10-5A2), IL-17A (SCPL1362), IFNγ (B27), TGFβ (TW4-9E7), also all from BD Biosciences. The excitation and emission spectra of the fluorochromes are in **Appendix 1**.

IgG isotype controls for the intracellular markers were included, each at the same concentration as the primary antibody. Unstained cells, and where necessary, fluorescence minus one (FMO) controls, were also prepared. For these controls, unstimulated and stimulated cells were separately stained. For compensation setup, excess cell suspensions of stimulated and unstimulated cells were combined, aliquoted out according to the number of colours in the panel, and stained with a single antibody conjugated with each fluorochrome. The staining panel, including all antibodies used, are listed in Table 1.

2.5.4. Flow cytometry analysis

For flow cytometry, cells were analysed on an LSRFortessa X-20 analytical flow cytometer (Becton Dickinson) equipped with four lasers: 488 nm, 635 nm, 405 nm and 355 nm. Generally 50,000 events (cells) were acquired, using the BD FACSDiva software version 8. The unstained and single colour controls were run first to calculate the compensation for overlapping fluorochromes, collecting 10,000 events **(Appendix 4)**. When processing the actual samples and isotype controls, 50,000 events were collected. Flow cytometry data were analysed using the same BD FACS Diva software (version 8), and presented in bi-exponential dotplots or histogram plots.

2.6. Future direction

2.6.1. Statistical analysis

Since the focus of this project was on optimising the flow cytometry protocol, only a few patient samples were analysed. Thus, more samples need to be processed in order to report robust data. The student's T-test (unpaired) would have been used to compare the mean percentages of T cell subsets from healthy donors and lymphoedema patients.

2.6.2. Cell sorting, TREC analysis and TCR sequencing

Due to unforeseen circumstances, not all aims of the project were accomplished in time. Nevertheless, the following plans were investigated: CD4 T cells were to be sorted according to definitions of recent thymic emigrants and peripherally expanded naïve T cells. Unfortunately, however, our staining panel was not compatible with the available cell sorters (i.e. limited in detection of BUV395, BUV737 and PerCP). DNA will have been isolated from the sorted cells, which will allow for TREC quantification by real-time quantitative PCR using the following primers (synthesized at Geneworks) for single joint TREC, forward, 5'-TCGTGAGAACGGTGAATGAAG-3', reverse, 5'-CCATGCTGACACCTCTGGTT-3' and probe: FAM-5'-CACGGTGATGCATAGGCACCTGC-3'-TAMRA (Fallen et al., 2003; Naylor et al., 2005).

DNA extracted from sorted cells will be sent for TCRβ sequencing using the ImmunoSEQ service (Adaptive Biotechnologies). The ImmunoSEQ assay uses a highly optimised multiplex PCR method identifying the V regions of human TCRβ cells, allowing studies on the TCR diversity between the naïve populations of interest.

Table 1. Staining Panels

A. CD4 T cell subset panel

(Tube)	Staining Description	Intracellular staining (Prepared in intracellular staining buffer)			Surface staining (Prepared in BV Brilliant Stain buffer)								
		PE	AF488	BV421	PerCP	APC-Cy7	APC	BV711	BV605	BV786	PECy7	BUV737	BUV395
(1)	Th1	IL-4	T-bet	IFNγ	CD3	CD4	CD8	CD183 (CXCR3)	CD194 (CCR4)	CD127 (IL-7R)	CD197 (CCR7)	CD27	CD62L
(2)	Th2	IL-4	GATA3	IL-13/ IFNγ									
(3)	Th17	IL-17A	RORγt	IFNγ									
(4)	Treg	TGFβ	FoxP3	IL-10									
(5)	Treg	TGFβ	FoxP3	IL-10			CD120b	CD25	CD11c		/CD56		
(6)	Isotype IgG	Ms IgG1κ (5.0µl)	Ms IgGκ (5.0 µl)	-			CD8	CD183 (CXCR3)	CD194 (CCR4)		CD197 (CCR7)		
(7)		Ms IgG1κ (1.2µl)	Ms IgG1κ (1.25µl)	-									
(8)		Ms IgG1κ (0.3µl)	Ms IgG1κ (0.5µl)	-									
(9)	Surface only	-	-	-									
(10)	Unstained	-	-	-	-	-	-	-	-	-	-	-	-

B. Naïve/memory T cell panel

FITC	PE	PE-Cy7	PerCP	APC	APC-Cy7	BV421	BV605	BV711	BUV395	BUV737
TCRαβ	CD45RO	CD197	CD3	CD8	CD4	CD45RA	CD31	CD183	CD62L	CD27

C. Compensation controls (each single colour only).

FITC	PE	PE-Cy7	PerCP	APC	APC-Cy7	BV421	BV605	BV711	BV786	BUV395	BUV737	BV510 (Aqua)
CD4	CD45RO/ TCRαβ	CD197	CD3	CD8	CD4	CD45RA	CD31	CD25	CD127	CD62L	CD27	50:50 Live or H_2O_2 treated

Footnotes: **Panel A** was designed by my supervisors LS and SA. **Panel B** was designed by me (NG)

3. Results

3.1. Experimental setup

3.1.1. Comparison of two permeabilisation buffers & PMA/ionomycin stimulation

Flow cytometry based detection of cell surface molecules is a well established technique. Surface molecules can, for example, distinguish CD4 T cells from CD8 T cells, but cannot differentiate CD4 subsets, such as Th1, Th2 and Th17 cell subtypes. Intracellular antigens/proteins must be detected for further subset discrimination (Mosmann and Coffman, 1989). However, the identification of intracellular proteins is more complex, as the detection of transcription factors and cytokines requires cells to be permeabilised to allow the staining reagents (i.e. antibodies) to penetrate the cell and nuclear membrane and bind to its target protein in the cytoplasm or nucleus. To establish the best intracellular staining protocol to simultaneously detect surface antigens with intracellular proteins, two staining protocols were directly compared. Protocol A involved the use of the eBioscience permeabilisation buffer. Protocol B involved the use of the BD Transcription Factor buffer set. Both resting and PMA/ionomycin activated human PBMCs from a normal (healthy) donor were examined.

First, cells were incubated with an FcR-specific antibody to prevent staining antibodies from binding to surface Fc-Receptors. Using the same cocktail of antibodies (Table 1–A), cells were first incubated with surface markers. Cells in protocol A were fixed in 2% PFA/PBS and incubated with the eBiosciences permeabilisation buffer; in protocol B, cells were treated with the BD TF buffer set (composed of Fix/Perm and Perm/Wash solutions), each according to the manufacturer's instructions. Following intracellular staining and the final wash, the cells were fixed in 2% PFA/PBS, and analysed the next day.

To ensure analysis was examining only single CD4 and CD8 T leukocytes, PMBCs were gated as follows: (1) side scatter (SSC)/forward scatter (FSC) **P1 lymphocyte gate** (based on typical morphological characteristics of human blood lymphocytes, (2) FWD-A/FWD-H **P2 single cell gate**, then (3) CD3/FWD **P3 CD3$^+$ T cell** gate, followed by (4) CD4/CD8 plots – **P4 CD4$^+$ T cells** and **P5 CD8$^+$ T cells** (for example, **Figure 5 –A and B**). Thus, cytokine and transcription factors were analysed in single CD4 or CD8 peripheral blood T cells.

When the two staining protocols were examined, focusing first on unstimulated cells, the first variation was seen in the SSC/FSC plots that would identify the lymphocyte population from other cell types. When the forward scattered light voltage was set at 560 for the cells treated with the eBioscience buffer (**Figure 5 -A**, **row 1**), the **P1** lymphocyte population was easily discernible from the dead cells (to the left) and other mononuclear populations such as monocytes (larger cells with greater SSC/FSC profile) to the right. However, for the cells treated with the BD buffers, the lymphocyte population shifted to the left when compared using the same FWD voltage settings (data not shown). Consequently, the FWD voltage settings had to be increased to 670 on cells treated with the BD Transcription Factor buffer, i.e. to distribute the cells along the x-axis in a way that still enabled the detection of a lymphocyte population separate from dead cells and larger cells (**Figure 5 –B, row 1**). This SSC/FSC difference between buffers was evident in both resting and PMA/ionomycin stimulated cells (**Figure 6 –B, row 1**).

A. eBioscience permeabilisation buffer – unstimulated cells

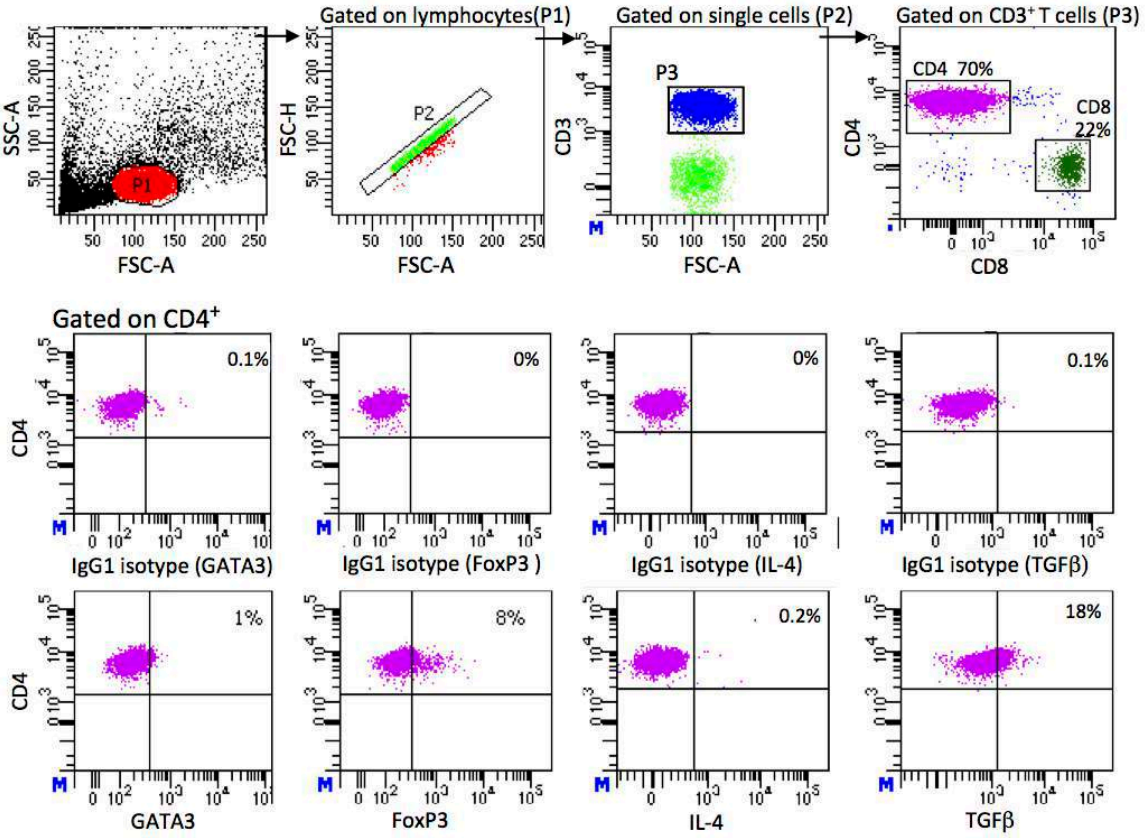

B. BD Transcription Factor buffer – unstimulated cells

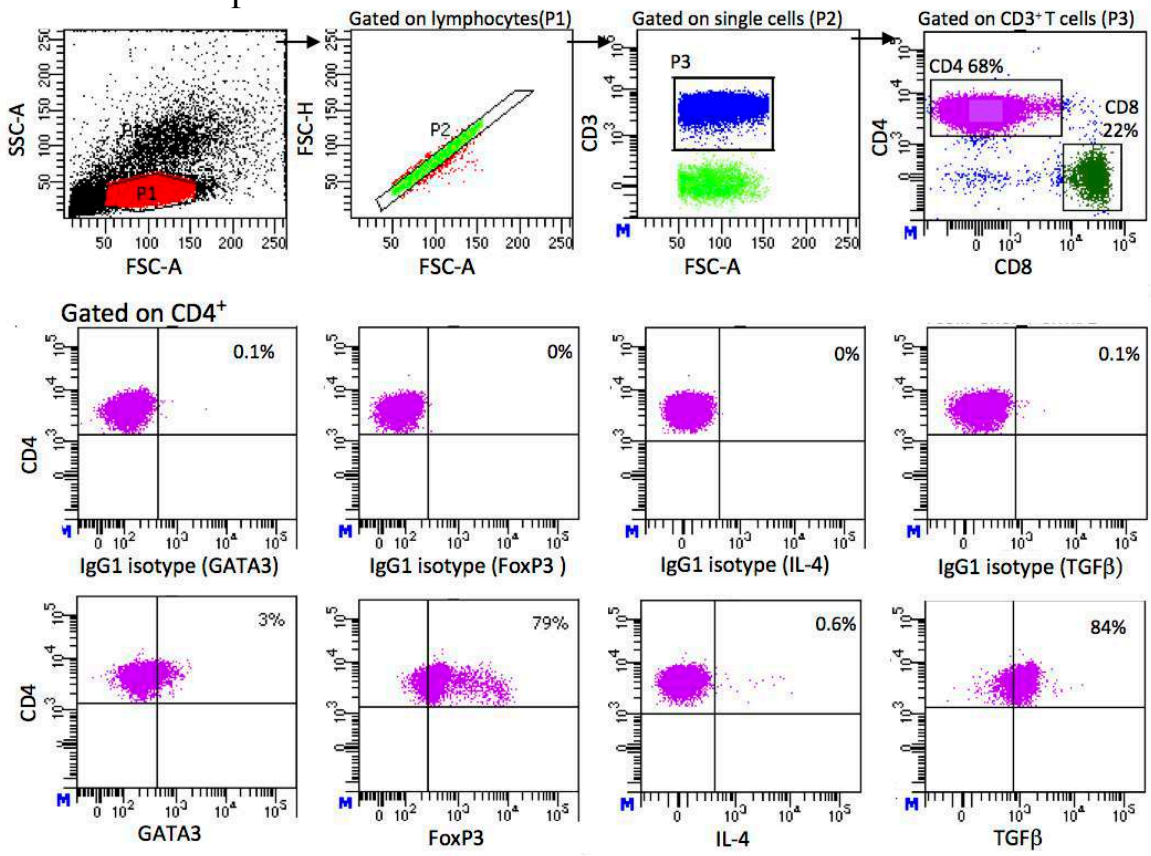

Figure 5. Comparison of eBiosciences and BD permeabilisation buffers on unstimulated PBMCs. Analysis was done using identical voltage settings, except for FSC. Cells treated with **A)** eBiosciences buffer had FSC voltage set at 570, and **B)** BD buffer had a higher setting at 620, since the lymphocyte population P1 shifted to the left (not shown). Gating on single-cell P2, $CD3^+$ P3 and $CD4^+$ T cells, representative intracellular staining is shown with gating based on isotype controls.

A. eBioscience permeabilisation buffer – PMA/ionomycin stimulated cells

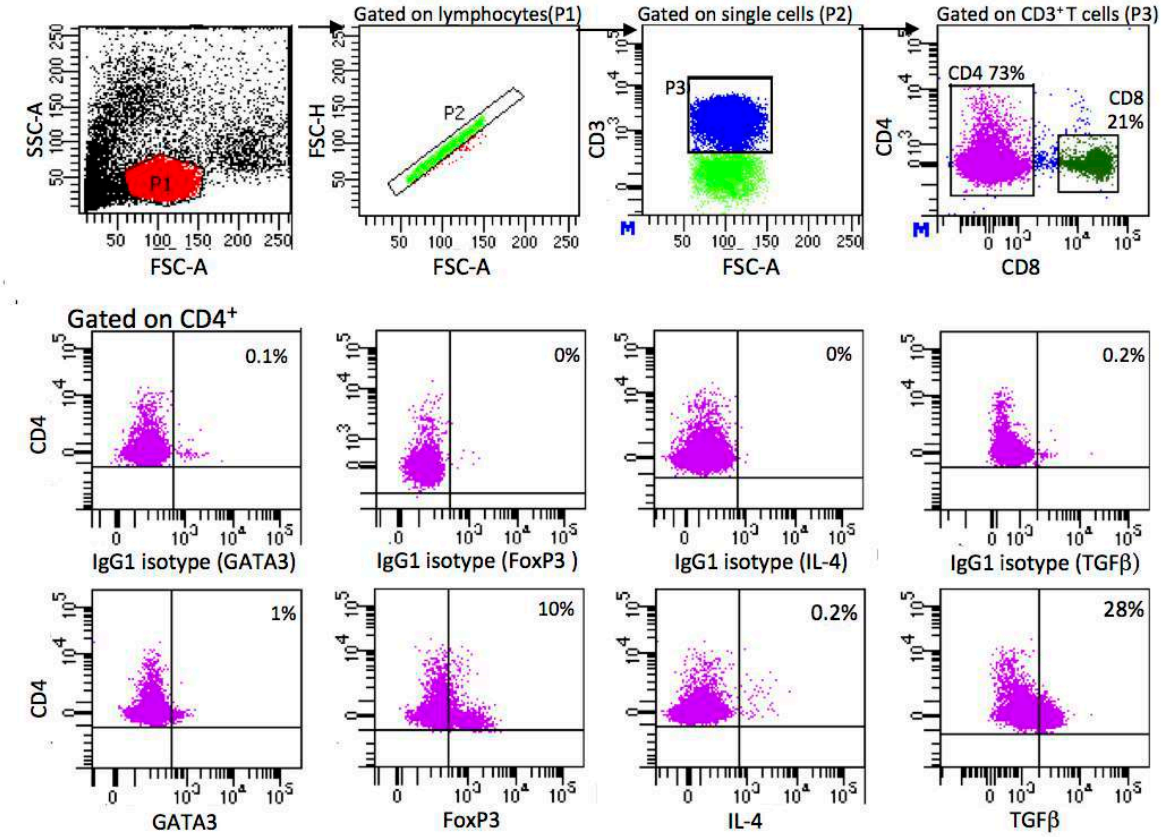

B. BD Transcription Factor buffer – PMA/ionomycin stimulated cells

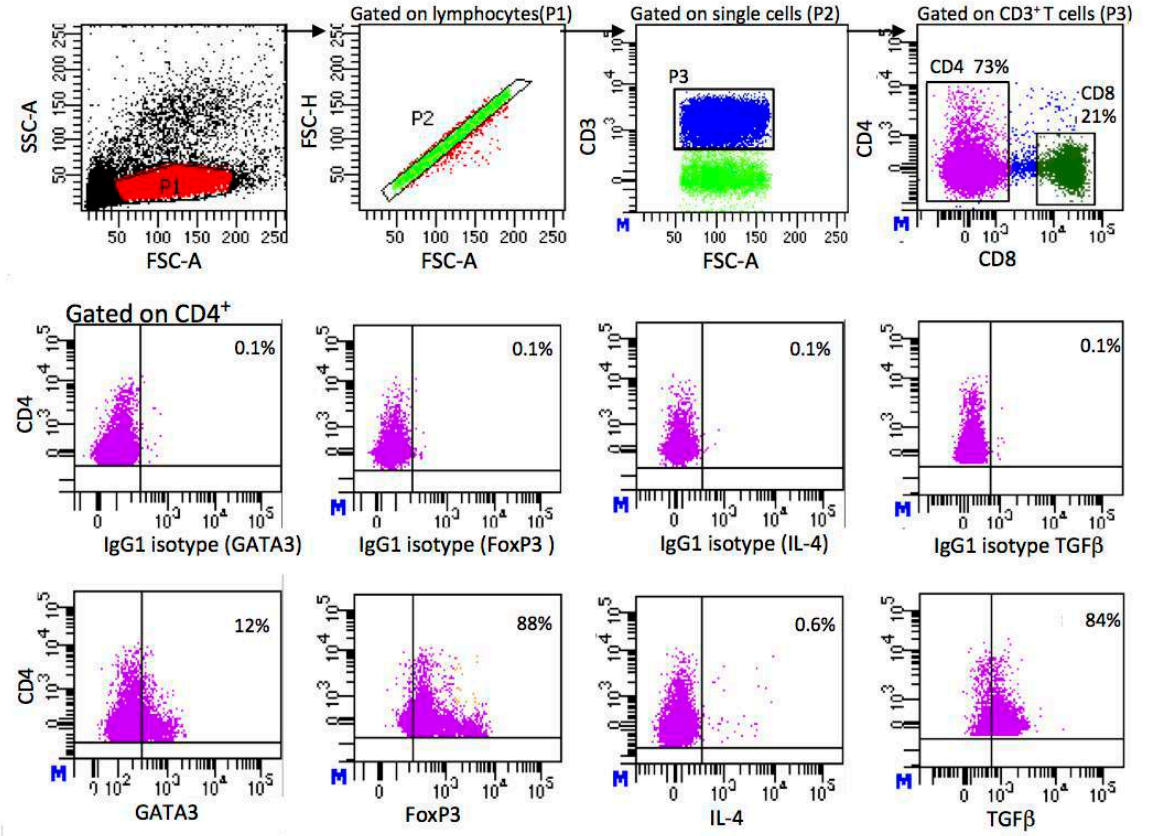

Figure 6. Comparison of eBiosciences and BD permeabilisation buffers on PMA/ionomycin stimulated PBMCs. Analysis was done using identical voltage settings, except for FSC (as above). **A)** Cells permeabilised with the eBiosciences buffer. **B)** Cells permeabilised with the BD buffer. Gating on single-cell P2, $CD3^+$ P3 and $CD4^+$ T cells. Due to CD4 downregulation, CD4 gates were widened. Representative intracellular staining is shown with gating based on isotype controls.

In unstimulated cells, CD4 and CD8 T cells were both clearly distinct and easy to gate on, as expected **(Figure 5 –A and B)**. CD3 negative cells were also present which are expected to include mostly B lymphocytes. Some CD4 negative and CD8 negative cells are also present – these could include either the double negative ($CD4^-CD8^-$) T cells, and NK T cells which express NK cell markers and CD3 but not CD4 or CD8 (Bendelac et al., 2007). Gating on CD4 T cells, examination of the presence of transcription factors and cytokines was performed with direct comparison to isotype-matched IgG antibodies conjugated to the same fluorochromes e.g. AF488 or PE. This analysis indicated that cells expressing FoxP3 were plainly detected with either the eBioscience or the BD buffer, but $GATA3^+$ cells were less clear. TGFβ was also detected, as indicated by fluorescence level above isotype control stained levels. However, it was unclear whether the TGFβ staining was an artefact as the whole population had shifted to the right compared to isotype IgG staining. Some, but very few, IL-4^+ cells were also present **(Figure 5 –A and B, row 3)**.

While some T cells, even in 'resting' unstimulated conditions, can constitutively express detectable levels of certain cytokines, in many situations T cells require stimulation to produce detectable levels of cytokines (Jung et al., 1993; Zheng and Flavell, 1997). Thus, cells were stimulated for 6 hours with PMA/ionomycin (with Brefeldin A added in the last 3 hours). Although this is a broadly used stimulation protocol for PBMCs (Chatila et al., 1989; Jung et al., 1993; Karlsson and Hassan-Zahraee, 2015; Olsen and Sollid, 2013; Rodríguez-Caballero et al., 2004), a noticeable loss of CD4 surface expression was found on PMA/ionomycin-stimulated T cells compared to unstimulated cells **(compare Figures 5 and 6, row 1)**. The CD4 gate was therefore adjusted downwards, to permit for further analysis of intracellular cytokines and transcription factors. Nevertheless, the prior gating on the **P3** $CD3^+$ gate ensured that the analysis was still specific largely to T lymphocytes.

In the analysis of the stimulated **P4** $CD4^+$ T cells comparing the two buffers, for cells stained with the BD buffer, there were more $GATA3^+$ cells, and even higher levels of FoxP3-expressing cells and TGFβ-producing cells compared those treated with the eBioscience buffer (**Figure 6– A and B**). The BD Transcription Factor buffer was therefore used for most of the subsequent experiments (unless otherwise noted).

3.1.2. Cell stimulation with anti-CD3 and anti-CD28

Due to the decreased surface expression of CD4 after PMA/ionomycin stimulation an alternative activation method was investigated. Anti-CD3/anti-CD28 agonistic antibody conjugated microbeads were tested, as this system activates T cells through their TCR and therefore mimics the binding of a T cell to an APC (Trickett and Kwan, 2003). PBMCs were prepared from normal blood by Ficoll density centrifugation, and anti-CD3/anti-CD28 magnetic beads were added in a 1:2 bead-to-cell ratio overnight to activate the T cells. On the following day, the cells were incubated in FcR-specific blocking antibody, stained with a cocktail of surface markers, fixed with 2% PFA/PBS, permeabilised with the eBiosciences permeabilisation buffer and then stained with the intracellular antibodies (Table 1 – A). The cells were fixed in 2% PFA/PBS, stored overnight and analysed the next day. Isotype controls for all the intracellular stains were also included.

A. Unstimulated cells

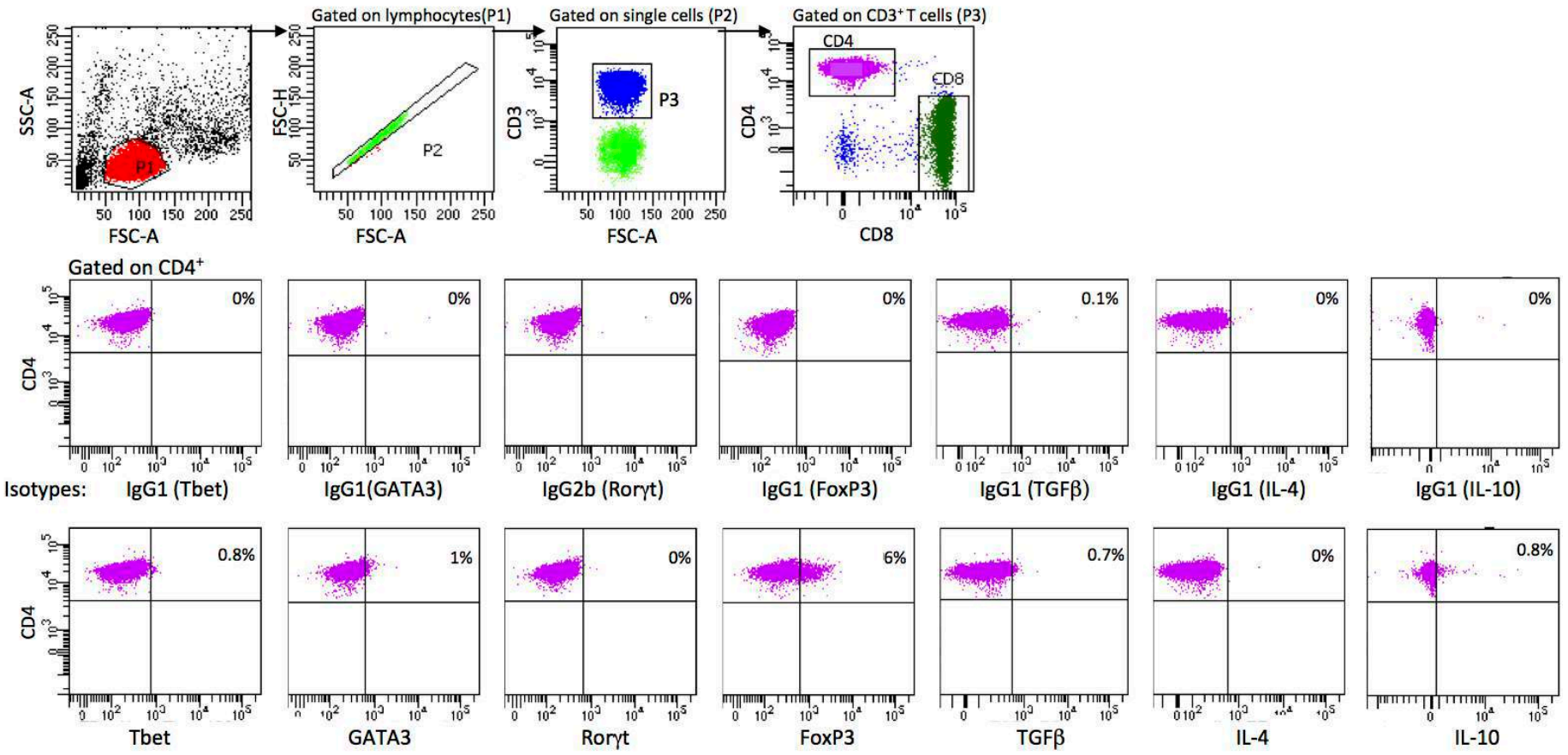

B. Anti-CD3/anti-CD28 activated T cells

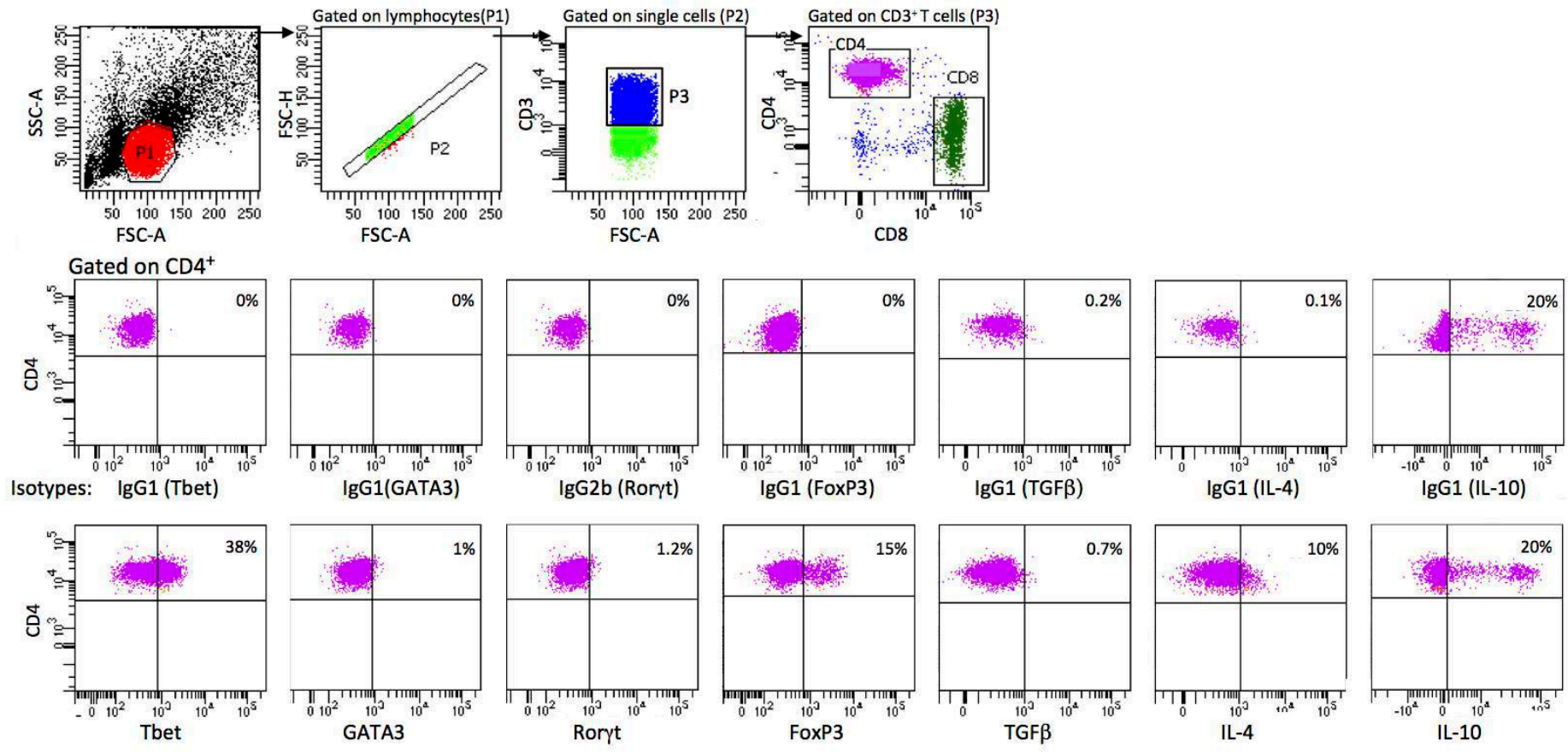

Figure 7. T cell activation with anti-CD3/anti-CD28 in normal blood, using the eBioscience permeabilisation buffer
A) Unstimulated control. **B**) Anti-CD3 and anti-CD28 bead activated cells. Gating on lymphocytes P1, single cells P2 and $CD3^+$ P3 cells, $CD4^+$ T cells are shown. Transcription factors and cytokines were gated based on isotype controls.

Unlike PMA and ionomycin **(Figure 6)**, the CD3/CD28 stimulation had no immediately obvious effect on the surface CD4 expression levels compared to unstimulated cells, and the preserved CD4 surface expression enabled easy gating on bona fide $CD4^+$ T cells (**Figure 7– A and B, rows 1**). Furthermore, although CD3 expression was slightly decreased, the expression of surface CD8 was essentially unchanged. Thus TCR-based activation permits easy gating on CD4, CD8, DN T cells, and NK T cells, without complications associated with the use of PMA/Ionomycin.

Gating on CD4+ T cells, expression of transcription factors and cytokines was analysed with direct comparison to isotype-matched IgGs. Compared to the unstimulated control (**Figure 7-A**), TCR activation resulted in high amounts of T-bet expression and greater FoxP3 expression, although GATA3 and RORγt positive cells remained infrequent (≥1%) (**Figure 7– B**). Expression of IL-4 was increased following TCR activation as well, although no additional production of TGFβ was detected. While IL-10 expression was seen at high amounts following TCR activation, the isotype control also showed positive staining (**Figure 7 – B, IL-10 panel**), leading to the possibility that this may represent false positive or artefactual staining.

3.1.3. Analysis of isotype control staining

The IL-10- and IFNγ- specific antibodies used in this staining panel are both mouse IgG1κ antibodies conjugated to the BV421 fluorochrome. There appeared to be non-specific staining issues with the isotype-matched IgG-BV421 antibody, even when used at identical concentrations in other earlier experiments. This included staining unstimulated cells or cells that had been activated with anti-CD3/anti-CD28 (**Figure 7– B, IL-10 panel**), and with PMA/ionomycin (**Figure 8– A**). The IL-10- and IFNγ-specific BV421-conjugated antibodies resulted in unexpectedly high level staining, both in the unstimulated and stimulated $CD4^+$ T cells processed with the BD buffer. The eBioscience buffer treated cells showed similar results (data not shown). Thus, this made identifying the truly positive cells difficult (or impossible). In contrast, staining with the PE-conjugated antibodies did not produce this artefact, and appeared to confirm that the intracellular staining protocol was appropriate (**Figure 8– B**). To address this problem, it was decided that instead of using an isotype control for BV421, FMO control would be used to set the positive gates for BV421-conjugated antibodies in future experiments.

3.2. Regulatory T cell identification

In staining for FoxP3 expression in resting and PMA/ionomycin stimulated CD4 T cells, it was noticeable that the lymphocyte population has shifted to the right more than expected, leading to a high percentage of FoxP3 positive cells (when the gate was set according to the isotype control) (**Figures 5 and 6– B**). Tregs usually comprise only 5-10% of human peripheral CD4 T cells in healthy individuals (Baecher-Allan et al., 2001). With such a large discrepancy in this experiment (~79-88% are $FoxP3^+CD4^+$ T cells, **Figures 5 and 6– B**), it was decided that additional markers were required to improve the identification of human peripheral blood Treg cells. Again, PBMCs were isolated, rested overnight, and PMA/ionomycin stimulated for 6 hours, or left unstimulated. After blocking with FcR-

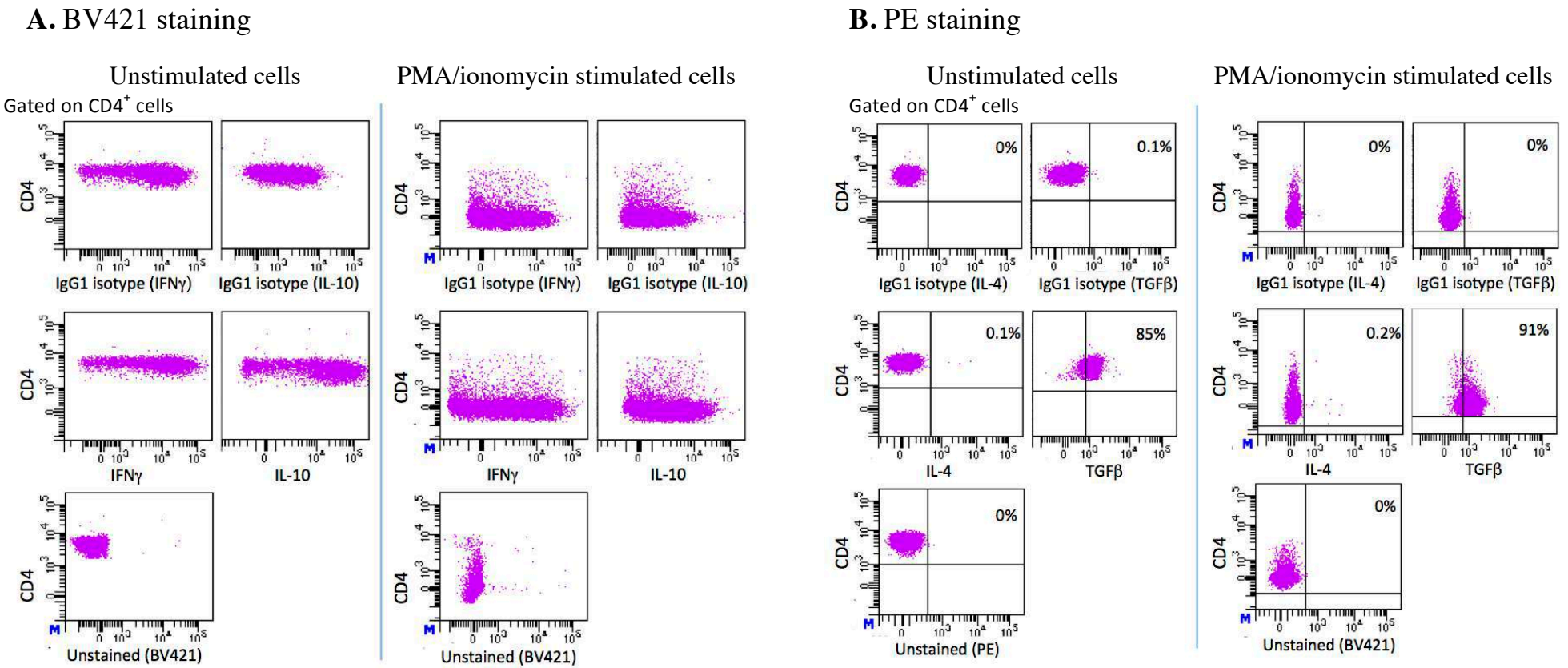

Figure 8. Intracellular staining with BV421- and PE-conjugated antibodies
The CD4 T cells were gated based on the cells treated with the BD buffer (Figures 5 and 6, B). The same was seen in the cells permeabilised with the eBioscience buffer (data not shown). **A)** Staining with BV421-conjugated antibodies revealed high positive staining on unstimulated (left) and stimulated (right) CD4 T cells. **B**) Intracellular staining on unstimulated (left) and stimulated (right) cells showed no issues with using PE-conjugated antibodies.

specific blocking antibody, cells were incubated with antibodies to surface markers (Table 1 – A): CD3, CD4, CD25 (IL-2Rα), IL-7R (CD127), and CD120b (TNFR2), permeabilised with the BD buffer and stained with antibodies to FoxP3, IL-10 and TGFβ. Isotype-matched IgG1 controls for FoxP3 and TGFβ were also included, but since the IgG1κ antibody specific for IL-10 was conjugated to BV421, an FMO unstained control was used (to avoid the problems described above). The cells were then analysed on the LSRFortessa X-20.

After gating on lymphocytes P1 and single cells P2, then gating on unstimulated $CD3^+$ **P3** and $CD4^+$ **P4** T cells, it was evident that at least 50% of CD4 T cells were $FoxP3^+$ (with gates set against the isotype-matched control) (**Figure 9– A)**. Of these $CD4^+FoxP3^+$ **P5** cells, ~14% were $CD25^+$, and 2% (of total CD4) appeared to express TGFβ. However, gating on the $FoxP3^+CD25^+$ **P6** population, the cells were examined for IL-7R expression and this indicated that ~10% were IL-$7R^{lo/-}$, and ~1.5% co-expressed TGFβ (percentages are of CD4 T cells). Lastly, an even more stringent gating strategy was used, where gating on $FoxP3^+CD25^+$IL-$7R^{lo/-}$ **P7** cells, and approximately 6% of total CD4 cells were $TNFR2^+$ and only approximately 1% were $TGFβ^+$. Finally, the **P8** population $FoxP3^+CD25^+$IL-$7R^{lo/-}TNFR2^+$ was backgated onto the CD4/FoxP3 plot, where they appear to be almost all $FoxP3^{hi}$ cells (**Figure 9– A, row 2**). Additionally, backgating for IL-10 and TGFβ expression indicated that this designation of $FoxP3^{hi}$ Tregs did not co-express IL-10, although some were $TGFβ^{lo/-}$ (**Figure 9– A, row 3**).

For the stimulated cells, $CD4^+$ downregulation was again observed, and hence a wider (i.e. lower) **P4** gate was set (**Figure 9– B**). Setting the gate for FoxP3 against the IgG1 isotype, it was evident that some 40% of CD4 T cells are initially seen as $FoxP3^+$. However, of the $CD4^+FoxP3^+$ **P5** cells, only ~6% are also $CD25^+$ and about 2% co-express TGFβ (of total CD4). Once again, gating on the $FoxP3^+CD25^+$ **P6** T cells, IL-$7R^{lo/-}$ expression is evident only in 5% of total CD4 T cells, and TGFβ expression was at ~1.3%. Finally, gating on the $FoxP3^+CD25^+$IL-$7R^{lo/-}$ **P7** T cells indicates that only 0.4% cells are $TNFR2^+$ **(Figure 9– B, row 2 and 3)**. Since the low TNFR2 levels are in contrast to detectable high levels in unstimulated cells, it appears that stimulation has downregulated TNFR2 expression. Thus, when analyzing PMA/ionomycin stimulated cells, Tregs are best defined via the $FoxP3^+CD25^+$IL-$7R^{lo-}$ **P7** population. This P7 population appeared to be mostly $FoxP3^{hi}$, and in backgating for IL-10/TGFβ expression, it was apparent that only a few cells are shown to co-express IL-10 or TGFβ **(Figure 9– B, row 2**).

In summary, in peripheral blood, human CD4 regulatory T cells can be defined by a $FoxP3^+CD25^+$IL-$7R^{lo-}$ phenotype, with or without the additional expression of $TNFR2^+$ depending on the method of stimulation, as these cells all express high levels of FoxP3 . It was also noticeable though in the backgating, that there may be some $FoxP3^{lo}$ cells. Nevertheless, taken together, it was clear that all future experiments should use either the P7 or P8 gating strategy to accurately identify Treg cells (at least in blood).

A. Unstimulated cells

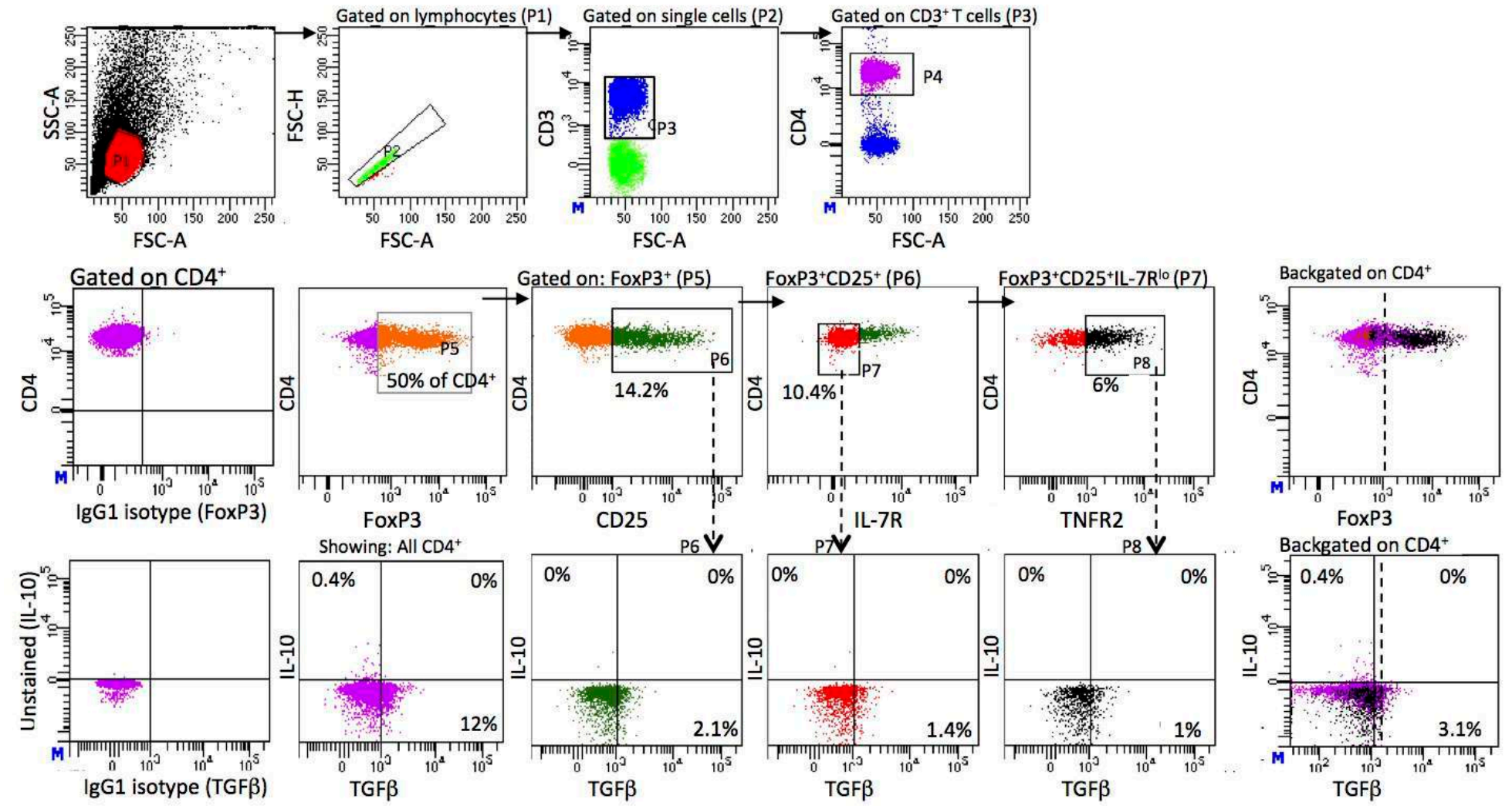

B. PMA/ionomycin stimulated cells

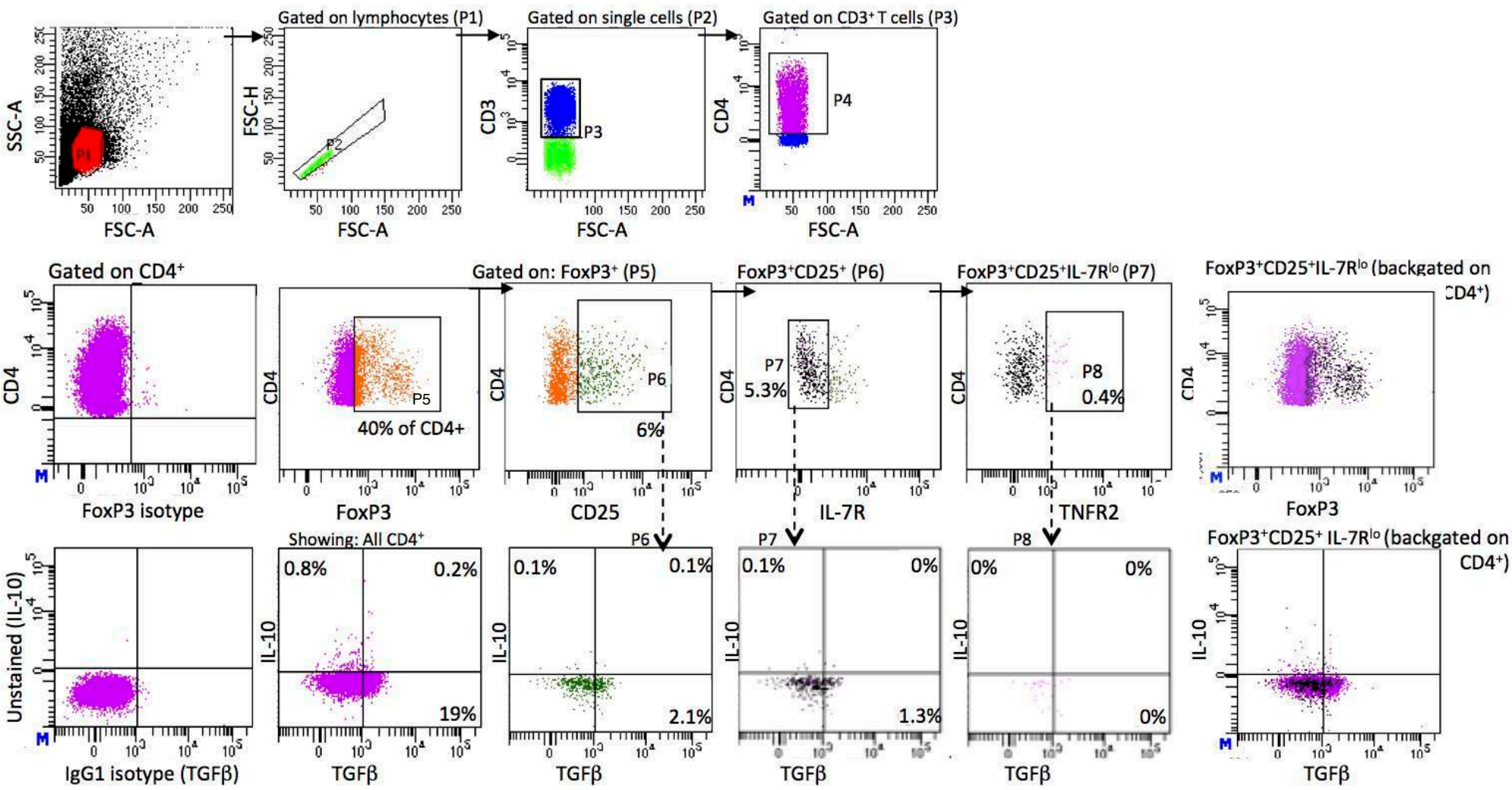

Figure 9. Identifying regulatory T cells using additional markers

Gating on lymphocytes P1, single cells P2, $CD3^+$ P3 and $CD4^+$ P4 cells, FoxP3 staining (gating based on the IgG isotype) reveal >40% FoxP3-positive cells. Subsequent gating was done on FoxP3+ **P5**, $FoxP3^+CD25^+$ **P6**, $FoxP3^+CD25^+IL\text{-}7R^{lo}$ **P7** and $FoxP3^+CD25^+IL\text{-}7R^{lo}TNFR2^+$ **P8** cells, and then plotted for IL-10/TGFβ expression (the gating set on an FMO and isotype control, respectively). In **A)** unstimulated cells, P8 was backgated on CD4/FoxP3 plots. In **B)** stimulated cells, P7 was backgated on CD4/FoxP3 plots.

3.3. Identifying T cell subsets in normal blood and in a pathology setting

With the staining cocktail and methods now established for PBMC analysis, the optimised protocol was used to determine if T cell subsets can be identified in normal blood as well as in situations of human pathology. For this reason, we examined blood and liposuction aspirate samples from a lymphoedema (LE) patient, collected at the time of liposuction surgery.

The following figures show representative data i.e. the analysis of normal and patient blood was performed in the same experiment using the BD buffer, and thus, stimulation, FcR-blocking conditions, antibody cocktails, staining incubation, washes, fixation and permeabilisation steps were identical, as described above. However, given the complexity of the collected tissue/starting material and the optimisation steps needed to stain SVF, the results presented of the SVF analysis are from another experiment (a different lymphoedema patient).

PBMCs were obtained from peripheral blood of one normal (healthy) donor and a lymphoedema patient, isolated by Ficoll density gradient centrifugation, and rested overnight. Adipose tissue collected from liposuction surgery was collagenase digested, gauze filtered, and centrifuged to separate the SVF. The SVF pellet was incubated in red cell lysis buffer, washed and resuspended in culture media with IL-2 for overnight resting. On the following day, PBMC and SVF cells were stimulated with PMA/ionomycin for 6 hrs, adding Brefeldin A in the final three hours. An unstimulated control cell sample was also included. Cells were incubated with the FcR-blocking antibody, and with the cocktail of antibodies for surface and intracellular markers (Table 1 – A). The PBMCs were fixed and permeabilised using the BD buffer. For the SVF, the eBiosciences permeabilisation buffer was used in this representative experiment. Finally, after washing, the cells were fixed with 2% PFA/PBS and analysed on the LSRFortessa X-20 cytometer the following day. The staining cocktail included antibodies specific to CD3, CD4, CD8, and intracellular markers, with matched IgG isotype controls for transcription factors T-bet, GATA3, RORγt, FoxP3, and cytokines IL-4, IFNγ, IL-13, IL-17A, IL-10 and TGFβ (or FMO control for BV421) (Table 1 – A). (Note: the staining panel used in the SVF does not include IL-13, with IFNγ used instead).

3.3.1. Characterisation of CD4 and CD8 T cell subsets in normal blood

First, analysing the healthy donor PBMCs, and gating on lymphocytes **P1** and single cells **P2**, then $CD3^+$ **P3** T cells, it was evident that approximately 67% of T cells are $CD4^+$ T cells, and approximately 21% are $CD8^+$ T cells, with small populations of $CD4^-CD8^-$ and $CD4^+CD8^+$ in unstimulated blood (**Figure 10– Part I. A**). Since PMA/ionomycin stimulation downregulated CD4 expression, gating on $CD3^+CD8^-$ was used to identify the CD4 and CD8 populations (**Figure 10– Part I. B**).

Expression of T-bet was abundant in both CD4 and CD8 T cells. More specifically, in unstimulated cells, at least 11% of $CD4^+$ T cells express T-bet, although most did not appear to produce IFNγ, nor (as expected) the Th2 signature cytokine IL-4 (**Figure 10– Part II. A**). Almost half of CD8 T cells express T-bet, although no cytokine production was detected (**Figure 10– Part II. C**). PMA/ionomycin stimulation doubled the CD4 T-bet positive cells,

and resulted in clear co-expression of T-bet and IFNγ in approximately 8.5% of cells; ≤1% of cells appeared to express IL-4, and a nominal population appeared to produce both cytokines (**Figure 10 – Part II. C**). There also appeared to be two distinct populations: a T-bet^{lo} and a T-bet^{hi} population. Further experiments will be required to define the significance of this finding. An increase in T-bet expression to 65% was also detected in CD8 T cells, with half of these producing IFNγ. There were also minor cell populations co-expressing IL-4, or both IL4 and IFNγ (**Figure 10– Part II. D**). Thus, after PMA stimulation, T-bet expressing cells appear relatively abundant and are easily identified in human peripheral blood, even from a healthy or otherwise uninfected individual.

There was a small population of GATA3^{+} CD4 T cells (8%) and also some GATA3^{+} CD8 (5%) T cells, although there was no cytokine expression detected in GATA^{+} cells when unstimulated (**Figure 10– Part III. A and C**). Stimulation increased the levels of GATA3 expression in CD4 cells to 11%, with a slight increase in CD8 cells. IL-13 production by GATA3^{+} cells was found in CD4 cells at 1%, and <1% in CD8 cells, but most of the cytokine production was by non-GATA3-expressing CD4 and CD8 T cells. IL-4, the cytokine produced by Th2 cells, is also minimally expressed (<1%), with other CD4 T cells appearing to produce it as well (**Figure 10– Part III. B and D**). This leads one to question as to whether these cells are truly fully differentiated i.e. bona fide Th2 GATA^{+} cells.

Among the T cell transcription factors, RORγt was the least represented in normal peripheral blood from this donor. Indeed, no more than ≤2% in both CD4 and CD8 cells appeared to be expressing detectable amounts of RORγt, even after stimulation **(Figure 10– Part IV**). Nevertheless the staining/and detection appears to be valid, as some of these CD4^{+} and CD8^{+} RORγt^{+} cells also co-express IL-17A, as they would be expected to do.

Assessing regulatory T cells, as defined by FoxP3^{+}CD25^{+}IL-7R$^{lo/-}$(and TNFR2^{+} in unstimulated) indicated that approximately 10% of the peripheral blood CD4 T cells were Tregs (**Figure 10– Part V**). This was independent of whether one analysed either unstimulated or stimulated cells. Interestingly, only a few of these Tregs produced IL-10 or TGFβ, although other CD4 T cells appear to produce these cytokines too (**Figure 10– Part V. A and B**). Even with the more stringent gating for Tregs, FoxP3 expression is still in ~2% of CD8 T cells, although these did not produce IL-10 or TGFβ. (**Figure 10– Part V. C and D**)

Taken together, these results indicate that CD4 T cell subsets – Th1 (T-bet, IFNγ), Th2 (GATA3, IL-4, IL-13), Th17 (RORγt, IL-17A) and Tregs (FoxP3, IL-10, TGFβ) can be identified in peripheral blood of an otherwise healthy individual, using these combinations of surface and intracellular markers. Furthermore, stimulation with PMA/ionomycin increased expression of most of the cytokines, particularly for IL-4, IL-13 and IFNγ. For the CD8 T cells, it was evident that they also express the transcription factors, specifically T-bet, but also RORγt and FoxP3, albeit at lower levels. CD8 T cells are also capable of producing the cytokines IL-4, IL-13 and IFNγ, especially after PMA/ionomycin stimulation. These results show that the staining protocols can detect T cell subsets in human peripheral blood.

Part I

A. Unstimulated cells

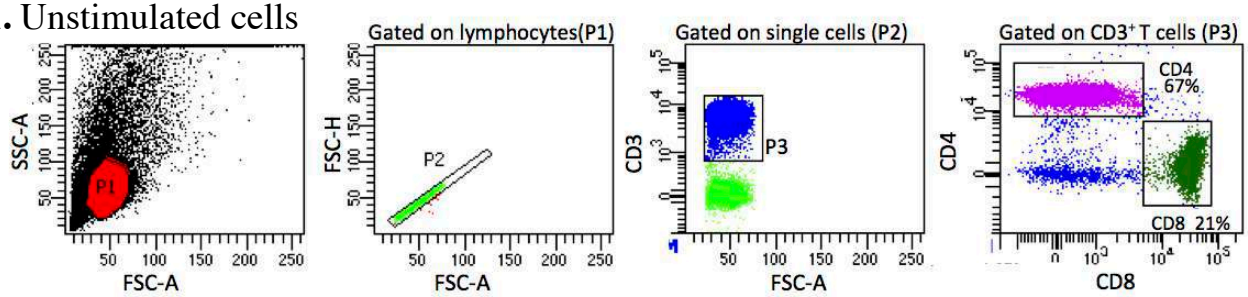

B. PMA/ionomycin stimulated cells

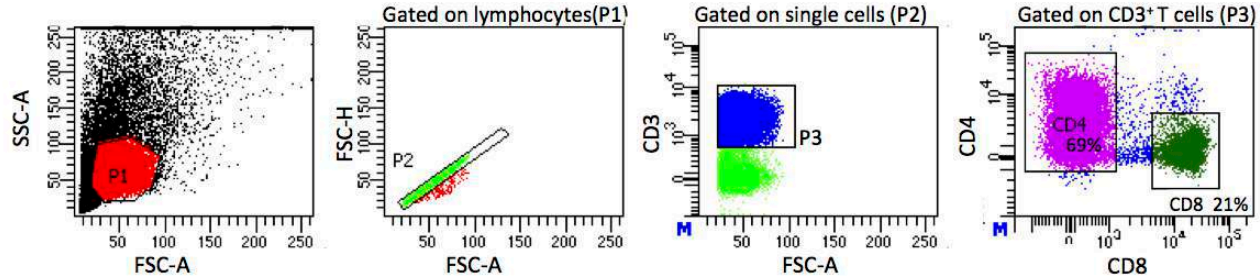

Figure 10. T cell subset identification on normal blood.

Part I. Gating strategy employed to isolate CD4 and CD8 T cells on **A)** unstimulated and **B)** PMA/ionomycin stimulated PBMCs permeabilised with the BD transcription factor buffer. Subsequent gating on lymphocytes **P1**, single cells **P2** and $CD3^+$ **P3** T cells identified the $CD4^+$ and $CD8^+$ T cells.

In the succeeding parts, 4 groups (A to D) of 6 plots are shown. A and B are gated on CD4 T cells, while C and D are gated on CD8 T cells. The top row (A, C) shows unstimulated cells, and the bottom row (B, D) shows PMA/ionomycin stimulated cells. On the first row, plot 1 shows the isotype control for the TF; plot 2 shows the unstained (BV421) and cytokine isotype (PE) controls, and 3 shows transcription factor-positive cells in blue (CD4) or orange (CD8). On the second row, plots 1 and 2 show co-expression of the TF and the indicated cytokine. Plot 3 shows expression of the two cytokines, backgated with TF-positive cells.

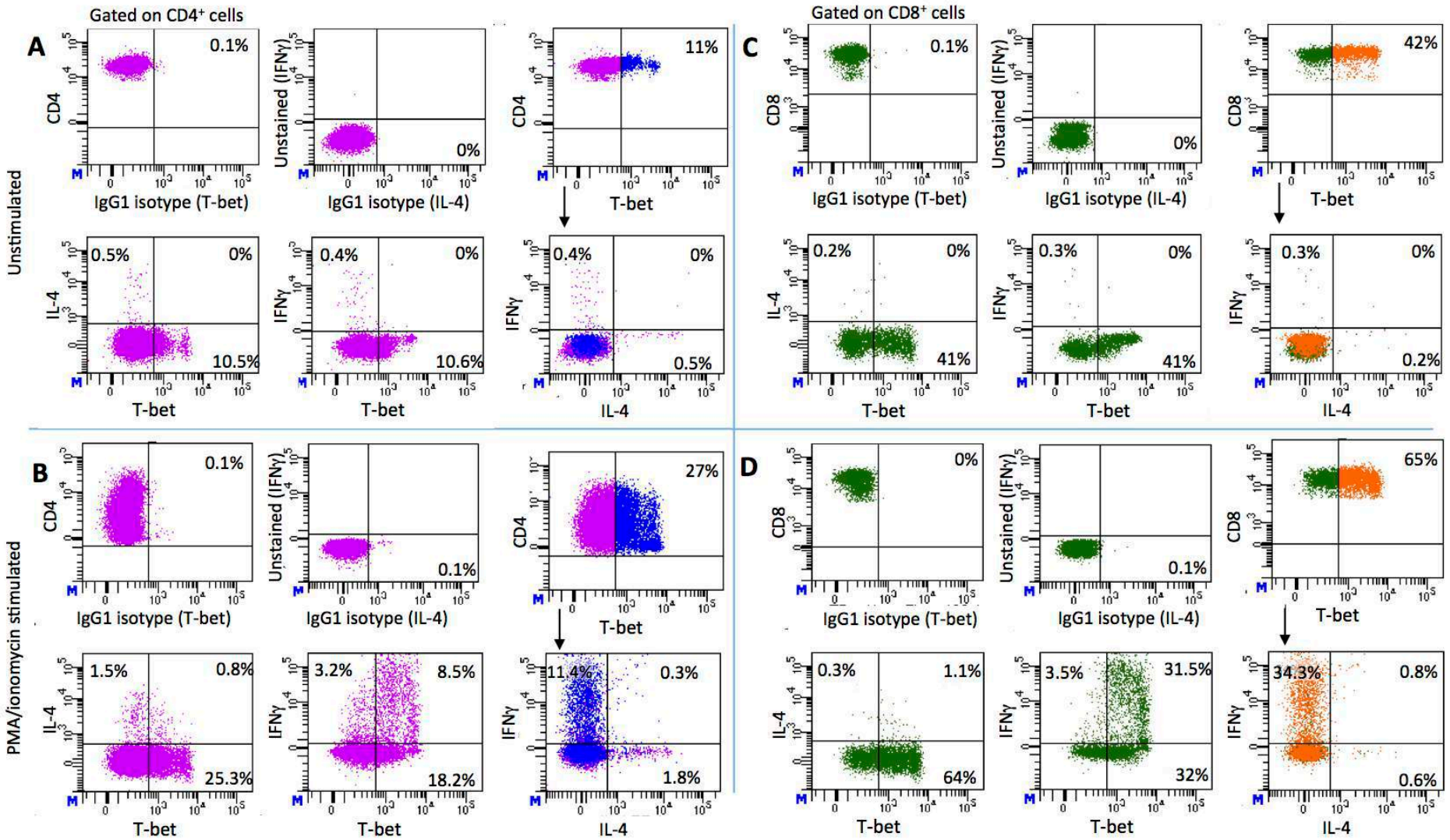

Figure 10 – Part II. T-bet, IFNγ, IL-4 staining on gated CD4 (A, B) and CD8 (C, D) T cells in normal blood. Gates were placed based on isotype and unstained controls. For CD4 T cells, T-bet and IFNγ expression identifies the Th1 cells. For CD8 T cells, IFNγ expression identifies the Tc1 cells.

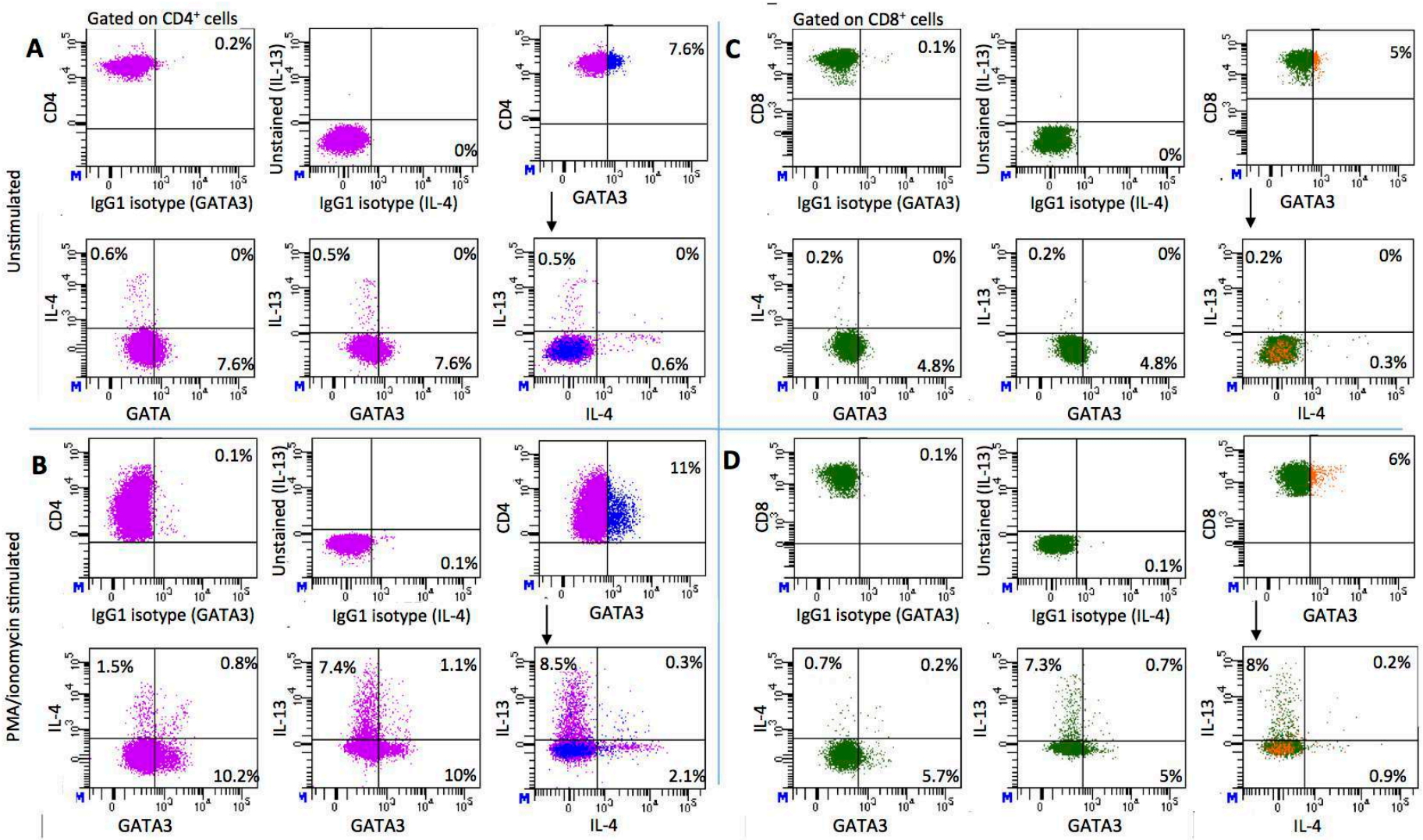

Figure 10 – Part III. GATA3, IL-4 and IL-13 staining on gated CD4 (A, B) and CD8 (C, D) T cells in normal blood.
Gates were placed based on isotype and unstained controls. For CD4 T cells, GATA3, IL-3 and IL-13 expression identifies the Th2 cells. For CD8 T cells, IL-4 expression identifies the Tc2 cells.

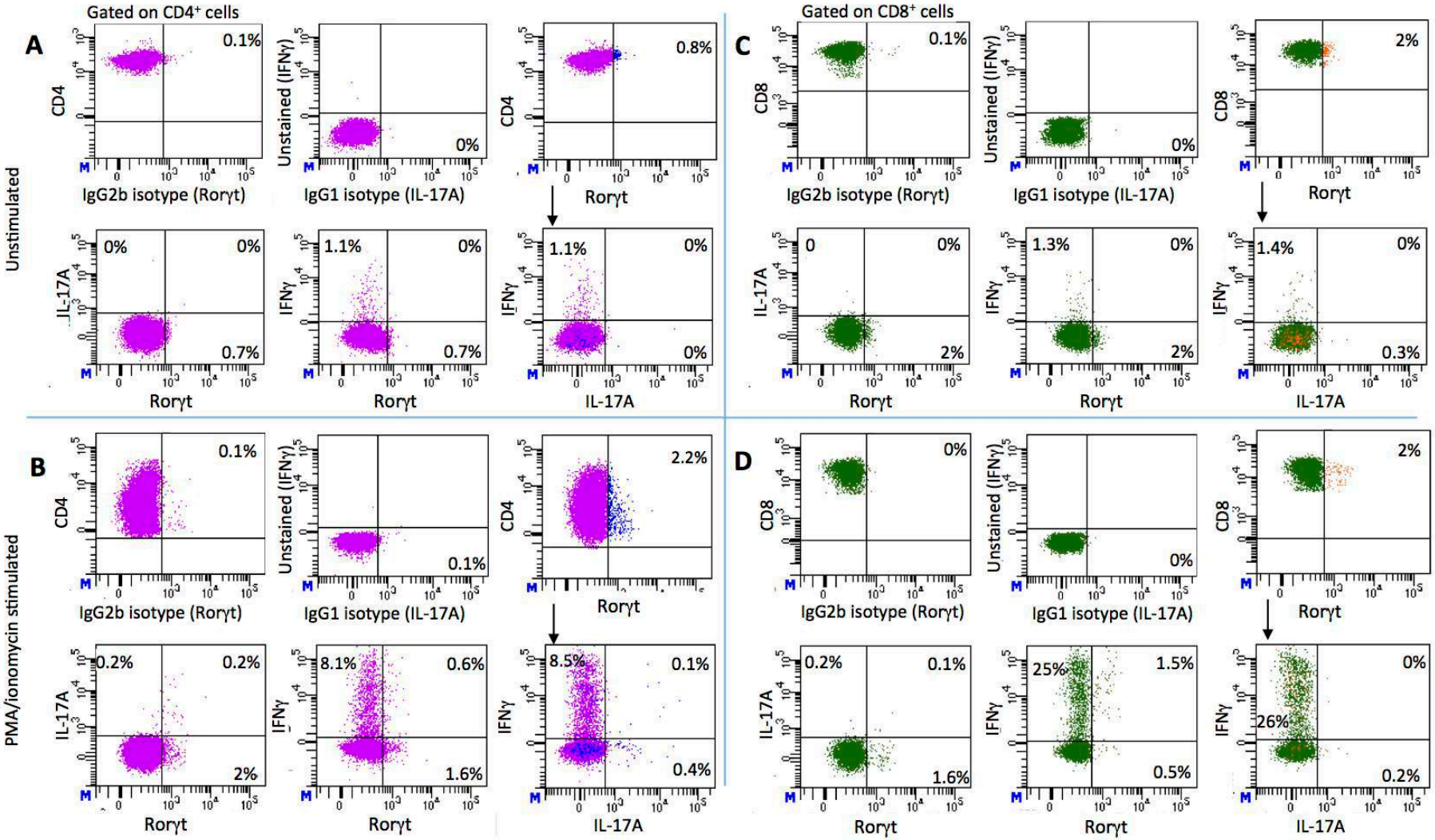

Figure 10 – Part IV. RORγt, IL-17A and IFNγ staining on gated CD4 (A, B) and CD8 (C, D) T cells in normal blood.
Gates were placed based on isotype and unstained controls. For CD4 T cells, RORγt and IL-17A expression identifies the Th17 cells. For CD8 T cells, IL-17A expression identifies the Tc17 cells.

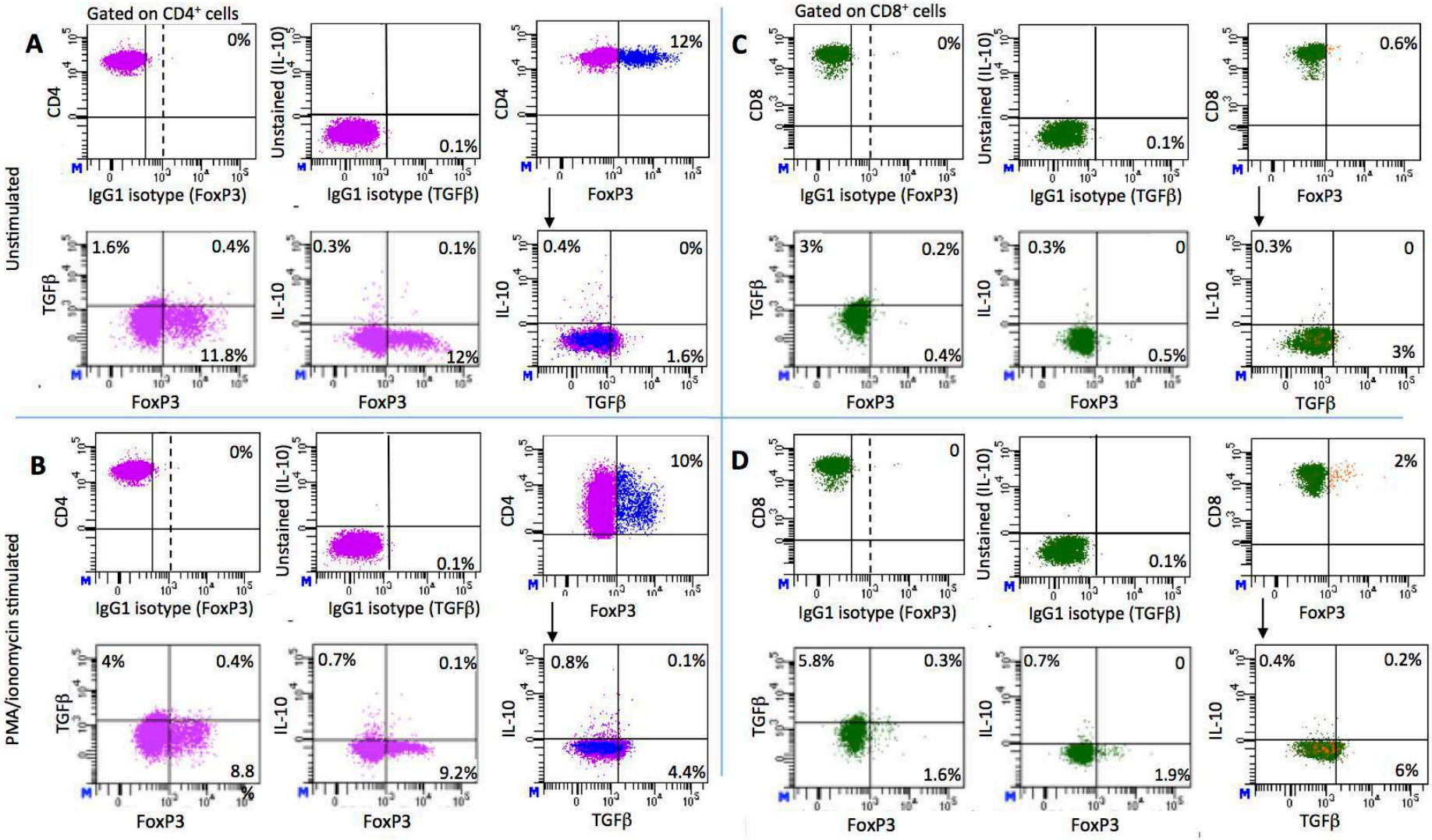

Figure 10 – Part V. FoxP3, IL-10 and TGFβ staining on gated CD4 (A, B) and CD8 (C, D) T cells in normal blood.
Based on Tregs defined as $CD25^{hi}IL\text{-}7R^{lo}TNFR2^{hi}$ in blood, the FoxP3 gate was moved (broken line) to include only $FoxP3^{hi}$ expression. Cytokine gates were based on isotype and unstained controls. For CD4 T cells, this identifies the regulatory T cells.

3.3.2. Characterisation of CD4 and CD8 T cell subsets in LE patient blood

The previous results clearly indicated that the early optimisation experiments have successfully established a reliable staining protocol to identify human T cell subsets. It remains to be determined how this staining protocol operates when examining samples obtained from pathology situations of human diseased tissues. Therefore to compare if there are differences in the expression of T cell subsets in a patient with lymphoedema, the peripheral blood collected at the time of liposuction surgery was processed and analysed as described above.

Gating first on lymphocytes P1 and single-cells P2, 69% of the $CD3^+$ cells were $CD4^+$ T cells while ~26% were $CD8^+$ T cells; a small population of $CD3^+$ T cells were DP or DN in unstimulated samples (**Figure 11– Part 1. A**). Stimulation with PMA/ionomycin downregulated CD4 expression (as expected), thus requiring to gate on $CD3^+CD8^-$ cells to identify the $CD4^+$ population, roughly maintaining the CD4/CD8 ratio seen in unstimulated cells (**Figure 11– Part 1. B**).

Expression of T-bet was evident in both CD4 and CD8 populations, with PMA/ionomycin stimulation almost doubling the T-bet positive cells to 50% of all CD4 T cells and 75% of CD8 T cells. Most strikingly, the majority of these T-bet^+ cells were also producing IFNγ, while almost all other CD4 and CD8 cells were also co-expressing IFNγ (**Figure 11– Part II**). It is possible that the cell populations have "shifted" after stimulation, and that only the $IFN\gamma^{hi}$ population shows true staining. Nevertheless, a similar staining on the panel with RORγt (Figure 11 – part IV. B and D) show increased IFNγ expression as well, and since this occurred only on the stimulated PBMC from the patient and not on the normal blood (Figure 10 – part II and IV) analysed on the same experiment, the IFNγ gate was retained as per the unstained control. Surprisingly, at least 2% of T-bet^+CD4^+ T cells and of T-bet^+CD8^+ T cells co-expressed IL-4 (**Figure 11– Part II. B and D**).

The expression of GATA3 on CD4 and CD8 T cells was also detectable especially after stimulation, with 7% of CD4 T cells and 10% of CD8 T cells staining positively for these factors **(Figure 11– Part III)**. Small populations (each ≤1%) of $GATA3^+$ cells co-expressed IL-4 or IL-13, or both IL-4 and IL-13. Of note, there appears to be $CD4^+GATA3^-$ and $CD8^+GATA3^-$ cells that produced IL-13 (**Figure 11– Part III. B and D**).

Compared to the normal peripheral blood, there was increased (9%) $CD4^+ROR\gamma t^+$ T cells in the patient blood detected after stimulation (**Figure 11– Part IV**). In this panel, IFNγ was noticeably highly positive, similar with Figure 11 – Part II. With the IFNγ gate placement unchanged and set according to the unstained control, of $CD4^+ROR\gamma t^+$ cells, over half produced IFNγ, and less than 1% also produced IL-17A. Interestingly, the population expressing IL-17A also appeared to co-express IFNγ **(Figure 11– Part IV. B)**. $CD8^+ROR\gamma t^+$ cells were also present, but these cells did not produce detectable levels of IL-17A and instead expressed IFNγ (**Figure 11– Part IV. D**).

Approximately the same levels of FoxP3^{hi} (gating defined by CD25^{+}IL-7R$^{lo/-}$(and TNFR2^{+} in unstimulated) cells were identified in CD4 T cells before (9.5%) and after stimulation (11%) (**Figure 11– Part V. A and B**). In the stimulated cells, ≤1% also produced IL-10, and there appeared to be some cells co-expressing TGFβ^{lo} **(Figure 11– Part V. B)**. Despite the gating on FoxP3^{hi}, at least 3% of CD8^{+} cells were FoxP3^{+}, with some cells possibly co-expressing IL-10 and TGFβ (**Figure 11– Part V. C and D**).

Taken together, Th1, Th2, Th17 and Treg cells, were clearly identified in the lymphoedema patient blood. According to transcription factor expression, Th1 cells dominated the CD4 T cell population, with nearly half of CD4 T cells being T-bet^{+} (especially after stimulation). In contrast, Th2 GATA3^{+} cells comprise only 7% of the CD4 T cells, and Th17 RORγt+ cells make up 9%. Treg FoxP3^{hi} T regulatory cells constitute 11% of all CD4 T cells. Cytokine expression was clearly evident, with the Th1 cytokine IFNγ being highly produced upon stimulation. IL-4, IL-13, IL-17 and IL-10 production were also detected. With respect to CD8 T cells, T-bet^{+} cells producing IFNγ were evident in blood, while there are smaller populations of GATA3^{+}, RORγt^{+} and FoxP3^{+} CD8 T cells.

Nevertheless, since we have only been able to analyse a few patients at this time, more patient samples, analysed simultaneously with matched normal blood, is needed in order to conclude if the differences in T cell subset quantities are significant. In any case this analysis has proven that the current protocol can be applied to examine patient blood, as well as healthy individuals, and it may be useful in investigating peripheral blood immune cells in the context of virtually any pathology/disease state.

3.3.3. Characterisation of CD4 and CD8 T cell subsets in the stromal vasculature fraction of an LE patient

The greatest challenge in analysing the stromal vasculature fraction of adipose tissue is that it contains diverse material compared to freshly isolated PBMCs, as seen in the SSC/FSC plots (**Figure 12– Part I**). Positioning of the lymphocyte gate **P1** had to be done while backgating on the CD3^{+}, CD4^{+} and CD8^{+} cells, and the gate was subjectively positioned on an area where the most cells stained for the T cell markers. Remarkably, the lymphocyte population was in a similar position when lymphocytes are examined in blood, although a wider single-cell gate was set to accommodate for the most number of cells. In collecting 50,000 events, in PBMCs, approximately 20-40% are CD3^{+} (Figure 10 and 11 – Part I), while only around ≤5% are CD3^{+} in the SVF . Also, in contrast to the uniform CD4^{hi} populations in unstimulated PBMC, CD4 expression in unstimulated cells in SVF appeared to have been downregulated to some extent (**Figure 12– Part I**), perhaps as a result of the collagenase enzyme exposure, and/or indicating that these cells are already in an activated state.

In CD4 T cells, high expression of T-bet was observed in both unstimulated and stimulated cells, with almost half of these cells also producing IFNγ, and a minor percentage producing IL-4. There also appeared to be T-bet negative IFNγ^{+}IL-4^{+} cells (**Figure 12– Part II. A and B**). Approximately 30-42% of CD8 T cells are also T-bet^{+}, with nearly half co-expressing

IFNγ. In addition, nearly 50% of $CD8^{-}IFN\gamma^{-}$ T cells produce IFNγ (**Figure 12– Part II. C and D**).

Upon stimulation, GATA3 expression was detected in 4% of CD4 T cells, with some cells also producing IL-4, IFNγ, and both IL-4 and IFNγ. As observed above (Figure 12– Part II), other CD4 (GATA3-negative) cells co-expressed IFNγ and IL4 (**Figure 12 – Part III. A and B**). With the small population of CD8 T cells identified in SVF, it is unclear if the 2% $GATA3^{+}$ CD8 T cells are true staining. Nevertheless, it was confirmed that virtually 50% of CD8 T cells produce IFNγ (**Figure 12 – Part III. C and D**).

RORγt expression in CD4 T cells was increased following stimulation in the SVF. Two per cent of $ROR\gamma t^{+}$ CD4 T cells also produced IL-17A, with some appearing to co-express both IL-17A and IFNγ (**Figure 12 – Part IV. A and B**). Some CD8 T cells also stained positively with the RORγt antibody, although these did not produce IL-17A or IFNγ **(Figure 12 – Part IV. C and D)**; as with the $GATA3^{+}$ CD8 T cells, it is currently unclear what the $ROR\gamma t^{+}$ CD8 T cells are.

In CD4 T cells, there was 4-6% $FoxP3^{+}$ expression before and after stimulation. The majority of these cells produced TGFβ, although IL-10 production was less clear (**Figure 12– Part V. A and B**). No CD8 T cells were found to be $FoxP3^{+}$ (**Figure 12– part V. C and D**). Surprisingly though, TGFβ production was detected in both CD4 and CD8 T cells in SVF, although not always by FoxP3-expressing cells.

Taken together, one must consider that lymphoedema adipose tissue is not well understood and has not been previously characterised in this manner. It has been reported that there are significantly more Treg cells in the visceral adipose tissue in normal mice but not in insulin-resistant models of obesity (Feuerer et al., 2009), so it remains to be seen how this relates to human lymphoedema adipose tissue. Even though there was a relatively small T cell ($CD3^{+}$) population identified within SVF, these data indicate that it is still possible to detect Th1, Th2, Th17 and Treg cells, even simply based on transcription factor expression. Detection of IL-4-, IFNγ-, IL-10-, TGFβ- and perhaps IL-17A- producing CD4 T cells has also been achieved. Likewise, CD8 T cells mostly expressed T-bet, while GATA3 and RORγt positive cells were possibly detected, with CD8 T cells producing the cytokines IFNγ, IL-10 and TGFβ.

In summary, when considering the data obtained across three different samples (blood from healthy individual, and blood and SVF from an LE patient), it is apparent that (i) there is an abundance of Th1 cells ($T\text{-}bet^{+}$ and $IFN\gamma^{+}$ cells), (ii) that FoxP3 expression is relatively stable (i.e. before and after PMA/ionomycin stimulation), and (iii) that some cells simultaneously exhibit Th1 and Th2 characteristics (such as $T\text{-}bet^{+}IL\text{-}4^{+}$).

A. Unstimulated PBMCs

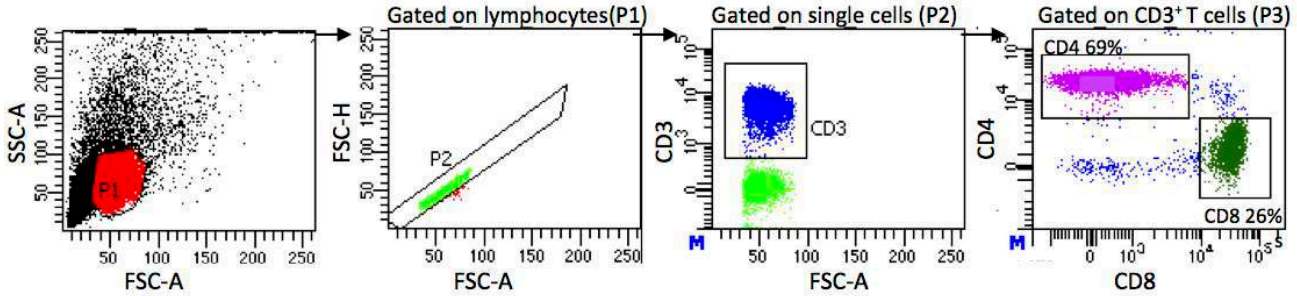

B. PMA/ionomycin activated cells

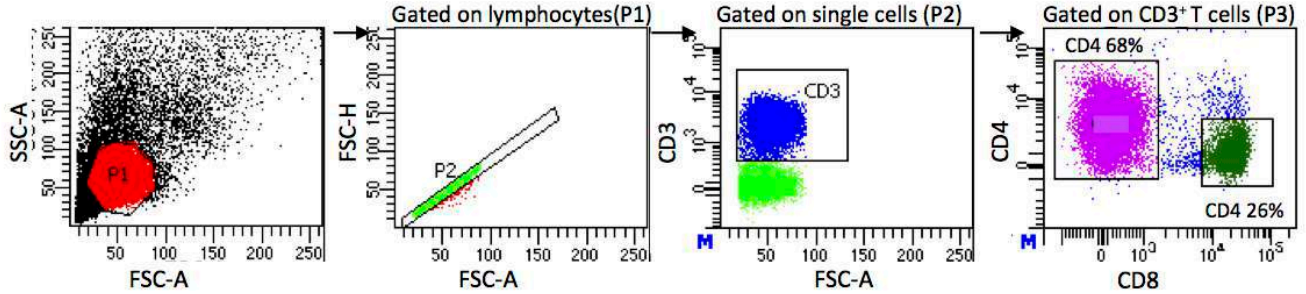

Figure 11. T cell subset identification on LE patient blood

Part I. Gating strategy employed to isolate CD4 and CD8 T cells on **A**) unstimulated and **B)** PMA/ionomycin stimulated PBMCs permeabilised with the BD Transcription Factor buffer. Subsequent gating on lymphocytes P1, single cells P2 and $CD3^+$ P3 T cells identified the $CD4^+$ and $CD8^+$ T cells.

In the succeeding parts, 4 groups (A to D) of 6 plots are shown. A and B are gated on CD4 T cells, while C and D are gated on CD8 T cells. The top row (A, C) shows unstimulated cells, and the bottom row (B, D) shows PMA/ionomycin stimulated cells. On the first row, plot 1 shows the isotype control for the TF; plot 2 shows the unstained (BV421) and cytokine isotype (PE) controls, and 3 shows transcription factor-positive cells in blue (CD4) or orange (CD8). On the second row, plots 1 and 2 show co-expression of the TF and the indicated cytokine. Plot 3 shows expression of the two cytokines, backgated with TF-positive cells.

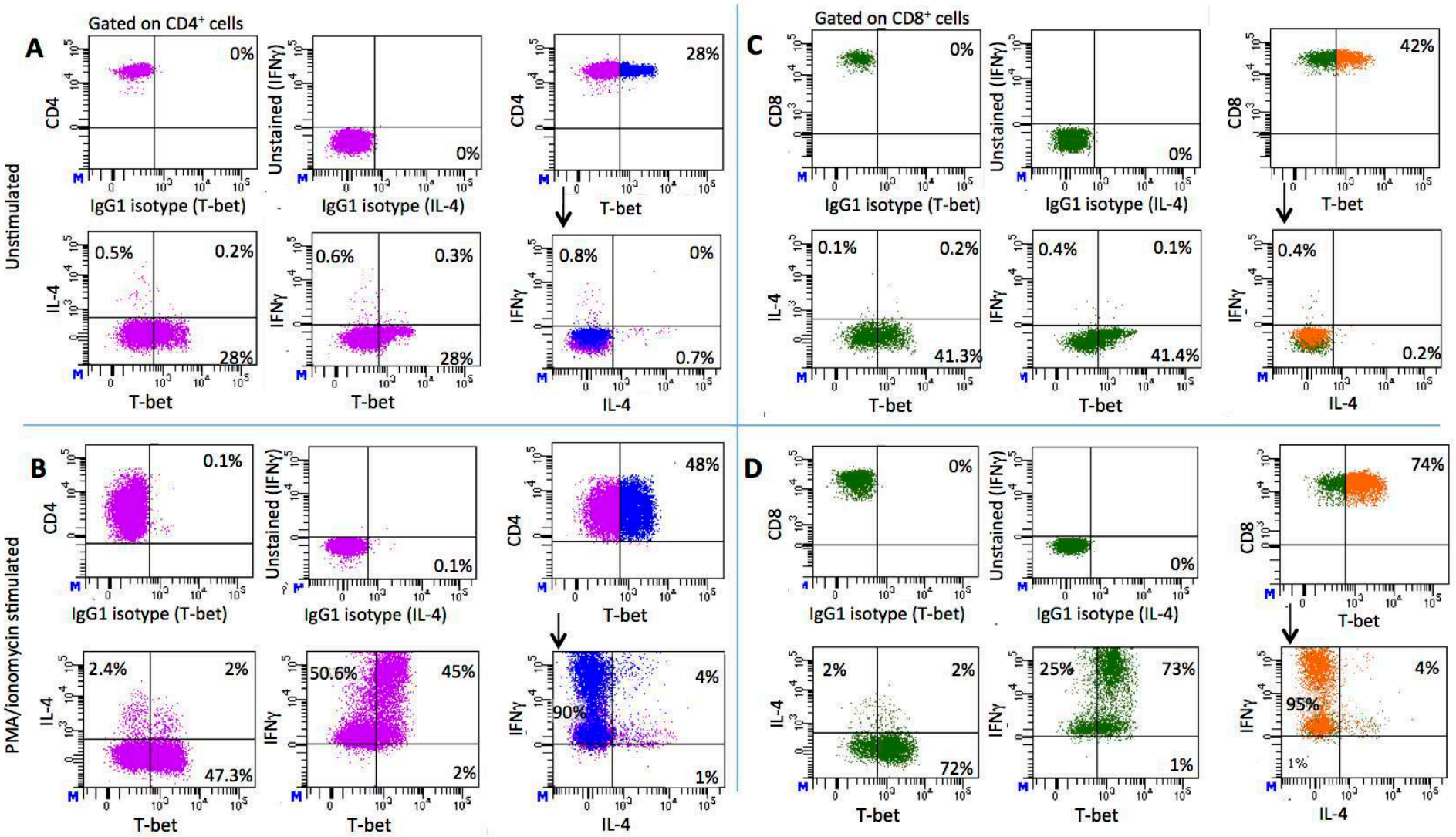

Figure 11 – Part II. T-bet, IFNγ, IL-4 staining on gated CD4 (A, B) and CD8 (C, D) T cells in patient blood.
Gates were placed based on isotype and unstained controls. For CD4 T cells, T-bet and IFNγ expression identifies the Th1 cells. For CD8 T cells, IFNγ expression identifies Tc1 cells.

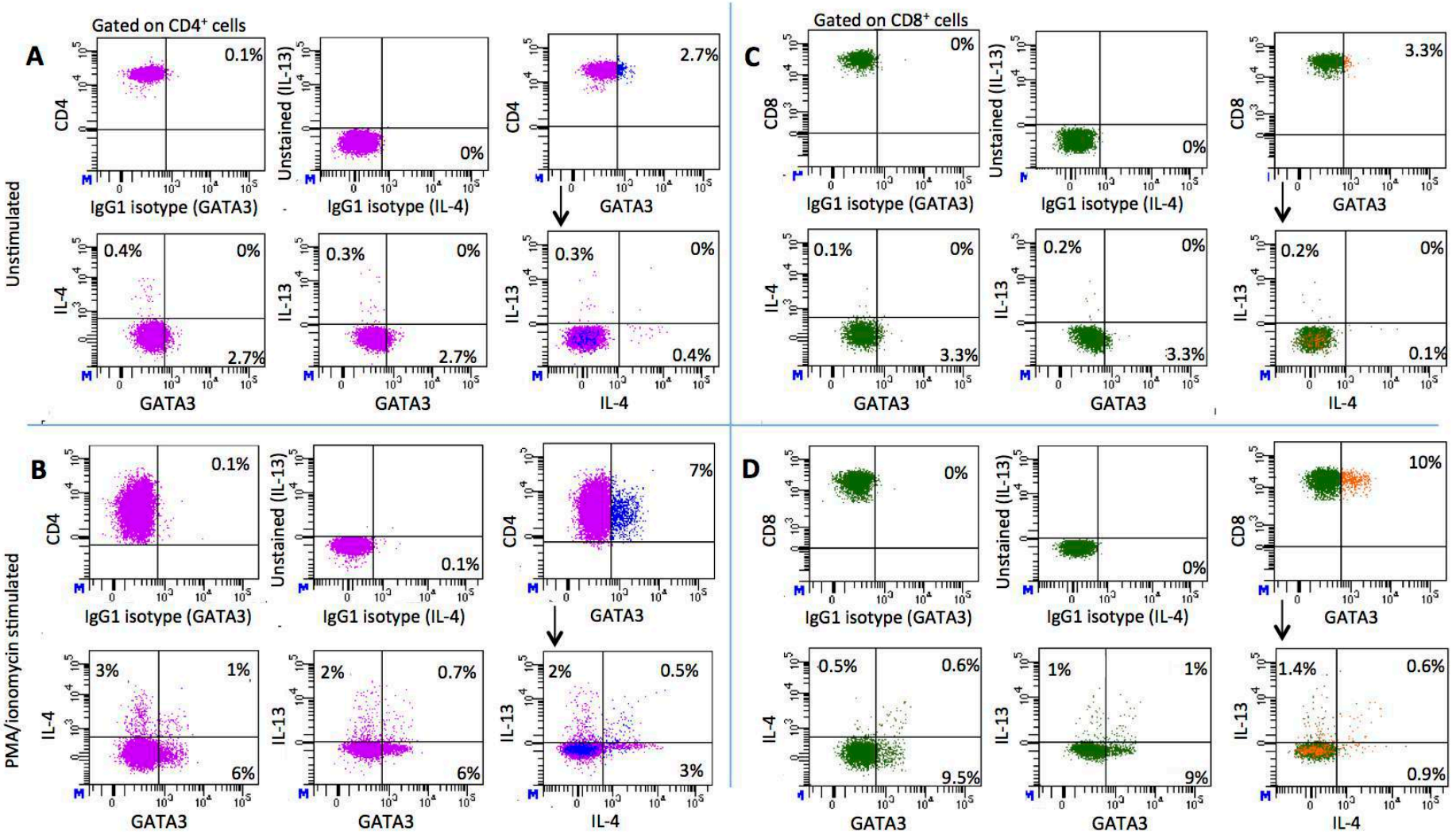

Figure 11 – Part III. GATA3, IL-4 and IL-13 staining on gated CD4 (A, B) and CD8 (C, D) T cells in patient blood.
Gates were placed based on isotype and unstained controls. For CD4 T cells, this identifies the Th2 cells.
For CD8 T cells, IL-4 expression identifies the Tc2 cells.

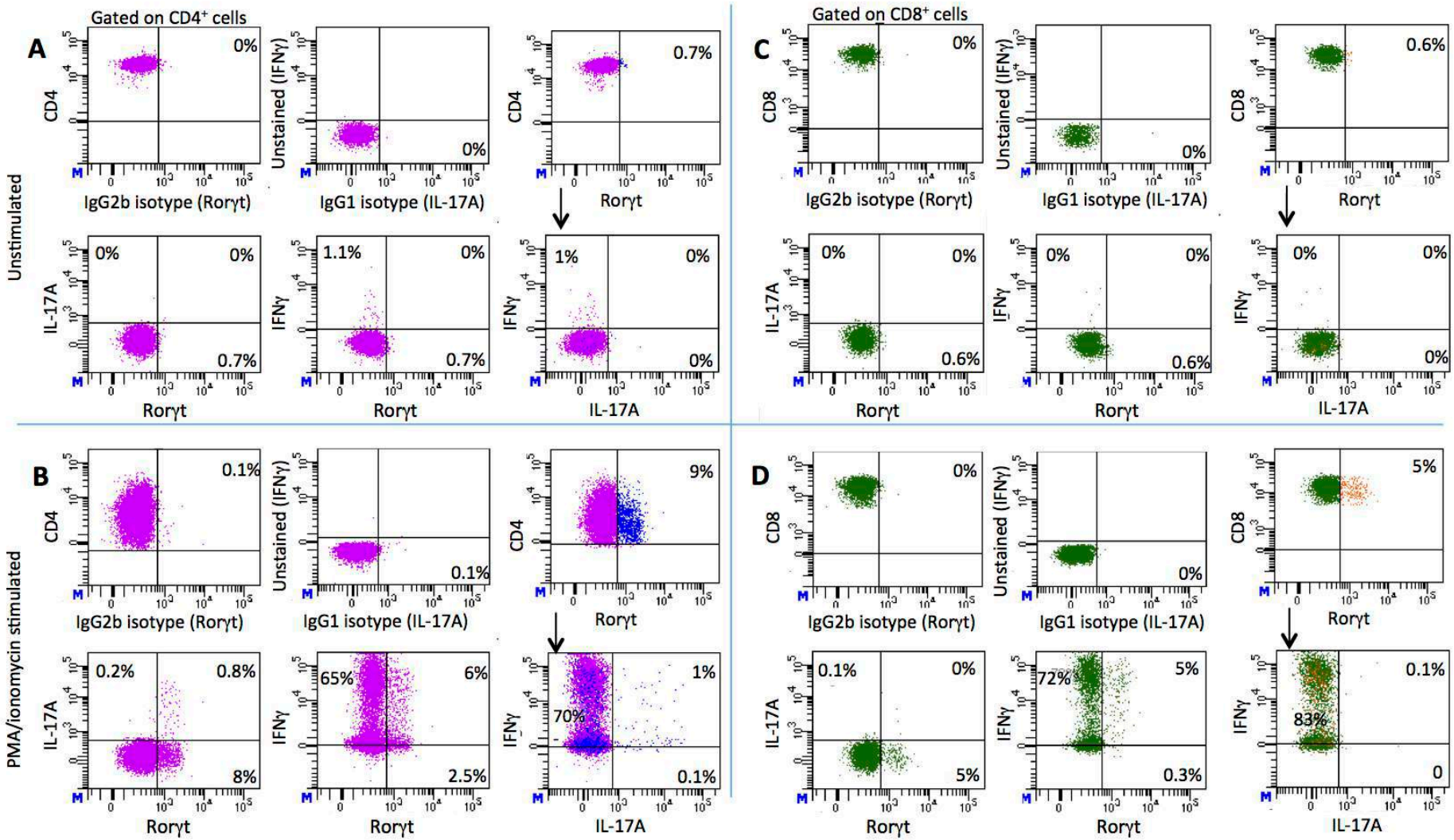

Figure 11 – Part IV. RORγt, IL-17A and IFNγ staining on gated CD4 (A, B) and CD8 (C, D) T cells in patient blood.
Gates were placed based on isotype and unstained controls. For CD4 T cells, GATA3 and IL-17A expression the Th17 cells. For CD8 T cells, IL-17A expression identifies Tc17 cells.

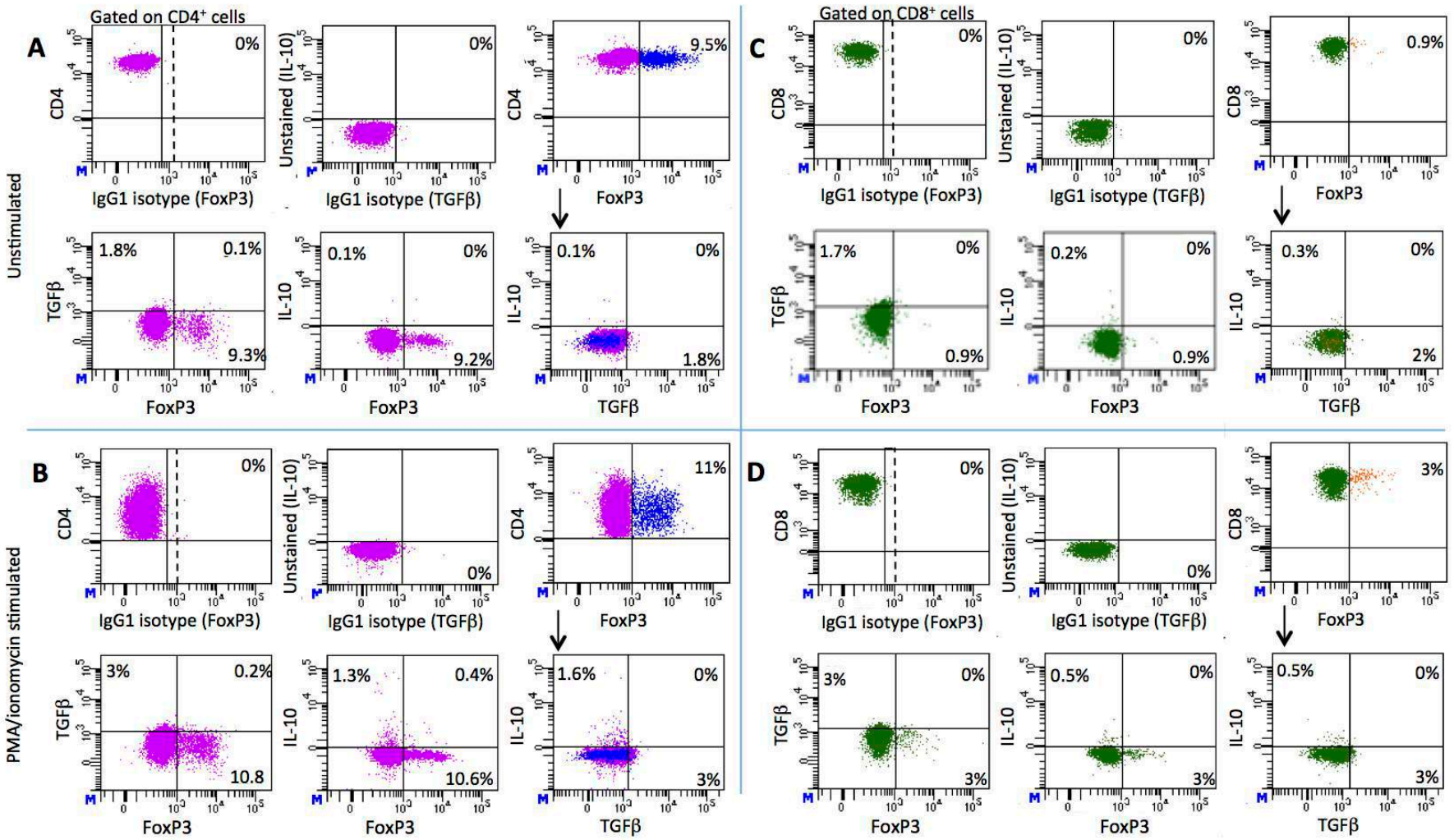

Figure 11 – Part V. FoxP3, IL-10 and TGFβ staining on gated CD4 (A, B) and CD8 (C, D) T cells in patient blood.
Based on Treg cells defined as $CD25^{hi}IL\text{-}7R^{lo}TNFR2^{hi}$ in blood, the FoxP3 gate was moved (broken lines) to include only $FoxP3^{hi}$ expression. Cytokine gates were based on isotype and unstained controls. For CD4 T cells, this identifies the regulatory T cells.

A. Unstimulated cells

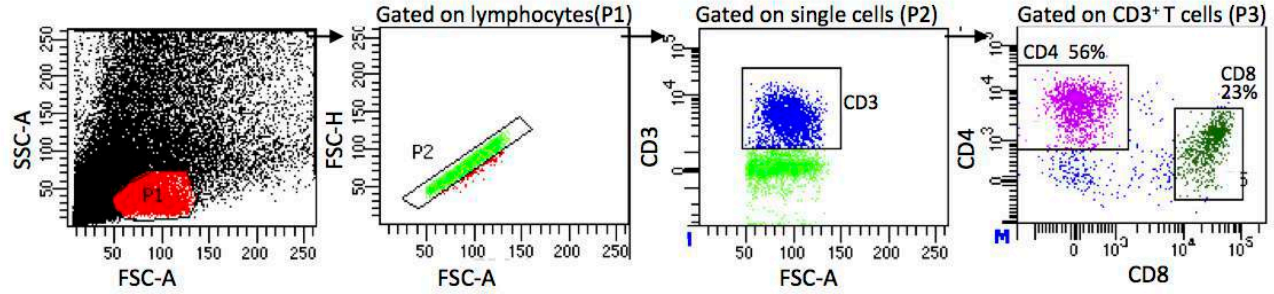

B. PMA/ionomycin activated cells

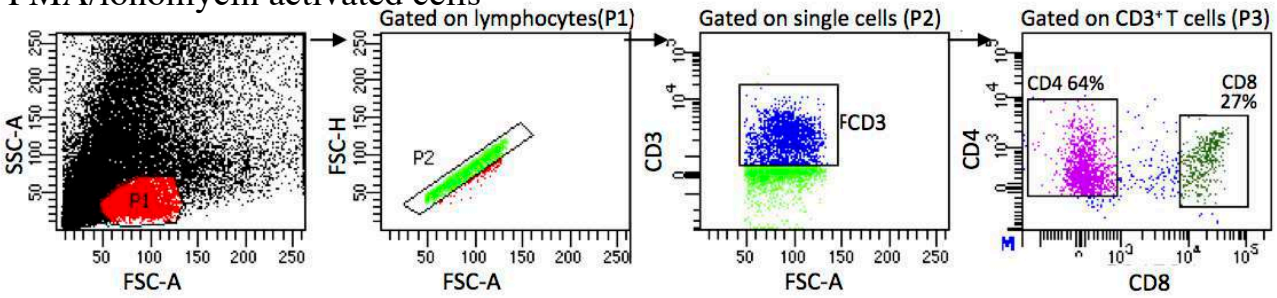

Figure 12. T cell subset identification on SVF of an LE patient.

Part I. Gating strategy employed to isolate CD4 and CD8 T cells on **A)** unstimulated and **B)** stimulated cells from SVF, permeabilised with the eBiosciences buffer. Subsequent gating on lymphocytes **P1**, single cells **P2** and $CD3^+$ **P3** T cells identified the $CD4^+$ and $CD8^+$ T cells.

In the succeeding parts, 4 groups (A to D) of 6 plots are shown. A and B are gated on CD4 T cells, while C and D are gated on CD8 T cells. The top row (A, C) shows unstimulated cells, and the bottom row (B, D) shows PMA/ionomycin stimulated cells. On the first row, plot 1 shows the isotype control for the TF; plot 2 shows the unstained (BV421) and cytokine isotype (PE) controls, and 3 shows transcription factor-positive cells in blue (CD4) or orange (CD8). On the second row, plots 1 and 2 show co-expression of the TF and the indicated cytokine. Plot 3 shows expression of the two cytokines, backgated with TF-positive cells.

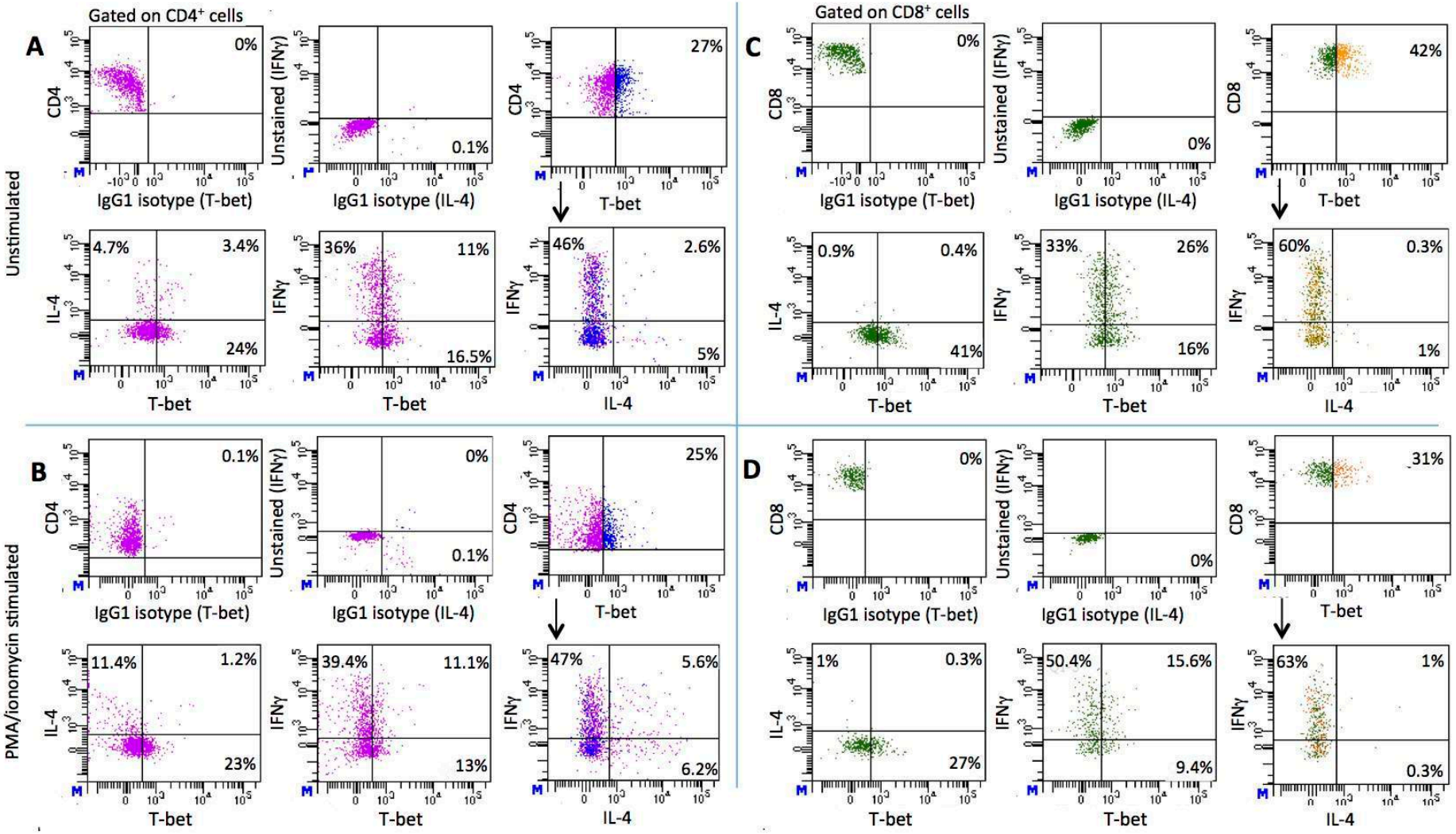

Figure 12 – Part II. T-bet, IFNγ, IL-4 staining on gated CD4 (A, B) and CD8 (C, D) T cells in SVF.
Gates were placed based on isotype and unstained controls. For CD4 T cells, T-bet and IFNγ expression identifies the Th1 cells. For CD8 T cells, IFNγ expression identifies Tc1 cells.

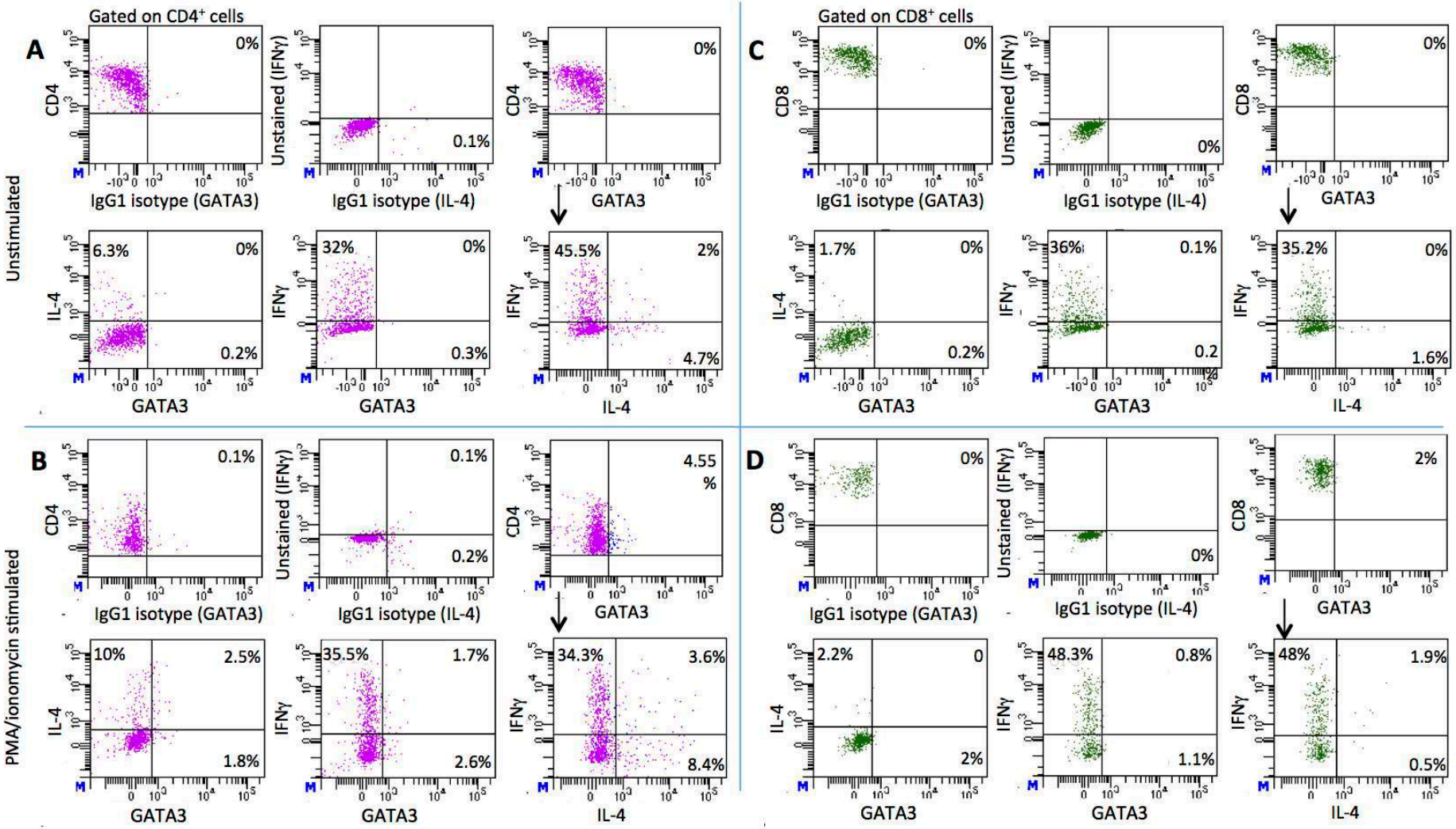

Figure 12 – Part III. GATA3, IL-4 and IL-13 staining on gated CD4 (A, B) and CD8 (C, D) T cells in SVF.
Gates were placed based on isotype and unstained controls. For CD4 T cells, GATA3, IL-4 and IL-13 expression identifies the Th2 cells. For CD8 T cells, IL-4 expression identifies the Tc2 cells.

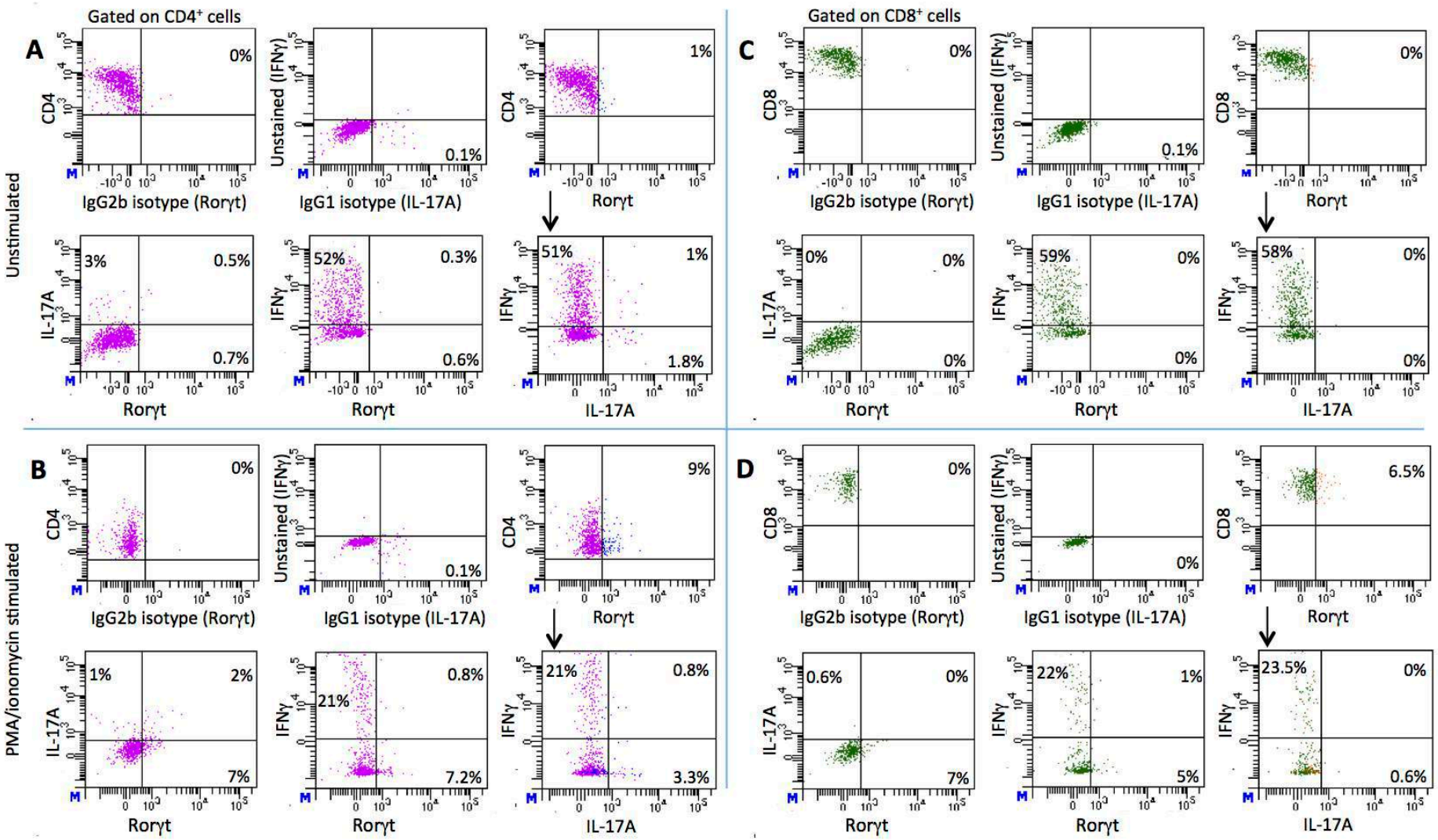

Figure 12 – Part IV. RORγt, IL-17A and IFNγ staining on gated CD4 (A, B) and CD8 (C, D) T cells in SVF.
Gates were placed based on isotype and unstained controls. For CD4 T cells, RORγt and IL-17A expression the Th17 cells. For CD8 T cells, IL-17A expression identifies Tc17 cells.

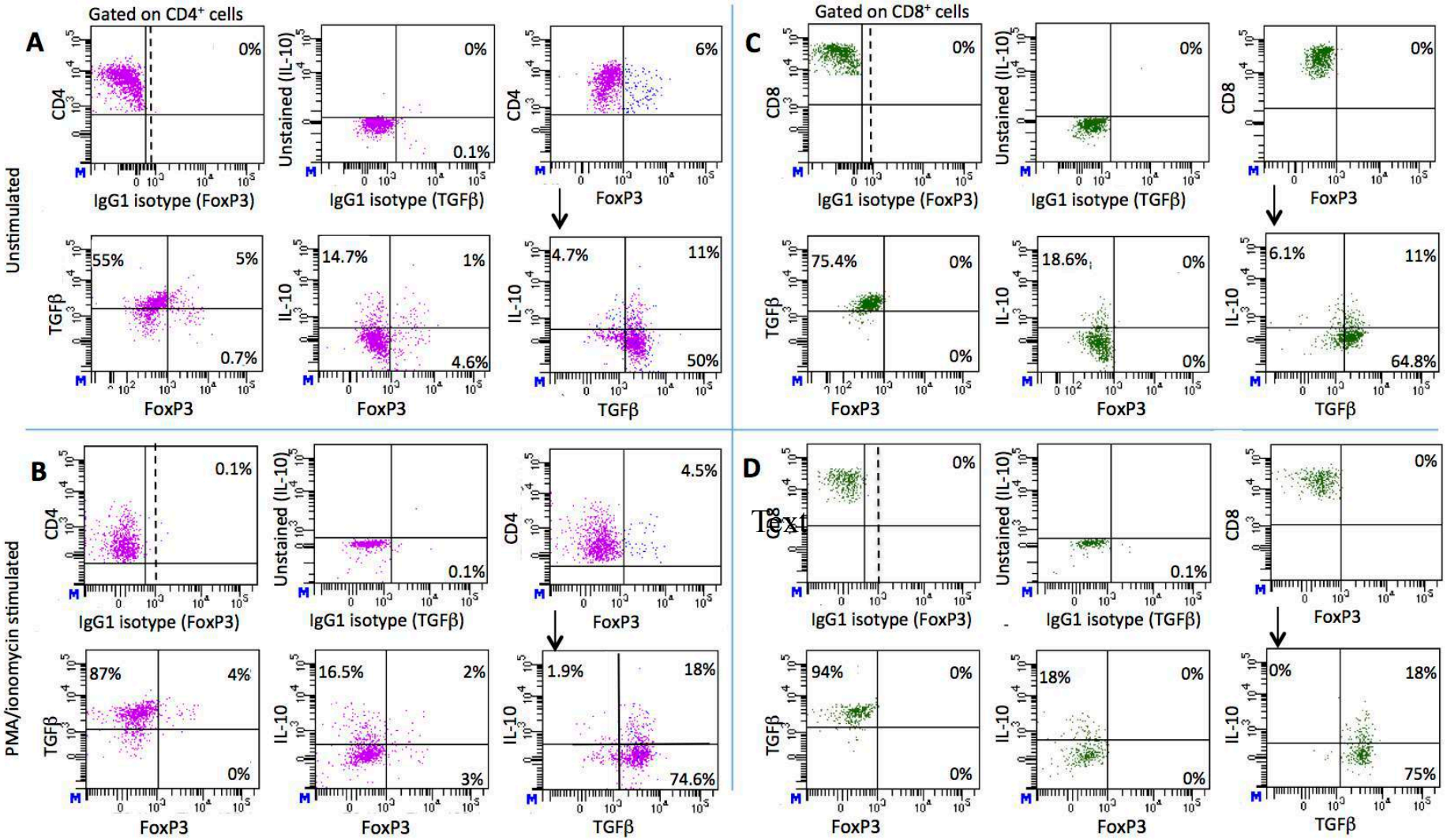

Figure 12 – Part V. FoxP3, IL-10 and TGFβ staining on gated CD4 (A, B) and CD8 (C, D) T cells in SVF

Based on regulatory T cells defined as $CD25^{hi}IL\text{-}7R^{lo}TNFR2^{hi}$ *in blood*, the FoxP3 gate was moved to include only $FoxP3^{hi}$ expression. Cytokine gates were based on isotype and unstained controls. For CD4 T cells, this identifies the regulatory T cells.

Table 2. Summary of T cell subset identification in blood & SVF

A. $CD3^+CD4^+$ T cell subsets		Normal blood		Patient blood		SVF	
		U	S	U	S	U	S
Th1	$T\text{-}bet^+ IFN\gamma^+$	-	++	+/-	+++	++	++
Th2	$GATA3^+ IL\text{-}4^+$	-	+/-	-	+/-	-	+
Th17	$ROR\gamma t^+ IL\text{-}17^+$	-	+/-	-	+/-	+/-	+
Treg	$FoxP3^{hi} IL\text{-}10^+$	+/-	+/-	-	+/-	+/-	+/-
Treg	$FoxP3^{hi} TGF\beta^{hi}$	+/-	+/-	+/-	+/-	+	+
Transcription factors	T-bet	+	++	++	+++	++	++
	GATA3	+	++	+/-	+	-	+
	RORγt	+/-	+	+/-	+	+/-	+
	$FoxP3^{hi}$	++	++	++	++	+	+
Cytokines	IFNγ	+/-	+	+/-	+++	++	+++
	TGFβ	+	+	+	+	++	+++
	IL-10	+/-	+/-	+/-	+/-	++	++
	IL-13	+/-	+	+/-	+	N/a	N/a
	IL-4	+/-	+	+/-	+	+	++
	IL-17A	-	+/-	-	+/-	+	+

B. $CD3^+CD8^+$ T cell subsets		Normal blood		Patient blood		SVF	
		U	S	U	S	U	S
	$T\text{-}bet^+IFN\gamma^+$	-	++	+/-	+++	++	++
	$GATA3^+IL\text{-}4^+$	-	+/-	-	+/-	-	-
	$ROR\gamma t^+IL\text{-}17^+$	-	+/-	-	-	-	-
	$FoxP3^{hi}IL\text{-}10^+$	+/-	+/-	-	-	-	-
	$FoxP3^{hi}$ $TGF\beta^{hi}$	-	-	-	-	-	-
Transcription factors	$T\text{-}bet^+$	++	+++	++	+++	++	++
	$GATA3^+$	+	+	+	++	-	+
	$ROR\gamma t^+$	+/-	+/-	+/-	+	-	+
	$FoxP3^{hi}$	+/-	+	+/-	+	-	-
Cytokines	$IFN\gamma^+$	+/-	++	+/-	+++	++	+++
	$TGF\beta^+$	+	++	++	+	++	+++
	$IL\text{-}10^+$	+/-	+/-	+/-	+/-	++	++
	$IL\text{-}13^+$	+/-	+	+/-	+	N/a	N/a
	$IL\text{-}4^+$	+/-	+/-	+/-	+	+/-	+/-
	$IL\text{-}17A^+$	-	+/-	-	+/-	-	+/-

Footnotes: Unstimulated U; PMA/ionomycin stimulated, S; Not available or not analysed, N/A.

3.4. Characterising T cells with the use of additional markers

In the first part, we analysed a series of suggested surrogate surface markers to identify and discriminate between Th1 and Th2 cells, etc. In later experiments, we have added the inclusion of a live/dead cell stain, and an antibody for TCRαβ. In addition, unstimulated frozen PBMC cells were thawed, stained, and examined for viability. Finally, a comprehensive panel of markers that identify naïve and memory T cells was assessed.

3.4.1. CD183 (CXCR3) and CD194 (CCR4) correlation with transcription factor expression in CD4 T cells

The use of surface markers to identify Th1 and Th2 cells may be useful, as current techniques rely on intracellular makers (T-bet and IFNγ, or GATA3 and IL-4) and thus requires cell fixation and permeabilisation, which does not permit experiments with live cells. For this reason, antibodies to CD183 and CD194 were added to the surface staining panel (Table 1 – A), to see if these markers correlated with the CD4 T cell subsets identified by use of transcription factor and cytokine staining as others have suggested (Bonecchi et al., 1998). This experiment was performed on the normal blood PBMCs, as shown in Figure 10 Part I, and the gating for CD4 transcription factor – positive cells were based in Parts II (T-bet), III (GATA3), IV (RORγt) and V (FoxP3). The placement for the CD183 and CD194 positive gates were based on the unstained control in unstimulated and PMA/ionomycin stimulated CD4 T cells **(Figure 13)**.

In unstimulated CD4 T cells, T-bet expression showed the highest association with CD183 expression, while some $GATA3^+$ and $FoxP3^+$ cells were also $CD183^+$ **(Figure 13– A. 1).** For CD194 expression, $GATA3^+$ and $FoxP3^+$ cells showed high CD194 expression, although some $T\text{-}bet^+$ cells also expressed CD194. Stimulation resulted in a loss in CD183 expression on CD4 T cells, although CD194 was preserved **(Figure 13– B)**. In stimulated cells, T-bet-, GATA3-, and FoxP3 -positive cells appear to co-express CD194.

Since the $CD183^+$ and $CD194^+$ cells did not create distinct positive populations, it was considered if perhaps only high expression of CD183 and CD194 would correlate better with Th1 and Th2 cells, respectively. Thus the $CD183^{hi}$ and $CD194^{hi}$ cells were gated, and co-expression of the transcription factor positive cells was scrutinised **(Figure 13– A. 2)**. Even with this more stringent analysis, T-bet expression was still more highly associated with $CD183^{hi}$ expression compared to the other T cell subsets, while some $GATA3^+$ and $FoxP3^+$ cells retained $CD183^{hi}$ expression. As for $CD194^{hi}$ cells, it appears that $GATA3^+$ and $FoxP3^+$ cells maintained $CD194^{hi}$ expression, while in T-bet and RORγt, it was minimal **(Figure 13-A. 2)**. Hence, even gating on only the $CD183^{hi}$ or $CD194^{hi}$ cells, these surface markers are not overwhelmingly convincing of T cell subset identification. (Please note that analysis of CD183hi or CD194hi cells after PMA/ionomycin stimulation is not shown due to the downregulation of CD183).

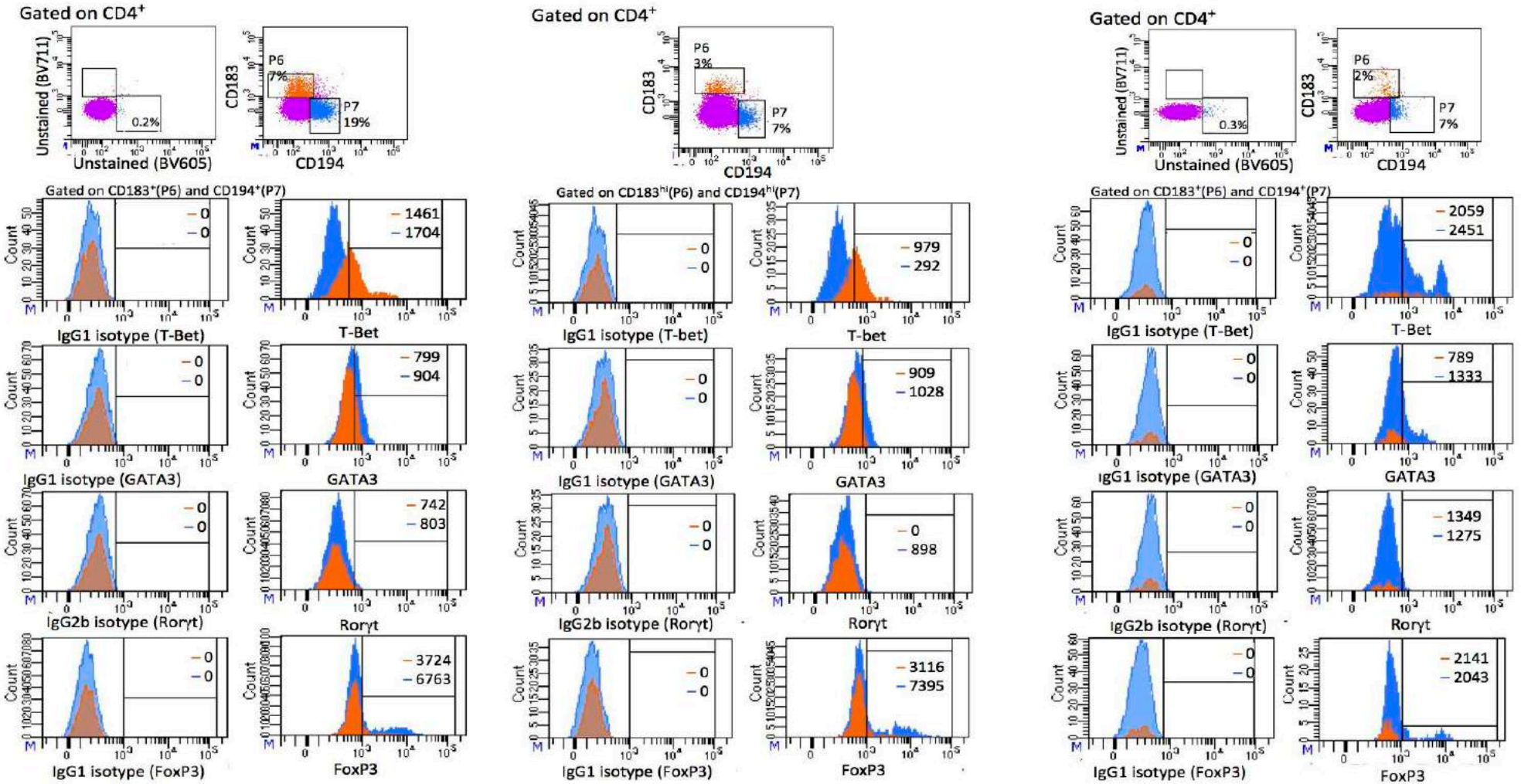

Figure 13. Correlation of CD183 (CXCR3) and CD194 (CCR4) expression with transcription factors on CD4 T cells in normal blood. In unstimulated cells, **A1)** gating on CD183- and CD194 – positive cells was based on the unstained control; **A2)** gating was moved to include only $CD183^{hi}$ or $CD194^{hi}$ cells. In stimulated cells **B)**, gating was based on the unstained control. Gating on transcription factors were placed according to isotype controls, except for $FoxP3^{hi}$ cells, which was based on $CD25^{hi}IL\text{-}7R^{lo}TNFR2^{hi}$.

3.4.2. Identification of live cells and CD3 T cells

A staining panel was designed that included (A) a dead cell stain, to confirm the viability of cells and to ensure dead cells do not cause nonspecific antibody binding, (B) TCRαβ, an additional T cell marker to verify CD4 and CD8 identity, and (C) a selection of surface markers to enhance identification of naïve and memory T cells, with the aim of achieving a better, or even more accurate, characterisation of T cells subsets (**Figure 14– A, B and C**). This experiment was performed with frozen PBMCs from a healthy donor, i.e. the cells were thawed, rested overnight, examined the following day. As the staining panel (Table 1– B) involved surface markers only, there were no PMA/ionomycin stimulation or permeabilisation steps required, and after staining, the cells were fixed in 2% PFA/PBS and immediately analysed on the LSRFortessa X-20.

A live/dead cell stain (Live/dead fixable Aqua 400) was used to determine the quality of the thawed PBMCs. Even with the freeze-thaw process, gating on single-cell lymphocytes (P1 and P2) resulted in approximately 96% viability (**P3**) (**Figure 14– A)**. This panel also accommodated the addition of TCRαβ, enabling a stricter definition of T cells **(Figure 14– A, CD3/TCRαβ panel).** Hence, gating only on the live P3 cells, it is apparent that approximately 1% of CD3 T cells are TCRαβ negative ($CD3^+TCR\alpha\beta^-$; **P5**). This staining and gating strategy therefore appear to be capable of identifying a population of CD3 positive cells in peripheral blood that are likely either NKT cells and/or $CD3^+TCR\gamma\delta$ cells. Further support of this idea comes from showing these cells on a CD4 and CD8 plot, where it is evident that the majority of this new P5 population does not co-express either CD4 or CD8 (**Figure 14– A, last panel**). Of the live cells, ~78% were $CD3^+TCR\alpha\beta^+$ **P4**, which accounts for the CD4, CD8, DN and DP T cells. The rest of the $CD3^-TCR\alpha\beta^-$ population most likely includes the B lymphocytes - which may be confirmed with the addition of the B cell marker CD19 (Meeker et al., 1984).

This experiment showed that even with previously frozen cells, the protocol for PBMC isolation, overnight culture, surface staining and fixation enable high cell recovery. Replicating this experiment on PMA/ionomycin stimulated cells with the dead cell stain is the next step in order to observe the effects of stimulation and permeabilisation on cell viability. Furthermore, the dead cell marker will be useful in analysing the highly heterogeneous SVF, and confer robustness to the data.

3.4.3. Naïve and Memory T cells

CD45RA and CD45RO have conventionally been used to differentiate naïve from memory cells (Akbar et al., 1988). Following on the gating of live, $CD3^+TCR\alpha\beta^+$ cells, and gating on CD4 T cells, approximately 45% were $CD45RA^{+/hi}CD45RO^{lo}$ **P8** identifying the naïve subset (**Figure 14– B, row 1**), and 51% are $CD45RO^+CD45RA^{lo}$ **P9**, identifying the memory subset (**Figure 14– B, row 2**). Gating on naïve CD4 T cells **(P8)** was subjective as there was no distinct delineation between the CD45RA- and CD45RO-positive populations. Hence, the addition of other markers proved useful in ensuring accurate identity. $CD45RA^+$ naïve cells have been described as $CD27^+CCR7^+CD62L^{hi}$ (De Rosa et al., 2001; Sallusto et al., 1999),

and as seen in **Figure 14– B**, approximately 97% of the $CD45RA^+$ cells co-express the first two markers CD27 and CCR7 (**P10**), although $CD62L^{lo/hi}$ expression was varied or mixed. This confirms that a fraction of $CD45RA^+$ cells may not be true naïve cells and the use of additional naïve markers is invaluable if exact characterisation of naivety is desired. Additionally, CD31 expression was examined. More than half of the $CD45RA^+CCR7^+CD27^+CD62L^+$ were RTE - identifying a subset of 'greater' antigen naivety. The CD31-negative naïve lymphocytes, involved in maintaining homeostasis of the peripheral CD4 T cell population makes up the rest of the naïve CD4 T cells (**Figure 14– B**).

With regards to the memory subset of CD4 T cells **(P9)**, the use of CCR7 and CD27 enables the identification of two memory subsets **(Figure 14 – B, row 2)**: effector memory cells ($CD27^-CCR7^{lo}$) **P11** and central memory cells, defined by $CD27^+CCR7^+$ (Sallusto et al., 1999). However, while the effector memory T cells were easily identified by this gating, the results show that there are possibly two subpopulations of the central memory cells: $CD27^+CCR7^{hi}$ **P12**, and $CD27^+CCR7^{lo}$ **P13**. These subsets were then plotted for CD62L and CD31 expression, and it is evident that the effector memory subset is mostly $CD62L^{lo}CD31^-$. Moreover, over half of the central memory subset was $CD62L^{hi}CD31^-$ and a quarter of these central memory cells are $CD62L^{lo}CD31^+$. Lastly, **P13,** despite being $CD27^+CCR7^{lo}$, more closely resembles the effector memory subset with low CD31 expression and a mostly $CD62L^{lo}$ phenotype **(Figure 14 – B, row 2)**.

With respect to CD8 T cells, gating on $CD45RA^+$ cells (**P14**) was more clear-cut, with 14% of CD8 T cells being naïve (**Figure 14 – C**). However, naïve CD8 T cells are also described to be $CD27^+CCR7^+$ (Berard and Tough, 2002), and tight gating on these cells (**P16**) show that only 60% of the initial gating are bona fide naïve CD8 T cells. Interestingly, the tightly gated naïve population is mostly $CD31^+$, possibly indicating that these cells are all recent thymic emigrants, and thereby suggesting that no CD8 naïve T cells are maintained at detectable levels in the periphery. The CD8 memory T cell subsets **(P15) (Figure 14 – C, row 2)** show similar proportions as with the CD4 memory cells, although when characterised by CD62L and CD31 expression, the distributions are different. The effector memory cells defined by $CCR7^{lo}CD27^-$ (**P17**) have an almost equal distribution of $CD62L^+CD31^-$, $CD62L^+CD3^+$, $CD62L^-CD31^-$ and $CD62L^-CD31^+$ cells, while central memory cells $CCR7^{hi}CD27^+$ (**P18)** are mostly $CD62L^+$, although roughly half are either $CD31^+$ or $CD31^-$, and of the population (**P19**) that is $CD27^+CCR7^{lo}$, half are $CD31^+CD62L^-$, and a near equivalent distribution on the other three ($CD62L^+CD3^+$, $CD62L^-CD31^-$ and $CD62L^-CD31^+$). Hence taken together the expression of CD62L and CD31 are markedly different between the memory subsets of CD4 and CD8 T cells, possibly highlighting the diversity of actions that T cells are capable of.

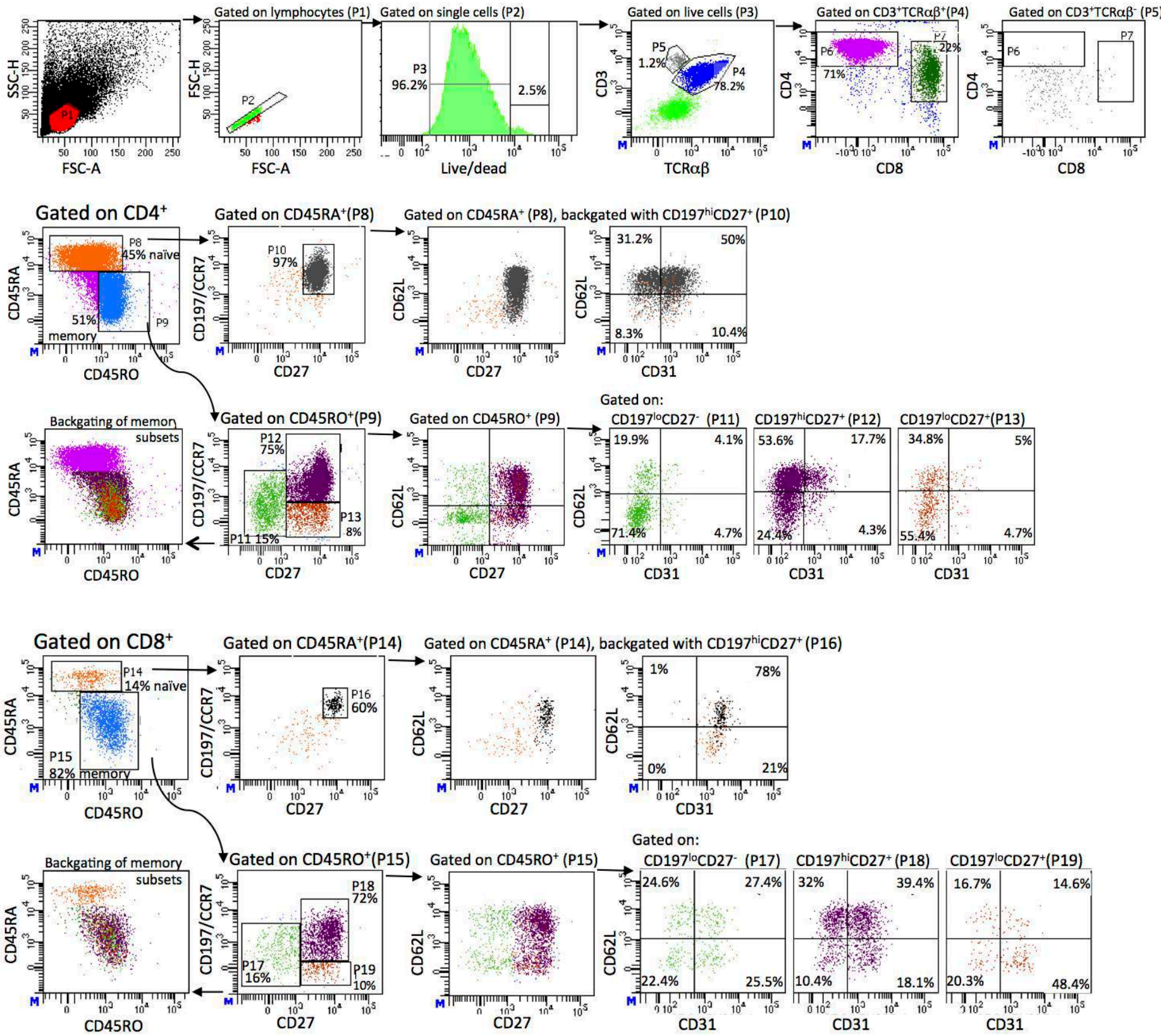

Figure 14. Naïve/memory staining panel incorporating the live/dead cell stain and TCRαβ on thawed, unstimulated, normal blood. **A)** Gating on lymphocytes P1, single cells P2, and live cells P3, $CD3^{+}TCR\alpha\beta$+ **P4** cells were distinguished from $CD3^{+}TCR\alpha\beta$- **P5** cells. P4 and P5 are then shown for CD4 and CD8 expression. Gating on **B)** $\mathbf{CD4^{+}}CD3^{+}TCR\alpha\beta^{+}$ T cells and **C)** $\mathbf{CD8^{+}}CD3^{+}TCR\alpha\beta^{+}$ T cells, naive and memory phenotypes were comprehensively characterized by the expression of surface markers CD45RA, CD45RO, CD197 (CCR7), CD27, CD62L and CD31.

4. Discussion

4.1 Protocol optimisation

4.1.1 Staining panel and controls

The staining panel designed for the identification of CD4 T cell subsets and the naïve and memory cell characterisation, included at most 12 colours. The excitation and emission spectra and the corresponding band pass filters of the fluorochromes are shown in **Appendix 1**. The dyes with the least spillover into other detectors were chosen, with the relatively brightest paired with intracellular markers (e.g. PE-IL-4, BV421-IFNγ), and the relatively dim dyes paired with highly expressed markers (e.g. APC-CD8, APC-Cy7-CD4, PerCP-CD3). The four transcription factors were detected with AF488, and although this is not necessarily a very bright fluorochrome, there is limited choice for commercially purchased antibodies to these transcription factors, and its use had to be weighed against the other available fluorophores for other surface and intracellular antigens being detected simultaneously.

Due to the complexity of the staining panel, control 'stains' were necessary to properly setup the flow cytometer during each run, especially with the inclusion of intracellular markers that may be expressed at low amounts and would otherwise prove difficult to interpret (Baumgarth and Roederer, 2000). A combination of IgG isotype-matched (for the transcription factors, IL-4 and TGFβ) and FMO controls (for IFNγ, IL-10) were included in antibody cocktails that contained the regular surface markers (CD3, CD4, CD8, etc.). An isotype control antibody has no specificity for the target cells, but retains the nonspecific characteristics of the staining antibody, thus confirming the specificity of the primary/real antibody binding. Used at the same concentration as the primary antibody, it can also show if proper washing has been done, as intracellular antibodies may stick and be trapped inside the cell (Baumgarth and Roederer, 2000).

Results from previous experiments with the BV421-conjugated antibodies (IFNγ and IL-10) indicated that the CD4 T cells stained highly positive with the BV421 antibodies, even with the IgG isotypes **(Figure 8– A)**. Although it was possible that the cells were insufficiently washed, staining with other intracellular markers showed no such issues (i.e. PE for IL-4 and TGFβ; **Figure 8– B**). This likely indicated that the problem was inherent to the BV421 dye or BV421-conjugated antibody. It is theoretically possible that non-specific staining (i.e. IgG1 binding) may have also occurred, although the cells were blocked with an anti-Fc receptor blocking antibody prior to staining. It is also possible that the voltage used for the BV421 channel was set too high in this particular experiment, or that compensation was incorrect, however this is unlikely due to the use of unstained and isotype control stained cells. Instead, the BV421 IgG1 isotype may be inherently 'sticky' and needed additional washing steps. Thus, in the following experiments, we decided to leave out the BV421 isotype control, and opting for a FMO control instead.

An FMO control contains all the fluorophores in the panel except for the one being measured, in order to detect the spillover of the other dyes into the channel of interest; this enables proper gate placement for the positive cells (Roederer, 2001). With using this control (for example, **Figure 10– Part II-V, IFNγ and IL-10 panels**), distinct populations of the

cytokine-positive cells were now properly detected. The possibility of the IFNγ antibody having a tendency to be 'sticky' and of being trapped inside the cells was not ruled out though, particularly for the patient blood where the cells shifted up the IFNγ axis and thus show very high amounts of IFNγ$^+$ cells **(Figure 11 – Part II and IV. B, IFNγ panels)**. Nonetheless, this might simply reflect the actual abundance of IFNγ–secreting T cells in blood. The high expression of T-bet$^+$ cells in both unstimulated and stimulated cells, and the low amounts of IFNγ detected in the unstimulated cells possibly confirm this hypothesis. Similarly, this shift was not detected in the normal blood that was analysed simultaneously (**Figure 10– Part II**).

The inclusion of single colour 'compensation controls' is also necessary in setting the LSRFortessa X-20 cytometer properly at the start of every run. Compensation controls are prepared by separately staining the same cells being investigated with each of the fluorophores in the panel (Table 1– C). The use of a single fluorochrome-conjugated antibody as a 'control dye' should stain brightly for the specific marker on the cells, to allow for accurate positive population identification (i.e. antibodies to CD4, CD8, CD45RO, CD45RA are ideal, but not for rare populations such as TCRγδ, [depending on the samples being examined] or intracellular cytokines etc. (Baumgarth and Roederer, 2000). This enables accurate (automatic) compensation calculation, wherein the spectral overlaps between two fluorochromes is algorithmically eliminated (Roederer, 2001). With the greater risk of artefacts brought by increasingly high number multi-colour staining panels, for example, spillover into another wavelength limited photomultiplier detector, reagent interactions, and compensation errors, having the necessary controls, namely: isotype, FMO/unstained, compensation, and unstimulated controls, are all vital in accurate data interpretation.

4.1.2 Lymphocyte gating

The differential light scattering of human leukocytes on the 488-nm wavelength laser (side scatter) and forward scatter is useful in identifying lymphocytes, monocytes and granulocytes, solely based on their natural or endogenous fluorescence and morphological differences (Loken et al., 1990; Salzman et al., 1975). Lymphocytes **P1** form a distinct cluster away from the origin of the two axes, which will contain small debris, platelets and dead cells, and to the right, the larger and more granular cells based on forward light scatter, which are likely to be monocytes, macrophages (for example, **Figure 1– A, SSC/FSC panel**) (Loken et al., 1990). Only these cells are expected to be mainly present in the blood samples that were analysed here, since the isolation of PBMCs by the Ficoll density gradient method mostly eliminates granulocytes and other polymorphonuclear cells (e.g. neutrophils and eosinophils) as well as erythrocytes (English and Andersen, 1974)**.**

Cell death, particularly by apoptosis, is characterised by cell shrinkage and membrane permeabilisation (Kerr et al., 1972), and have thus been found to interfere with flow cytometry analysis. Dead cells have a tendency for nonspecific uptake of antibodies and fluorophores, increased background autofluorescence, leakage of DNA fragments and intracellular proteins, all of which makes its exclusion necessary (Afanasyev et al., 1993; O'Brien and Bolton, 1995). Dead cell exclusion gating is commonly done by simply not

including the smallest events (dead cells sit near the origin of the two axes in a SSC/FSC plot) during P1 gating). Although dead cell exclusion is a suitable strategy, particularly in relatively homogenous samples such as PBMCs, the addition of a dead cell stain guarantees that only live cells have been analysed. In a trial run of the dead cell stain using frozen, unstimulated PBMCs from a healthy donor, ~96% cell viability was detected on the **P1** lymphocytes (**Figure 14 – A**), which is a frequency we expect in previous experiments, when a dead cell exclusion during **P1** gating was done, especially as all the blood analysed were freshly collected and never frozen. Nevertheless, adding a viability stain adds robustness to the assay, and improves data quality, especially when investigating permeabilised and stimulated cells, and, moreover, when examining extremely heterogeneous samples such as the SVF and other tissue-derived single cells suspensions (e.g. as produced by enzymatic digestion methods), including solid tumour tissues (O'Brien and Bolton, 1995).

Upon selection of the cell population of interest i.e. lymphocytes, a single-cell gate **P2** on a forward scatter plot (FSC-height and FSC-area) was done, which would eliminate doublets, since cell clumps will have a longer transit time through the laser beam, altering the area of the signal (Shapiro, 2005). This causes doublets and clumps to deviate from the single-cell population, which appears in a diagonal line in the plot due to proportional FSC height and area values (for example, **Figure 1– A, FSC-H/FSC-A panel**). Doublet discrimination also increases purity and reduces false double positives, which is vitally important especially in the context of studying lymphocytes, where rare double positive $CD4^+CD8^+$ blood T cells may be of interest - $CD4^+CD8^+$ lymphocytes are normally only present within the thymus (Nettenstrom et al., 2013; Shapiro, 2005). Hence, ensuring that analysis is performed on live, single/distinct cells, improves the quality of data, especially when detecting rare populations (e.g. cytokine-producing cells) using a high parameter multi-colour panel of surface and intracellular markers.

4.1.3 Cell permeabilisation

Most of the T cell subsets (e.g. Th1, Th2 and Th17) are characterised by the transcription factors and cytokines they express (Mosmann and Coffman, 1989; Szabo et al., 2000; Zheng and Flavell, 1997). Since these proteins are intracellular, cells need to be permeabilised to allow dyes such as fluorochrome-conjugated antibodies to bind with the protein of interest in the cytoplasm or nucleus (Sander et al., 1991). Two commercially available permeabilisation buffers (eBioscience permeabilisation buffer and BD Transcription Factor buffer) were compared to see if the cytokine and transcription factor detection differed between the two.

The different scatter profiles of the PBMCs between the two buffers likely reflect a variation in reagent compositions (**Figure 5 – compare A and B).** In cells treated with the eBioscience buffer (**A**), at a FSC voltage of 560, the lymphocyte population **P1** was distinct and easy to gate on. Since the cells were fixed first before permeabilisation using the saponin-containing eBioscience buffer, it is possible that less membrane disruption has occurred using this buffer. On the other hand, the FSC voltage during analysis of the cells treated with the BD buffers had to be increased to 670 in this experiment (**B**), since the lymphocytes were hard to distinguish. [The lymphocyte shift towards the left of the FSC axis is seen Figure 10 – Part I,

when FSC voltage was set at 570]. The BD Fix/Perm solution contains methanol in addition to saponin, which could have allowed greater membrane dissolution that had then altered the cell size and caused the cells to shift along the FSC axis.

Saponin, the main component of both permeabilisation buffers, solubilises membrane cholesterol, leaving pores on the membrane whilst retaining membrane structure integrity. This allows discrimination of cell types based on morphology (i.e. by forward and side scatter), while not affecting antigen membrane expression (Jacob et al., 1991). Saponin permeabilises both cytoplasmic and nuclear membranes, allowing stains/antibodies to penetrate the cytoplasm and through to the nucleus, and bind with DNA and other intranuclear antigens (Glauert et al., 1962). Other permeabilisation detergents include Triton X-100 and Tween-20, but these target subcellular membranes, are non-selective and may remove proteins simultaneously with the lipids, and thereby lead to false negative staining results (Jamur and Oliver, 2010). Organic solvents are also available for cell membrane permeabilisation, one of which is methanol, a component in the BD Fix/Perm buffer. Methanol dissolves membrane lipids, creating additional pores through which antibodies can pass through (Pollice et al., 1992). In addition, it can coagulate proteins, making it useful for fixing cells simultaneously to membrane permeabilisation (Jamur and Oliver, 2010).

Aside from the apparent altered cell morphology, the increased pore formation by saponin and methanol (BD buffer) likely has an effect on antibody binding efficiency. The greater capacity for permeability appeared to have allowed more antibodies to enter the cytoplasm and nucleoplasm, resulting to more cells staining positive for transcription factors and cytokines (specifically GATA3 and TGFβ), compared to the cells treated with the saponin-only (eBioscience) permeabilisation buffer (**Figure 6– A and B**). Since the same PBMC sample and an aliquot from the same antibody cocktail was used across the four tubes (unstimulated and stimulated cells on eBioscience and BD permeabilisation buffers), it is assumed that the combination of saponin and methanol in the BD buffer allowed greater access for intracellular staining reagents. For these reasons, the BD Transcription Factor buffer set was preferred in subsequent experiments. While the choice of buffer depends on availability and the needs of the experiment, it is still noteworthy to see that the permeabilisation buffer may influence the efficiency of antibody staining and is a factor to consider in intracellular staining.

4.1.4 T cell stimulation with PMA/ionomycin and anti-CD3/anti-CD28

In unstimulated CD4 or CD8 T cells, expression of some transcription factors and cytokines can already be detected (**for example, Figure 5 – A and B)**. However, to increase cytokine expression, cells have to be induced to produce cytokines, and this is achieved through the addition of gene expression stimulation agents (Jung et al., 1993). It is generally accepted that *ex vivo* cell stimulation drives cells formerly activated by physiological stimuli to express the transcription factors and cytokines they were producing *in vivo*. A commonly used method involves incubation with PMA and a calcium ionophore such as ionomycin (Jung et al., 1993). The addition of Brefeldin A is useful as it blocks the Golgi-mediated secretion systems and thus allows cytokines to accumulate within the cytoplasm - allowing for enhanced cytokine detection (Klausner et al., 1992).

The combination of PMA and ionomycin is a widely used polyclonal stimulus that induces T cell cytokine production as well as monocyte differentiation (Karlsson and Hassan-Zahraee, 2015; Kemp and Bruunsgaard, 2001; Pala et al., 2000; Rodríguez-Caballero et al., 2004; Tsuchiya et al., 1982). In T cells, PMA bypasses the TCR signalling complex and directly activates protein kinase C (PKC), which then targets transcription factors nuclear factor kappa-B (NF-κB) and activator protein 1 (AP-1) (Manger et al., 1987). Ionomycin activates Ca^{2+}/calmodulin-dependent signalling pathways by increasing cytoplasmic calcium (Chatila et al., 1989), activating the calcium-dependent phosphatase calcineurin, which then activates the transcription factor nuclear factor of activated T cells (NFAT) (Manger et al., 1987). Ionomycin works synergistically with PMA by also enhancing PKC activation (Chatila et al., 1989) (**Figure 15**). The activation of NF-κB, AP-1 and NFAT are vital in driving cellular responses such as gene-expression, cell proliferation and cytokine production, particularly in T cells were these transcription factors are abundant. (Berridge and Irvine, 1984)

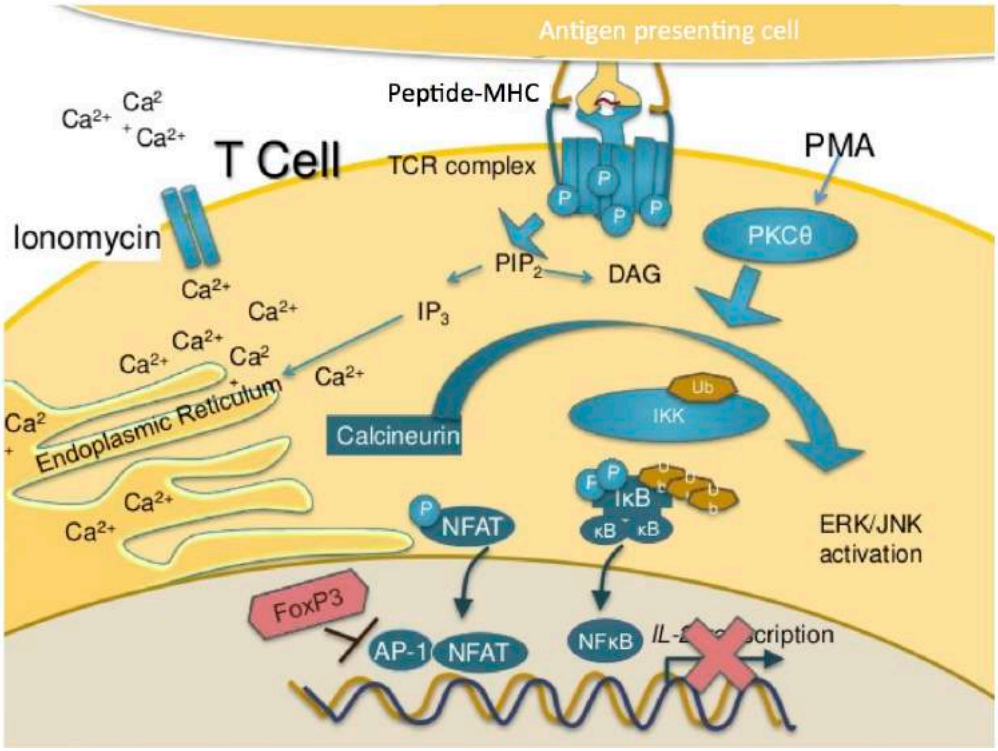

Figure 15. T cell stimulation by PMA/ionomycin or by TCR (CD3/CD28) activation. PMA/ionomycin bypasses TCR signalling to activate transcription factors AP-1, NFAT and NF-kB that control various cellular activities. Anti-CD3/anti-CD28 mimics TCR-MHC engagement type signalling. Shown here is an example of how FoxP3 can regulate cytokine gene expression (Manger et al., 1987).

Moreover, since PMA/ionomycin diffuses through the cell membrane and into the cytoplasm in an irreversible manner (Truneh et al., 1985), it may be toxic to cells at increasing concentrations and longer incubation times (Pala et al., 2000). However, since each cytokine's kinetics differ, the optimal concentration and incubation time depends on the cytokine(s) of interest. *Ex vivo* stimulation for 4-6 hours is adequate to drive most cytokine production, with

reported peak times of production as such: TNFα – 2 hours, with a rapid decline thereafter (Mascher et al., 1999), IL-4 4-to-6 hrs then declining (Baran et al., 2001; Pala et al., 2000) , IFNγ – between 4 to 8 hrs and sustained through to at least 48 hrs (Jung et al., 1993; Mascher et al., 1999; Pala et al., 2000), IL-17 - > 6 hrs (Olsen and Sollid, 2013) and IL-10 – >24 hours (Baran et al., 2001; Olsen and Sollid, 2013). Since each cytokine's expression kinetics varies greatly, setting the stimulus concentration and incubation time is dependent on the cytokine of interest and should be adjusted according to experimental needs. This may explain the low detection of IL-4, IL-17A and IL-10 in the experimental data, while IFNγ was detected in abundance. A longer incubation time with PMA/ionomycin may be implemented to see if cytokine detection is increased.

While PMA/ionomycin stimulation increases transcription factor and cytokine expression, it however adversely affects CD4 expression, evident in the loss of $CD4^{hi}$ cells and the formation of a broad $CD3^+CD8^-$ population with decreasing CD4 expression **(compare Figure 5 and 6, CD4/CD8 panels)**. In contrast, CD8 expression remains minimally affected, while a slight downregulation of CD3 expression was also evident. PMA is known to cause a transient phosphorylation of the CD4 cytoplasmic domain (Acres et al., 1986), by dissociating CD4 from its associated tyrosine protein kinase p56-lck, which aides TCR signalling, releasing CD4 and consequently inducing CD4 down-modulation by endocytosis (Pelchen-Matthews et al., 1993). PMA also directly increases the association of CD4 with endocytic coated pits and vesicles, thus increasing CD4 internalisation (Pelchen-Matthews et al., 1993). While there is some degree of CD8 phosphorylation, it is not readily modulated away from the cell surface compared to CD4 (Blue et al., 1987), making it a useful marker since gating for $CD4^+$ cells is therefore now ambiguous. It has been suggested that $CD3^+CD8^-$ gating may be used to deduce the $CD4^+$ population (Halvorsen et al., 2011; Kemp and Bruunsgaard, 2001; Li et al., 2013), however, double negative ($CD3^+CD4^-CD8^-$) populations need to be taken into consideration. This approach may also include the NKT cells, known to produce cytokines such as IL-17A, IFNγ, IL-4, IL-10 and IL-13 after PMA/ionomycin stimulation, which may therefore otherwise overestimate the number of true T cells producing these cytokines (Coquet et al., 2008; Godfrey et al., 2004) . The addition of an NK marker (CD56) can be beneficial, especially if there is a high amount of $CD3^+CD4^-CD8^-$ cells in the unstimulated control (Lanier et al., 1989). In fact, we have also included CD56 in our more extensive staining panel, but the data was not included as this study was limited to T cell subsets. Furthermore, in disease conditions associated with a significantly large DN T cell population, such as systemic lupus erythematosus, where these cells produce large amounts of inflammatory IL-17 and IFNγ that contributes to the pathogenesis of the disease (Crispin et al., 2008) alternative surface staining and/or different activating stimuli.

Activation by anti-CD3/anti-CD28 beads was tested to observe if this may be a suitable alternative for PMA/ionomycin stimulation (**Figure 7**). Anti-CD3/Anti-CD28 activation mimics the peptide presentation of APC to the TCR signalling complex (Reinherz et al., 1980; Tsoukas et al., 1985), inducing hydrolysis of phosphatidylinositol biphosphate (PIP_2) into (1) inositol triphosphate (IP3), which releases calcium from cytoplasmic stores that drives NFAT activation, and (2) diacylglycerol, which activates PKC to induce NF-κB and

AP-1 activation (Berridge and Irvine, 1984), thus activating T cell production of cytokines, among others (**Figure 15**).

The greatest advantage of CD3 or TCR activation over PMA/ionomycin stimulation is that it does not cause CD4 downregulation, as apparent in our data, thus permitting easy and accurate gating analysis of activated CD4 T cells as well as DN and NK T cells (**Figure 7, compare A and B**). With regards to intracellular staining, representative plots showing only $CD3^+CD4^+$ T cells are presented. Here, high expression of T-bet and FoxP3 was observed, and CD4 T cells produced detectable levels of IL-4 and IL-10, although TGFβ expression was undetected. While results of a single experiment using this stimulus do not give conclusive results, others have observed less cytokine (IL-17 and IFNγ) production compared to PMA/ionomycin stimulation (Olsen and Sollid, 2013; Pala et al., 2000; Rostaing et al., 1999). Only IL-10 was reportedly increased with CD3/CD28 activation (Olsen and Sollid, 2013), which makes this ideal for studies focusing on IL-10 expression, which is characteristic of regulatory T cells.

Another widely used stimulation agent is phytohaemagglutinin, which has been shown not to downregulate CD4, and it reportedly induces more production of IL-10 and TNFβ compared to PMA in cells stimulated for 48 hrs (Baran et al., 2001). Clearly, the choice of stimulating agent depends on the cytokines and specific cells of interest being studied; the PMA/ionomycin activation method was used in our experiments to accommodate simultaneous analysis of monocytes and other cells present within the adipose tissue SVF, i.e. cells which anti-CD3/anti-CD28 is not capable of activating.

4.2 T Cell identification by surface markers

4.2.1 Key T cell markers

With the appropriate gating set on single-cell, (live) lymphocytes based on light scatter, the next step is identifying the cells of interest using cell-specific markers. The gated lymphocytes **P1** will include the T cells and B cells. To distinguish between the two, an antibody to CD3 was added to the panel, which is a T cell co-receptor present in all T cells (Van Agthoven et al., 1981). T cells can be further categorised as: the MHC-restricted TCRαβ T cells, which are the $CD4^+$ and $CD8^+$ T cells (Cantor and Boyse, 1975; Reinherz et al., 1979, 1980), the MHC-unrestricted TCRγδ T cell (Bluestone et al., 1988), and natural killer T cells (MacDonald, 1995). The use of the CD4 and CD8 markers allows for parallel analysis on CD4 and CD8 T cell populations, the major cells involved in most cellular immune responses, as well as the isolation of rare DN or DP cells. In our investigations, of the $CD3^+$ T cells, approximately 68% were $CD4^+$, while ~20% were $CD8^+$, and 1-2% were double negative $CD4^-CD8^-$ and 1-2% were double positive $CD4^+CD8^+$, in resting or unstimulated cells. This ratio was similar across the blood samples from the healthy donors and LE patients **(Figures 10 and 11, Part I).**

CD56, an NK marker, is expressed on natural killer cells and NKT cells, which mediate MHC-unrestricted cytotoxicity (Lanier et al., 1989). This marker can be added to the staining panel to distinguish the NKT cells which will be $CD3^+CD56^+$, from NK cells ($CD3^-CD56^+$),

although a sub-population of $CD3^+CD8^+$ also co-express CD56, which possess cytolytic effector function (Pittet et al., 2000). In addition, the TCRαβ receptor recognises peptides presented in the MHC of antigen presenting cells, which then leads to T cell activation; it is expressed in all CD4 and CD8 T cells (Cantor and Boyse, 1975). A TCRαβ antibody can be added to improve separation between DN cells ($TCR\alpha\beta^+CD3^+CD4^-CD8^-$) and $TCR\gamma\delta^+$ T cells ($TCR\alpha\beta^-CD3^+CD4^-CD8^-$), or NKT cells which do not express a TCR ($TCR\alpha\beta^-CD3^+CD4^-CD8^-CD56^+$). We included the TCRαβ antibody in a separate staining panel (Table 1 – B), and the true DN cells were identified, with the rest of the $TCR\alpha\beta^-CD3^+$ cells in **P5** confirmed to be $CD4^-CD8^-$ (**Figure 14- A, CD4/CD8 panels**). As $TCR\gamma\delta^+$ T cells are more abundant in the skin and gut mucosa, this additional marker may prove useful when studying normal or diseased tissue samples from these sites (Bluestone et al., 1988).

Apart from lymphocyte populations are the larger mononuclear cells that will therefore have a greater forward scatter profile. These include monocytes, macrophages and also possibly dendritic cells, which are characterized by the expression of a combination of surface markers including, but not limited to, CD14, CD11c, CD11b and MHC-II, among others (Dzionek et al., 2000; Griffin et al., 1981; Murray and Wynn, 2011)

4.2.2 T cell subset surrogate markers

4.2.2.1 CD183 (CXCR3) and CD194 (CCR4) and its correlation with transcription factor expression in CD4 T cells

Chemokines are molecules that direct leukocyte recruitment processes. Their receptors are defined according to four structural motifs (C, CC, CXC, and CX3C) as dictated by the position of Cysteine tandems (reviewed in Zlotnik and Yoshie, 2000). Chemokine receptor expression was found to differ between Th1 and Th2 subsets, showing that cells migrate differentially in response to different chemokines (Murphy, 1994). CD183 (CXCR3) was found to be preferentially expressed by Th1 cells (Bonecchi et al., 1998; Thivierge et al., 2015), and CD194 (CCR4) by Th2 cells (Bonecchi et al., 1998). However, based on our results, in unstimulated cells, although most Th1 $T\text{-}bet^+$ cells co-expressed CD183, Treg $FoxP3^{hi}$ cells also co-express CD183. Of the Th2 $GATA3^+$ cells identified, these expressed CD194, with Treg $FoxP3^{hi}$ cells also co-expressing CD194. However, upon PMA/ionomycin stimulation, CD183 expression appeared to be lost, and less CD183 positive cells were detected. CD194 expression remained but was found in $T\text{-}bet^+$, $GATA3^+$ and $FoxP3^+$ cells.

CD183 is described to be mostly present in effector memory T cells, and its correlation with Th1 cells indicate that they play a role in cell homing and migration to Th1-driven sites of inflammation (Groom and Luster, 2011). However, they have also been found in small populations of IL-4-producing Th2 cells and IL-17-producing Th17 cells (Lim et al., 2008; Qin et al., 1998). CD194 is found in activated memory T cells, and is associated with Th2 effector cells, although it has also been found in Th17 and $FoxP3^+$ Tregs (Chen et al., 2010; Lim et al., 2008). Moreover, CD194 has also been found to be co-expressed with CD183 (Andrew et al., 2001; Issekutz et al., 2011). Hence, while there may be a preference for Th1 and Th2 cells to express CD183 and CD194, respectively, reports that other cell types also co-express these chemokine receptors indicate that these markers alone are insufficient to

identify or segregating pure populations of Th1 and Th2 cells. While the addition of other markers (CCR5 for Th1 and CCR3, CCR8 for Th2) may improve identification (Bonecchi et al., 1998), combinations of surface and intracellular markers may still be required for optimal T cell subset characterisation.

4.2.2.2 Precise identification of regulatory T cells

In preliminary experiments using the FoxP3 antibody, if gating was based on the matched isotype control, it was apparent that there was high expression of $FoxP3^{+}$ cells following activation of $CD3^{+}CD4^{+}$ cells, (**Figure 6, FoxP3 panels**). And although Tregs are relatively abundant in human blood, the high expression levels was thought to be unlikely, prompting us to add additional parameters to improve Treg identification. (Chen et al., 2003; Levings et al., 2001)

Prior to the availability of intracellular markers, Tregs were defined as CD4 T cells that highly express the IL-2 receptor-α, CD25 (Baecher-Allan et al., 2001; Levings et al., 2001). However, approximately 20% of T cells may also be $CD25^{+(lo)}$, thus requiring additional markers for bona fide Treg identification. CD127/ IL-7R was found to inversely correlate with FoxP3 expression (Liu et al., 2006; Seddiki et al., 2006), while high co-expression of CD120b, or TNFR2, also aids in identifying CD25+FoxP3+ regulatory CD4 T cells (Chen et al., 2010). Together, these surface markers are ideal for Treg identification in live cells, where fixation and permeabilisation in order to stain for FoxP3 is not useful.

Subsequent gating on $CD3^{+}CD4^{+}FoxP3^{hi}CD25^{hi}IL\text{-}7R^{lo}TNFR2^{hi}$ cells decreased the $FoxP3^{+}$ population from up to 50% to approximately 6% Tregs in unstimulated CD4 T cells **(Figure 9 – A**). Of note, PMA/ionomycin stimulation appeared to have caused TNFR2 downregulation, so the $FoxP3^{hi}CD25^{hi}IL\text{-}7R^{lo}$ population remains an optimal identification profile (**Figure 9 – B**). Backgating with these stringently defined populations allowed better gating of FoxP3 expression to identify bona fide Tregs, and was how the gates for the succeeding FoxP3 staining plots were set. The $FoxP3^{hi}$ cells also create a marginally distinct population that is separate from the rest of the CD4 $FoxP3^{-/lo}$ cells, giving confidence to the use of $FoxP3^{hi}$ expression to aid in identifying Tregs.

In the peripheral blood of a healthy donor, IL-10 production was not correlated with FoxP3 expression, while TGFβ expression, while vaguely positive, appeared to not be all produced by Tregs. Furthermore, it was challenging to set the gating for TGFβ even with the isotype control, since the positive cells are perhaps $TGF\beta^{lo}$. It is possible that there were still issues with either nonspecific binding or excessive antibody uptake, resulting to false positives. Washing and fluorochrome (PE) issues have been ruled out, as this is not seen in other staining panels. It is likely then that the combination of the antibody itself and permeabilisation protocol has contributed to this issue. Hence, it is probable that staining (and stimulation) for TGFβ may still need to be optimised. Nevertheless, while regulatory T cells characteristically produce IL-10 and/or TGFβ, these cytokines are not always directly required for Treg suppressive function (Levings et al., 2001; Suri-Payer and Cantor, 2001). Tregs can inhibit proliferation of other T cells by cell contact-dependent mechanisms that are

cytokine independent (Levings et al., 2001; Thornton and Shevach, 1998), and, indeed, suppression of diseases such as in autoimmune gastritis is IL-10 independent (Suri-Payer and Cantor, 2001). Also, Tregs can act by virtue of their high expression of CD25, sequestering IL-2 and removing it from being biologically available for non-Treg T cells, which require IL-2 for their viability and proliferation (**Figure 15**). Conversely, it has also been reported that FoxP3 is not a prerequisite for $CD4^+CD25^+IL\text{-}10^+$ regulatory T cells to functionally exhibit suppressive activity (Vieira et al., 2004). These factors indicate the value of using multiple markers in identifying the Treg subset, as varying Treg surface marker and transcription factor expression and cytokine production may influence the ability (or inability) to identify this CD4 T cell population.

4.3 Identifying T cell subsets in normal blood and in a pathology setting

With the experimental setup established, the optimised staining panel was applied to identify CD4 T cell subsets in peripheral blood from not only healthy donors but also LE patients, as well as for examination of the SVF from liposuction AT aspirates from the lymphoedema patient.

Th1 cells, characterized by T-bet (Szabo et al., 2000), and the secretion of IFNγ (Mosmann and Coffman, 1989), were identified in blood and SVF especially after stimulation **(Figures 10-12 – Part II).** The secretion of the proinflammatory cytokine IFNγ, as well as IL-2 and TNFβ, activates macrophages and CD8 T cells to combat intracellular pathogens (Zhu and Paul, 2010). The detection of abundant Th1 cells in normal and patient blood and SVF may thus signify a state of active and ongoing inflammation. Likewise, Th2 cells, which produce IL-4 (Mosmann and Coffman, 1989), IL-13 and express GATA3 (Zheng and Flavell, 1997), were detected in all samples after stimulation (**Figures 10-12 – Part III).** The presence of these Th2 cells may indicate that the inflammation is not limited only to Th1 cells, but that it likely also involved Th2 cells and/or Th2 cytokines.

Of particular interest is the small population of $T\text{-}bet^+$ cells co-expressing IL-4, traditionally a Th2 cytokine, and at least in SVF, $GATA3^+IFN\gamma^+$ cells **(Figures 10-12 – Part II, and Figure 12, part III)**. The plasticity of CD4 T cell lineages is possibly reflected by these results. Naïve T cells, together with IFNγ, IL-4, IL-12 signals, are able to simultaneously commit to Th1 and Th2 differentiation programs (Peine et al., 2013). Similarly, in certain situations, Th2 cells, with TCR stimulation, IFNγ, IL-4 and IL-12 signals and T-bet, can revert to a Th1/2 hybrid (Hegazy et al., 2010). The hybrid Th1/2 cells are notably described to stably express both $T\text{-}bet^+GATA3^+$, be maintained in memory cells, and secrete both Th1 and Th2 cytokines albeit at lower amounts. They may represent cells that are not fully or terminally committed to Th1 or Th2 differentiation. Likewise, the presence of these hybrid phenotype cells is suggested to be a potential reprogramming mechanism that permits unfavourably differentiated Th1 or Th2 cells to redefine themselves in different conditions (Hegazy et al., 2010); or that they are capable of exerting a self-limiting course or repose i.e. to moderate inflammation (Peine et al., 2013). Combining the staining antibodies for T-bet, GATA3, IFNγ and IL-4 in the current panel may prove useful in identifying these hybrid Th1/Th2 cells, especially in the context of disease states of patient samples investigated.

Th17 cells, characterized by the production of cytokines such as IL-17A, IL-17F, and the expression of RORγt (Ivanov et al., 2007) were also detected in all the samples **(Figures 10-12 – Part IV)**. These cells are involved in inflammation to eliminate certain extracellular bacteria, autoimmunity and allergic disorders (Zhu et al., 2010). In addition, RORγt+IL-17^{+}IFNγ^{+} cells have also been identified in the blood samples, a population previously reported in mice (Duhen et al., 2013). Also, despite the high number of IFNγ-producing cells in the adipose SFV, there did not appear to be high numbers of Th17 cells in this tissue in LE; thus, Th17 cells do not appear to be integral to inflammation in lymphoedema.

Lastly, regulatory T cells, characterised to express FoxP3^{hi} (Fontenot et al., 2003), were identified in all samples **(Figures 10-12 – Part V).** This demonstrates the presence of Tregs, that in blood correspond to normal reported levels (~10% of CD4 T cells) (Chen et al., 2010; Levings et al., 2001), are constitutively present in controlling immune responses. Of interest is the observation that the percentage of FoxP3^{+} cells are relatively conserved after PMA/ionomycin stimulation, and that their production of cytokines IL-10 and TGFβ was not increased. This may indicate that Tregs require different stimuli to be activated, and this idea is supported by observations that PHA and anti-CD3/anti-CD28 activation induces more cytokine production by Tregs (Baran et al., 2001; Olsen and Sollid, 2013).

Ultimately, the designed staining panel can only detect a single transcription factors at once; combining them might aid in the further characterisation of nonconventional co-expressing cells such as Th1/2 hybrids (T-bet^{+}GATA3^{+}IL-4^{+}IFNγ^{+}) and RORγt^{+}IL-17^{+}IFNγ^{+} cells, and other T cells described but not identified here such as T-bet^{+}FoxP3^{+} cells (McPherson et al., 2015), FoxP3^{+}RORγt^{+}IL-17^{+} cells (which may have a link to glomerulonephritis) (Kluger et al., 2015; Voo et al., 2009), FoxP3^{+}IFNγ^{+} (which are in increased levels in patients with Type 1 diabetes) (McClymont et al., 2011).

With regards to CD8 T cell subsets, these cells are characterised according to cytokine secretion and not with the same transcription factors as used to identify CD4 T cell subsets. Analogous to Th1, Th2 and Th17 cells, Type 1 CD8 Tc1 cells produce IFNγ, Tc2 produce IL-4, and Tc17 produce IL-17 and some IFNγ, all to exert the cytotoxic effects CD8 T cells are defined by (Kondo et al., 2009; Mosmann et al., 1997). In the samples investigated in this study, we can conclude that Tc1 and Tc2 were detected, as well as IL-13 and IL-10-producing CD8 T cells, but no Tc17 were identified. As for the transcription factors, T-bet was highly expressed, and this was expected as it is a master regulator for CD8 T cell differentiation (Intlekofer et al., 2005), with at least half of these CD8 T-bet^{+} cells appearing to secrete IFNγ as well. GATA3, expressed at low levels, is believed to facilitate homeostasis and activation of CD8 T cells, as well as required for optimal IL-4 production in Tc2 cells (Tai et al., 2013). RORγt appeared to not be present in CD8 T cells. Lastly, CD8^{+}FoxP3^{+} cells were also identified, although the transcription factor function is generally unknown in CD8 lineage cell types.

4.3.1 Potential relevance to lymphoedema

Lymphoedema is a chronic condition in which there is an excessive build up of interstitial fluid in tissues, causing abnormal swelling (reviewed in Szuba and Rockson, 1998). Acquired or secondary lymphoedema is estimated to occur in ~50% of breast cancer patients, when treatment involves axillary surgery to remove lymph nodes, and the lymphatic system is affected (DiSipio et al., 2013). If left untreated, chronic LE promotes lipogenesis and accumulation of subcutaneous adipose tissue AT, leading to increased fibrogenesis and connective tissue overgrowth (Szuba and Rockson, 1998)s. Currently, little is known about AT development in lymphoedema.

The SVF of adipose tissue is known to contain various immune cells such as macrophages and T cells (Riordan et al., 2009). Thus, in conjunction with identifying T cell subsets in blood, we have analysed the SVF from liposuction AT aspirate samples collected from lymphoedema patients who have undergone liposuction surgery to remove the excess tissue. One notable result from this analysis was the observation that even in unstimulated SVF, CD4 expression already appears slightly downregulated, unlike in unstimulated blood that was $CD4^{hi}$ (compare **Figure 10 and 12 – A, Part I)**. This may be due to the collagenase treatment (cell extraction procedure). Alternatively, it is also possible that the CD4 lymphocytes present in the adipose SVF are already in an activated state, and this is supported by the observation that T-bet and FoxP3 expression in CD4 T cells is relatively the same even before PMA/ionomycin stimulation, and IFNγ, TGFβ (and relatively low IL-10) production are already detectable, i.e. even in unstimulated $CD4^+$ (and $CD8^+$ cells). This may reflect the chronic inflammation state described in lymphoedema (Szuba and Rockson, 1998), and is supported here by high numbers of IFNγ-producing cells. Furthermore, Tregs in the SFV appear to be constitutively producing IL-10, and particularly TGFβ. TGFβ is a regulatory cytokine that maintains peripheral tolerance; it is also an inflammatory cytokine, driving further production of IL-17 and IFNγ by certain cells (Wan and Flavell, 2009). Thus, the increased levels of TGFβ, especially in the unstimulated cells, may indicate that perhaps these cells are constantly activated, ameliorating the ongoing chronic inflammation associated with adipose tissue deposition in lymphoedema (Brestoff et al., 2015). Whether suppressive or inflammatory, the constitutive presence of adipose tissue TGFβ is likely to be linked to the development and increasing fibrotic nature of the tissue pathology - a hallmark of chronic advanced lymphoedema (Szuba and Rockson, 1998).

With the myriad of mononuclear cell types, such as monocytes/macrophages, fibroblasts, mesenchymal stem cells and lymphocytes contained in SVF, (Riordan et al., 2009) and the low frequency of T cell populations we have identified in these experiments, future patient samples will be required to substantiate this hypothesis and to ensure robustness of data. It would also be ideal if patient blood and SVF can be optimally investigated at the same time. Currently, the T cell subset staining in SVF has yielded varying results, given the low initial amount of T cells ($CD3^+$ cells) collected during flow cytometry analysis. Still, it is remarkable to see that in spite of the highly heterogeneous tissue sample, and the stringent gating on lymphocytes, single-cells, and CD3, CD4 and CD8 expression, intracellular staining for transcription factors and cytokine expression using the staining protocol has been possible.

With time we hope to generate enough data that will expand the current knowledge on pathological mechanism that are active in cancer related lymphoedema.

4.4 Naïve and memory T cells

Naïve and memory CD4 T cells have traditionally been characterised by the expression of $CD45RA^+$ or $CD45RO^+$ markers (Akbar et al., 1988). However, it has been described that naïve $CD45RA^+$ T cells can express functional activities upon activation, and that CD45RA may be re-expressed by 'previously activated' memory T cells (De Rosa et al., 2001). Consequently, there is a need for the inclusion of additional markers to correctly distinguish naïve from memory cells. Currently, only CD62L, CCR7 (CD197) and CD27 are normally included in the T cell phenotype subset staining panel. Thus, a more comprehensive staining panel for naïve and memory T cell characterisation was designed that incorporated antibodies for CD45RA, CD45RO and CD31 (Table 1 – B). This improves our capacity to profile T cells, particularly for the activated, transcription factor-positive and cytokine-secreting cells.

Naïve T cells travel to secondary lymphoid organs in search of antigens presented by antigen presenting cells. Upon activation, they proliferate and differentiate into effector memory cells that home to sites where they are needed. CCR7 is a chemokine receptor that mediates migration to secondary lymphoid organs (Förster et al., 1999), and although expressed in naïve T cells, it also distinguishes between two memory T cell subsets: (1) effector memory ($CD45RO^+CCR7^-$) cells that exhibit immediate effector function upon migration to inflammation sites; and (2) central memory ($CD45RO^+CCR7^+$) cells that lack immediate function, but display lymph node homing receptors and can stimulate dendritic cells and convert to a $CCR7^{lo/-}$ phenotype following secondary stimulation (Sallusto et al., 1999). The CD62L (L-selectin) receptor aids in recirculation of T cells between blood and lymph nodes by binding to ligands in endothelial cells, inducing signals to permit entry of the T cell into secondary lymphoid organs (Hengel et al., 2003). Like CCR7, it is also expressed in naïve T cells and central memory ($CCR7^+$) cells, allowing these cells to enter secondary lymphoid organs where they may be activated by APCs (Hengel et al., 2003). CD27 is a costimulatory receptor belonging to the TNF-Receptor superfamily of molecules, and is expressed on naïve CD4 T cells, whose ligand binding aids cell activation upon antigen stimulation. Its loss marks the activation of the T cell into an effector phenotype (Kobata et al., 1994; Morimoto and Schlossman, 1993). Also, as mentioned, CD31 is a surface marker for recent thymic emigrants in naïve CD4 T cells and its loss indicates peripheral expansion and therefore homeostatic expansion and/or antigen experience (Kimmig, 2002).

In the CD4 T cell panel, naïve T cells are first identified (**Figure 14– B**) by one marker (CD45RA, **P8**), but this is somewhat subjective due to the lack of a distinct boundary from $CD45RO^+$ memory cells (**P9**) and $CD45RO^-$ naïve cells. In fact, by gating on CD27 and CCR7, **(P10)** only 97% of the $CD45RA^+$ T cells originally identified were truly naïve. Although this may seem like a high percentage, it may still have significant implications for functional studies that require absolutely pure naïve T cell populations. Furthermore, when assessed on CD62L and CD31 expression, it is evident that more than half are recent thymic

emigrants, indicating active thymic output i.e. of newly produced naïve T cells with broad TCR specificities (Kimmig, 2002).

Populations of effector memory (**P11**) and central memory (**P12**) T cells can be identified by expression of CCR7 and CD62L. The expression of CD31 on memory cells was unexpected though, although it is apparent that effector memory cells are mostly $CD31^{negative}$, and it was the central memory cells that are $CD31^{+}$. Maintaining CD31 on central memory cells may imply a role in aiding re-activation of lymphocytes and/or in mediating the recruitment of immune cells to inflammatory sites (Marelli-Berg et al., 2013).

In the CD8 T cells (**Figure 14– C**) tight gating on CD45RA+$CD27^{+}CCR7^{+}$ (**P16**) revealed that only 60% of the initially identified $CD45RA^{+}$ **P14** cells are truly naïve. Interestingly, these cells are most, if not all, $CD31^{+}$, possibly indicating that naïve CD8 T cells do not undergo peripheral expansion, and are continuously released by the thymus. However, the correlation between CD31 and RTE in CD8 T cells is seen only in healthy individuals and not in patients with HIV; thus, CD31 may not be a reliable marker for identifying recent thymic emigrants in certain disease states like HIV (Tanaskovic et al., 2010) or potentially other chronic or persistent virus infections. The memory subsets in CD8 T cells have been similarly identified and characterised by the use of multiple markers (Tomiyama et al., 2002), suggesting the various modes of actions these cytotoxic T cells are capable of.

Finally, the transcription factor positive cells from the experiment investigating the normal blood are shown in CCR7 (CD197)/CD27 and CD27/CD62L plots **(CD4 T cells in Appendix 2, CD8 T cells in Appendix 3)**. These cells are mostly $CD62L^{+}$, $CD27^{hi}$, $CCR7^{hi/lo}$ and with the assumption that these transcription factor-positive cells signify an activated state (i.e. $CD45RO^{+}$), it is noticeable that majority of CD4 T cells are in the central memory subset, and the T-bet^{hi} population highlighted in orange (gating not shown), are mostly $CD27^{-}$ and thus of an effector memory phenotype. Upon PMA/ionomycin stimulation, the most noticeable result is the downregulation of CD62L, a phenomenon that was expected, as it is known to be caused by an L-selectin sheddase induced by PMA (Preece et al., 1996).

4.5 Future direction

One of the original aims of this project involved sorting on the $CD31^{+}$ and $CD31^{-}$ cells defined by $CD3^{+}CD4^{+}CD45RA^{+}CCR7^{+}CD27^{+}CD62L^{+}$, analysing the DNA for the TREC content, and finally having the TCR sequenced to determine the clonality of each subpopulation. However, the staining panel we have established was designed for use on our 4-laser LSRFortessa X-20 analytical cytometer, and it appears that the UV-excitable BUV395 and BUV737 fluorochromes are not capable of being detected on Influx sorters – even those with UV 355 nm excitation lasers. The reasons for this are currently unclear and being actively investigated by Becton Dickinson technicians. Interestingly, it is worth considering that the influx is a jet-in-air–based cell sorter, and fluorescence under these conditions appears to be quite different when in a liquid environment as per quartz cuvette flow cells. Unfortunately, without availability of cell sorters able to detect these fluorochromes, we either have to purchase new antibody and re-design the staining panel, or wait until this issue is

resolved by Becton Dickinson. The next steps of this project are therefore currently unavoidably delayed.

Since naïve CD4 T cells are classically defined to be antigen-inexperienced, they are expected to possess a highly diverse TCR repertoire, having not undergone clonal selection that occurs upon antigen activation (Calis and Rosenberg, 2014). However, this definition was challenged, when naïve T cells in mice studies were shown to actually require continuous contact with self-MHC molecules (Takeda et al., 1996), and that the lack of MHC contact affected the survival of the naïve T cell (Kirberg et al., 1997; Rooke et al., 1997; Viret et al., 1999). It was then found that recognition of positively selecting self-peptides is necessary to stimulate homeostatic proliferation (Ernst et al., 1999; Moses et al., 2003; Viret et al., 1999). This post-thymic positive selection of the TCR repertoire occurs in order to optimise the antigen recognition capacity of peripheral naïve T cells, which encourages efficient response upon foreign antigen activation (Ernst et al., 1999; Stefanová et al., 2002). By this definition, peripherally expanded 'naïve' T cells will have already experienced TCR engagement and possess skewed TCR repertoires, confounding the original definition of an 'antigen-inexperienced' naïve T cell.

Thus, CD31 was added to the panel to differentiate between the two subsets of naïve CD4 T cells. The value of distinguishing RTE is in its potential significance in health and diseases. A broad TCR repertoire, which is conferred by $CD31^+$ recent thymic emigrants, is required for robust antigen recognition. Knowledge of the naive TCR profile may shed light on developing enhanced vaccines especially for populations with reduced vaccine response such as the elderly (Naylor et al., 2005). It may also expand the knowledge on conditions where the lack of available naïve antigen-specific T cells/ skewed TCR repertoires renders a deficient immune response (Funauchi et al., 1995). Conversely, peripheral expansion of naïve T cells ($CD31^-$) can be investigated. Lymphoepenia, the loss of T cells, induces strong homeostatic proliferation to compensate for the cells lost (Tanchot et al., 1997). It is also a condition linked to autoimmunity, whereby auto-reactive naïve T cells are accumulated due to peripheral proliferation (King et al., 2004), as observed in diseases such as multiple sclerosis, where homeostatic abnormalities have been observed in the peripheral naïve T cells but not in the thymic emigrants (Duszczyszyn et al., 2006)

Finally, TREC analysis would have further confirmed CD31 expression, and TCR sequencing would have confirmed the extent of clonality of each population, since there is a discrepancy among studies that used CDR3 spectratyping to determine if $CD31^+$ cells are indeed more polyclonal compared to $CD31^-$ that have a more restricted clonotype repertoire due to a selection process during proliferation (Kilpatrick et al., 2008; Kohler et al., 2005). Currently, no studies have yet reported on using the more accurate method of TCR sequencing to confirm clonality of recent thymic emigrants and peripherally expanded naïve T cells, but the protocols established in this research have the exciting capacity to accomplish this once the cell sorting issues are resolved in the near future.

5. Acknowledgements

First and foremost, the utmost gratitude to my supervisor Dr Lisa Sedger, who has made this year possible. Thank you for your relentless enthusiasm, patience and encouragement. It has been a crazy ride, considering I started the year not knowing what a flow cytometer was! You have been an inspiration in rekindling my love for science and research.

To my co-supervisor Dr Seray Adams, and Dr Benjamin Heng, my sincere thanks for your advice and assistance in the lab, and for teaching me tricks that made things run a tad easier.
To Andrew Lim (BD) and Christopher Brownlee (UNSW), thank you for the technical advice in the flow cytometry analysis and cell sorting.

And to my family, whose unending encouragement and support kept me sane (and fed) during my sleepless nights. This is the fourth one, and I promise the fifth will be the last!

We also thank Macquarie University for the financial support. This project was supported by the Macquarie University Grand Cancer Research grant (awarded to my supervisor LS), and by two Macquarie University Research and Development grants (awarded to LS, and also to BH and Prof Gilles Guillemin)

6. References

Acres, R. B., Conlon, P. J., Mochizuki, D. Y., and Gallis, B. (1986). Rapid phosphorylation and modulation of the T4 antigen on cloned helper T cells induced by phorbol myristate acetate or antigen. *J. Biol. Chem.* 261, 16210–4.

Afanasyev, V. N., Korol, B. A., Matylevich, N. P., Pechatnikov, V. A., and Umansky, S. R. (1993). The use of flow cytometry for the investigation of cell death. *Cytometry* 14, 603– 9.

Van Agthoven, A., Terhorst, C., Reinherz, E., and Schlossman, S. (1981). Characterization of T cell surface glycoproteins T 1 and T 3 present on all human peripheral T lymphocytes and functionally mature thymocytes. *Eur. J. Immunol.* 11, 18–21.

Akbar, A. N., Terry, L., Timms, A., Beverley, P. C., and Janossy, G. (1988). Loss of CD45R and gain of UCHL1 reactivity is a feature of primed T cells. *J. Immunol.* 140, 2171–8.

Andrew, D. P., Ruffing, N., Kim, C. H., Miao, W., Heath, H., Li, Y., et al. (2001). C-C chemokine receptor 4 expression defines a major subset of circulating nonintestinal memory T cells of both Th1 and Th2 potential. *J. Immunol.* 166, 103–11.

Annunziato, F., and Romagnani, S. (2009). Heterogeneity of human effector CD4(+)T cells. *Arthritis Res. Ther.* 11, 257.

Appay, V., van Lier, R. A. W., Sallusto, F., and Roederer, M. (2008). Phenotype and function of human T lymphocyte subsets: consensus and issues. *Cytometry. A* 73, 975–83.

Baecher-Allan, C., Brown, J. A., Freeman, G. J., and Hafler, D. A. (2001). CD4+CD25high regulatory cells in human peripheral blood. *J. Immunol.* 167, 1245–1253.

Baecher-Allan, C., Wolf, E., and Hafler, D. A. (2005). Functional analysis of highly defined, FACS-isolated populations of human regulatory CD4+ CD25+ T cells. *Clin. Immunol.* 115, 10–8.

Bailey, S. R., Nelson, M. H., Himes, R. A., Li, Z., Mehrotra, S., and Paulos, C. M. (2014). Th17 cells in cancer: the ultimate identity crisis. *Front. Immunol.* 5.

Baran, J., Kowalczyk, D., Ozóg, M., and Zembala, M. (2001). Three-color flow cytometry detection of intracellular cytokines in peripheral blood mononuclear cells: comparative analysis of phorbol myristate acetate-ionomycin and phytohemagglutinin stimulation. *Clin. Diagn. Lab. Immunol.* 8, 303–13. doi:10.1128/CDLI.8.2.303-313.2001.

Baumgarth, N., and Roederer, M. (2000). A practical approach to multicolor flow cytometry for immunophenotyping. *J. Immunol. Methods* 243, 77–97.

Beck, R. C., Stahl, S., O'Keefe, C. L., Maciejewski, J. P., Theil, K. S., and Hsi, E. D. (2003). Detection of mature T-cell leukemias by flow cytometry using anti–T-cell receptor Vβantibodies. *Am. J. Clin. Pathol.* 120, 785–794.

Bendelac, A., Savage, P. B., and Teyton, L. (2007). The biology of NKT cells. *Annu. Rev. Immunol.* 25, 297–336.

Berard, M., and Tough, D. F. (2002). Qualitative differences between naïve and memory T cells. *Immunology* 106, 127–38.

Berridge, M. J., and Irvine, R. F. (1984). Inositol trisphosphate, a novel second messenger in cellular signal transduction. *Nature* 312, 315–321.

Blue, M. L., Hafler, D. A., Craig, K. A., Levine, H., and Schlossman, S. F. (1987). Phosphorylation of CD4 and CD8 molecules following T cell triggering. *J. Immunol.* 139 , 3949–3954.

Bluestone, J. A., Cron, R. Q., Cotterman, M., Houlden, B. A., and Matis, L. A. (1988). Structure and specificity of T cell receptor gamma/delta on major histocompatibility complex antigen-specific CD3+, CD4-, CD8- T lymphocytes. *J. Exp. Med.* 168, 1899– 916.

Bonecchi, R., Bianchi, G., Bordignon, P. P., D'Ambrosio, D., Lang, R., Borsatti, A., et al. (1998). Differential expression of chemokine receptors and chemotactic responsiveness of type 1 T helper cells (Th1s) and Th2s. *J. Exp. Med.* 187, 129–34.

Brestoff, J. R., Kim, B. S., Saenz, S. A., Stine, R. R., Monticelli, L. A., Sonnenberg, G. F., et al. (2015). Group 2 innate lymphoid cells promote beiging of white adipose tissue and limit obesity. *Nature* 519, 242–6. doi:10.1038/nature14115.

Britanova, O. V, Putintseva, E. V, Shugay, M., Merzlyak, E. M., Turchaninova, M. A., Staroverov, D. B., et al. (2014). Age-Related Decrease in TCR repertoire diversity measured with deep and normalized sequence profiling. *J. Immunol.* 192, 2689–2698.

Brusko, T. M., Putnam, A. L., and Bluestone, J. A. (2008). Human regulatory T cells: role in autoimmune disease and therapeutic opportunities. *Immunol. Rev.* 223, 371–90.

Calis, J. J. A., and Rosenberg, B. R. (2014). Characterizing immune repertoires by high throughput sequencing: strategies and applications. *Trends Immunol.* 35, 581–590.

Campbell, J. J., Murphy, K. E., Kunkel, E. J., Brightling, C. E., Soler, D., Shen, Z., et al. (2001). CCR7 Expression and Memory T Cell Diversity in Humans. *J. Immunol.* 166, 877–884.

Cantor, H., and Boyse, E. A. (1975). Functional subclasses of T-lymphocytes bearing different Ly antigens. I. The generation of functionally distinct T-cell subclasses is a differentiative process independent of antigen. *J. Exp. Med.* 141, 1376–89.

Chatila, T., Silverman, L., Miller, R., and Geha, R. (1989). Mechanisms of T cell activation by the calcium ionophore ionomycin. *J. Immunol.* 143, 1283–9.

Chen, W., Jin, W., Hardegen, N., Lei, K., Li, L., Marinos, N., et al. (2003). Conversion ofperipheral CD4+CD25− naive T cells to CD4+CD25+ regulatory T cells by TGF-β induction of transcription factor Foxp3. *J. Exp. Med.* 198, 1875–1886.

Chen, X., Subleski, J. J., Hamano, R., Howard, O. M. Z., Wiltrout, R. H., and Oppenheim, J. J. (2010). Co-expression of TNFR2 and CD25 identifies more of the functional CD4+FOXP3+ regulatory T cells in human peripheral blood. *Eur. J. Immunol.* 40, 1099– 106.

Connors, M., Kovacs, J. A., Krevat, S., Gea-Banacloche, J. C., Sneller, M. C., Flanigan, M., et al. (1997). HIV infection induces changes in CD4+ T-cell phenotype and depletions within the CD4+ T-cell repertoire that are not immediately restored by antiviral or immune-based therapies. *Nat. Med.* 3, 533–540.

Coquet, J. M., Chakravarti, S., Kyparissoudis, K., McNab, F. W., Pitt, L. A., McKenzie, B. S., et al. (2008). Diverse cytokine production by NKT cell subsets and identification of an IL-17-producing CD4-NK1.1- NKT cell population. *Proc. Natl. Acad. Sci. U. S. A.* 105, 11287–92.

Crispin, J. C., Oukka, M., Bayliss, G., Cohen, R. A., Van Beek, C. A., Stillman, I. E., et al. (2008). Expanded double negative T cells in patients with systemic supus erythematosus produce IL-17 and infiltrate the kidneys. *J. Immunol.* 181, 8761–8766.

DiSipio, T., Rye, S., Newman, B., and Hayes, S. (2013). Incidence of unilateral arm lymphoedema after breast cancer: a systematic review and meta-analysis. *Lancet. Oncol.* 14, 500–15.

Douek, D. C., McFarland, R. D., Keiser, P. H., Gage, E. A., Massey, J. M., Haynes, B. F., et al. (1998). Changes in thymic function with age and during the treatment of HIV infection. *Nature* 396, 690–5.

Duhen, R., Glatigny, S., Arbelaez, C. A., Blair, T. C., Oukka, M., and Bettelli, E. (2013). Cutting edge: the pathogenicity of IFN-γ-producing Th17 cells is independent of T-bet. *J. Immunol.* 190, 4478–82.

Duszczyszyn, D. A., Beck, J. D., Antel, J., Bar-Or, A., Lapierre, Y., Gadag, V., et al. (2006). Altered naive CD4 and CD8 T cell homeostasis in patients with relapsing-remitting multiple sclerosis: thymic versus peripheral (non-thymic) mechanisms. *Clin. Exp. Immunol.* 143, 305–313.

Dzionek, A., Fuchs, A., Schmidt, P., Cremer, S., Zysk, M., Miltenyi, S., et al. (2000). BDCA- 2, BDCA-3, and BDCA-4: Three markers for distinct subsets of dendritic cells in human peripheral blood. *J. Immunol.* 165, 6037–6046.

English, D., and Andersen, B. R. (1974). Single-step separation of red blood cells, granulocytes and mononuclear leukocytes on discontinuous density gradients of Ficoll- Hypaque. *J. Immunol. Methods* 5, 249–252.

Ernst, B., Lee, D.-S., Chang, J. M., Sprent, J., and Surh, C. D. (1999). The Peptide Ligands Mediating Positive Selection in the Thymus Control T Cell Survival and Homeostatic Proliferation in the Periphery. *Immunity* 11, 173–181.

Fallen, P. R., Duarte, R. F., McGreavey, L., Potter, M., Ethell, M., Prentice, H. G., et al. (2003). Identification of non-naïve CD4+CD45RA+ T cell subsets in adult allogeneic haematopoietic cell transplant recipients. *Bone Marrow Transplant.* 32, 609–16.

Feuerer, M., Herrero, L., Cipolletta, D., Naaz, A., Wong, J., Nayer, A., et al. (2009). Lean, but not obese, fat is enriched for a unique population of regulatory T cells that affect metabolic parameters. *Nat. Med.* 15, 930–9.

Fontenot, J. D., Gavin, M. A., and Rudensky, A. Y. (2003). Foxp3 programs the development and function of CD4+CD25+ regulatory T cells. *Nat. Immunol.* 4, 330–6.

Förster, R., Schubel, A., Breitfeld, D., Kremmer, E., Renner-Müller, I., Wolf, E., et al. (1999). CCR7 coordinates the primary immune response by establishing functional microenvironments in secondary lymphoid organs. *Cell* 99, 23–33.

Funauchi, M., Farrant, J., Moreno, C., and Webster, A. D. (1995). Defects in antigen-driven lymphocyte responses in common variable immunodeficiency (CVID) are due to a reduction in the number of antigen-specific CD4+ T cells. *Clin. Exp. Immunol.* 101, 82– 8.

Glauert, A. M., Dingle, J. T., and Lucy, J. A. (1962). Action of saponin on biological Cell Membranes. *Nature* 196, 953–955.

Godfrey, D. I., MacDonald, H. R., Kronenberg, M., Smyth, M. J., and Kaer, L. Van (2004). Opinion: NKT cells: what's in a name? *Nat. Rev. Immunol.* 4, 231–237.

Grant, C. R., Liberal, R., Mieli-Vergani, G., Vergani, D., and Longhi, M. S. (2015). Regulatory T-cells in autoimmune diseases: challenges, controversies and--yet-- unanswered questions. *Autoimmun. Rev.* 14, 105–16.

Griffin, J. D., Ritz, J., Nadler, L. M., and Schlossman, S. F. (1981). Expression of myeloid differentiation antigens on normal and malignant myeloid cells. *J. Clin. Invest.* 68, 932– 41.

Groom, J. R., and Luster, A. D. (2011). CXCR3 ligands: redundant, collaborative and antagonistic functions. *Immunol. Cell Biol.* 89, 207–215.

Halvorsen, E. H., Strønen, E., Hammer, H. B., Goll, G. L., Sollid, L. M., and Molberg, Ø. (2011). Interleukin-15 induces interleukin-17 production by synovial T cell lines from patients with rheumatoid arthritis. *Scand. J. Immunol.* 73, 243–249.

Harding, C. V, and Unanue, E. R. (1990). Quantitation of antigen-presenting cell MHC class II/peptide complexes necessary for T-cell stimulation. *Nature* 346, 574–6.

Hegazy, A. N., Peine, M., Helmstetter, C., Panse, I., Fröhlich, A., Bergthaler, A., et al. (2010). Interferons direct Th2 cell reprogramming to generate a stable GATA-3(+)T- bet(+) cell subset with combined Th2 and Th1 cell functions. *Immunity* 32, 116–28.

Van Heijst, J., Ceberio, I., Lipuma, L. B., Samilo, D. W., Wasilewski, G. D., Gonzales, A. M. R., et al. (2013). Quantitative assessment of Tcell repertoire recovery after hematopoietic stem cell transplantation. *Nat Med* 19, 372–377.

Hengel, R. L., Thaker, V., Pavlick, M. V., Metcalf, J. A., Dennis, G., Yang, J., et al. (2003). Cutting edge: L-selectin (CD62L) expression distinguishes small resting memory CD4+ T cells that preferentially respond to recall Antigen. *J. Immunol.* 170, 28–32.

Hulett, H. R., Bonner, W. A., Barrett, J., and Herzenberg, L. A. (1969). Cell sorting: automated separation of mammalian cells as a function of intracellular fluorescence. *Science (80-.).* 166, 747–749.

Hutloff, A., Dittrich, A. M., Beier, K. C., Eljaschewitsch, B., Kraft, R., Anagnostopoulos, I., et al. (1999). ICOS is an inducible T-cell co-stimulator structurally and functionally related to CD28. *Nature* 402, 21–24.

Intlekofer, A. M., Takemoto, N., Wherry, E. J., Longworth, S. A., Northrup, J. T., Palanivel, V. R., et al. (2005). Effector and memory CD8+ T cell fate coupled by T-bet and eomesodermin. *Nat. Immunol.* 6, 1236–44.

Issekutz, A. C., Quinn, P. J., Lang, B., Ramsey, S., Huber, A. M., Rowter, D., et al. (2011). Coexpression of chemokine receptors CCR5, CXCR3, and CCR4 and ligands for P- and E-selectin on T lymphocytes of patients with juvenile idiopathic arthritis. *Arthritis Rheum.* 63, 3467–76.

Ivanov, I. I., Zhou, L., and Littman, D. R. (2007). Transcriptional regulation of Th17 cell differentiation. *Semin. Immunol.* 19, 409–17.

Jacob, M. C., Favre, M., and Bensa, J. C. (1991). Membrane cell permeabilization with saponin and multiparametric analysis by flow cytometry. *Cytometry* 12, 550–8.

Jamur, M. C., and Oliver, C. (2010). Permeabilization of cell membranes. *Methods Mol. Biol.* 588, 63–6.

Janeway, C., Murphy, K., Travers, P., and Walport, M. (2008). *Janeway's immunobiology*. Garland Science.

Janeway CA Jr, Travers P, Walport M, and Shlomchik M J (2008). *Immunobiology: The immune system in health and disease*. 7th ed. New York: Garland Science.

Jung, T., Schauer, U., Heusser, C., Neumann, C., and Rieger, C. (1993). Detection of intracellular cytokines by flow cytometry. *J. Immunol. Methods* 159, 197–207.

Karlsson, F., and Hassan-Zahraee, M. (2015). Quantification of Th1 and Th17 cells with intracellular staining following PMA/Ionomycin stimulation. *Curr. Protoc. Cytom.* 71, 6.35.1–7.

Kedzierska, K., La Gruta, N. L., Stambas, J., Turner, S. J., and Doherty, P. C. (2008). Tracking phenotypically and functionally distinct T cell subsets via T cell repertoire diversity. *Mol. Immunol.* 45, 607–618.

Kemp, K., and Bruunsgaard, H. (2001). Identification of IFN-gamma-producing CD4+ T cells following PMA stimulation. *J. Interferon Cytokine Res.* 21, 503–6.

Kerr, J. F., Wyllie, A. H., and Currie, A. R. (1972). Apoptosis: a basic biological phenomenon with wide-ranging implications in tissue kinetics. *Br. J. Cancer* 26, 239–57.

Kilpatrick, R. D., Rickabaugh, T., Hultin, L. E., Hultin, P., Hausner, M. A., Detels, R., et al. (2008). Homeostasis of the naive CD4+ T cell compartment during Aging. *J. Immunol.* 180, 1499–1507.

Kimmig, S. (2002). Two subsets of naive T helper cells with distinct T cell receptor excision circle content in human adult peripheral blood. *J. Exp. Med.* 195, 789–794.

King, C., Ilic, A., Koelsch, K., and Sarvetnick, N. (2004). Homeostatic expansion of T cells during immune insufficiency generates autoimmunity. *Cell* 117, 265–77.

Kirberg, J., Berns, A., and Boehmer, H. v. (1997). Peripheral T cell survival requires continual ligation of the T cell receptor to major histocompatibility complex-encoded molecules. *J. Exp. Med.* 186, 1269–1275.

Klausner, R. D., Donaldson, J. G., and Lippincott-Schwartz, J. (1992). Brefeldin A: insights into the control of membrane traffic and organelle structure. *J. Cell Biol.* 116, 1071–80.

Kluger, M. A., Meyer, M. C., Nosko, A., Goerke, B., Luig, M., Wegscheid, C., et al. (2015). ROR t+Foxp3+ cells are an independent bifunctional regulatory T cell lineage and mediate crescentic GN. *J. Am. Soc. Nephrol.*

Kobata, T., Agematsu, K., Kameoka, J., Schlossman, S. F., and Morimoto, C. (1994). CD27 is a signal-transducing molecule involved in CD45RA+ naive T cell costimulation. *J. Immunol.* 153, 5422–32.

Kohler, S., and Thiel, A. (2009). Life after the thymus: CD31+ and CD31- human naive CD4+ T-cell subsets. *Blood* 113, 769–74.

Kohler, S., Wagner, U., Pierer, M., Kimmig, S., Oppmann, B., Möwes, B., et al. (2005). Post-thymic in vivo proliferation of naive CD4+ T cells constrains the TCR repertoire in healthy human adults. *Eur. J. Immunol.* 35, 1987–94.

Kondo, T., Takata, H., Matsuki, F., and Takiguchi, M. (2009). Cutting edge: Phenotypic characterization and differentiation of human CD8+ T cells producing IL-17. *J. Immunol.* 182, 1794–8.

Korn, T., Bettelli, E., Oukka, M., and Kuchroo, V. K. (2009). IL-17 and Th17 Cells. *Annu. Rev. Immunol.* 27, 485–517.

Krell, P. F. I., Reuther, S., Fischer, U., Keller, T., Weber, S., Gombert, M., et al. (2013). Next-generation-sequencing-spectratyping reveals public T-cell receptor repertoires in pediatric very severe aplastic anemia and identifies a β chain CDR3 sequence associated with hepatitis-induced pathogenesis. *Haematologica* 98, 1388–1396.

Lanier, L. L., Testi, R., Bindl, J., and Phillips, J. H. (1989). Identity of Leu-19 (CD56) leukocyte differentiation antigen and neural cell adhesion molecule. *J. Exp. Med.* 169, 2233–8.

Levings, M. K., Sangregorio, R., and Roncarolo, M. G. (2001). Human cd25(+)cd4(+) t regulatory cells suppress naive and memory T cell proliferation and can be expanded in vitro without loss of function. *J. Exp. Med.* 193, 1295–302.

Li, S., Lefranc, M. P., Miles, J. J., Alamyar, E., Giudicelli, V., Duroux, P., et al. (2013). IMGT/HighV QUEST paradigm for T cell receptor IMGT clonotype diversity and next generation repertoire immunoprofiling. *Nat Commun* 4, 2333.

Lim, H. W., Lee, J., Hillsamer, P., and Kim, C. H. (2008). Human Th17 cells share major trafficking receptors with both polarized effector T cells and FOXP3+ regulatory T cells. *J.*

Immunol. 180, 122–9.

Liu, W., Putnam, A. L., Xu-Yu, Z., Szot, G. L., Lee, M. R., Zhu, S., et al. (2006). CD127 expression inversely correlates with FoxP3 and suppressive function of human CD4+ T reg cells. *J. Exp. Med.* 203, 1701–11.

Loken, M. R., Brosnan, J. M., Bach, B. A., and Ault, K. A. (1990). Establishing optimal lymphocyte gates for immunophenotyping by flow cytometry. *Cytometry* 11, 453–459.

Lovett-Racke, A. E., Yang, Y., and Racke, M. K. (2011). Th1 Versus Th17: Are T cell cytokines relevant in multiple sclerosis? *Biochim. Biophys. Acta* 1812, 246–251.

MacDonald, H. R. (1995). NK1.1+ T cell receptor-alpha/beta+ cells: new clues to their origin, specificity, and function. *J. Exp. Med.* 182, 633–8.

Manger, B., Weiss, A., Imboden, J., Laing, T., and Stobo, J. D. (1987). The role of protein kinase C in transmembrane signaling by the T cell antigen receptor complex. Effects of stimulation with soluble or immobilized CD3 antibodies. *J. Immunol.* 139, 2755–60.

Marelli-Berg, F. M., Clement, M., Mauro, C., and Caligiuri, G. (2013). An immunologist's guide to CD31 function in T-cells. *J. Cell Sci.* 126, 2343–52.

Mascher, B., Schlenke, P., and Seyfarth, M. (1999). Expression and kinetics of cytokines determined by intracellular staining using flow cytometry. *J. Immunol. Methods* 223, 115–121.

Matsumoto, Y., Matsuo, H., Sakuma, H., Park, I.-K., Tsukada, Y., Kohyama, K., et al. (2006). CDR3 Spectratyping analysis of the TCR repertoire in myasthenia gravis. *J. Immunol.* 176, 5100–5107.

McClymont, S. A., Putnam, A. L., Lee, M. R., Esensten, J. H., Liu, W., Hulme, M. A., et al. (2011). Plasticity of human regulatory T cells in healthy subjects and patients with type 1 diabetes. *J. Immunol.* 186, 3918–26.

McPherson, R. C., Turner, D. G., Mair, I., O'Connor, R. A., and Anderton, S. M. (2015). T- bet expression by Foxp3(+) T regulatory cells is not essential for their suppressive function in CNS autoimmune disease or colitis. *Front. Immunol.* 6, 69.

Meeker, T. C., Miller, R. A., Link, M. P., Bindl, J., Warnke, R., and Levy, R. (1984). A unique human B lymphocyte antigen defined by a monoclonal antibody. *Hybridoma* 3, 305–20.

Morimoto, C., and Schlossman, S. F. (1993). Human naive and memory T cells revisited: new markers (CD31 and CD27) that help define CD4+ T cell subsets. *Clin. Exp. Rheumatol.* 11,241-7.

Moses, C. T., Thorstenson, K. M., Jameson, S. C., and Khoruts, A. (2003). Competition for self ligands restrains homeostatic proliferation of naive CD4 T cells. *Proc. Natl. Acad. Sci. U. S. A.* 100, 1185–90. doi:10.1073/pnas.0334572100.

Mosmann, T. R., and Coffman, R. L. (1989a). TH1 and TH2 Cells: Different patterns of lymphokine lecretion lead to different functional properties. *Annu. Rev. Immunol.* 7, 145–173.

Mosmann, T. R., and Coffman, R. L. (1989b). TH1 and TH2 cells: different patterns of

lymphokine secretion lead to different functional properties. *Annu. Rev. Immunol.* 7, 145–73.

Mosmann, T. R., Li, L., and Sad, S. (1997). Functions of CD8 T-cell subsets secreting different cytokine patterns. *Semin. Immunol.* 9, 87–92.

Muraro, P. A., Robins, H., Malhotra, S., Howell, M., Phippard, D., Desmarais, C., et al. (2014). T cell repertoire following autologous stem cell transplantation for multiple sclerosis. *J. Clin. Invest.* 124, 1168–1172.

Murphy, P. M. (1994). The molecular biology of leukocyte chemoattractant receptors. *Annu. Rev. Immunol.* 12, 593–633. doi:10.1146/annurev.iy.12.040194.003113.

Murray, P. J., and Wynn, T. A. (2011). Protective and pathogenic functions of macrophage subsets. *Nat. Rev. Immunol.* 11, 723–37.

Naylor, K., Li, G., Vallejo, A. N., Lee, W.-W., Koetz, K., Bryl, E., et al. (2005). The influence of age on T cell generation and TCR diversity. *J. Immunol.* 174, 7446–7452.

Nettenstrom, L., Alderson, K., Raschke, E. E., Evans, M. D., Sondel, P. M., Olek, S., et al. (2013). An optimized multi-parameter flow cytometry protocol for human T regulatory cell analysis on fresh and viably frozen cells, correlation with epigenetic analysis, and comparison of cord and adult blood. *J. Immunol. Methods* 387, 81–8.

O'Brien, M. C., and Bolton, W. E. (1995). Comparison of cell viability probes compatible with fixation and permeabilization for combined surface and intracellular staining in flow cytometry. *Cytometry* 19, 243–55.

O'Garra, A., and Arai, N. (2000). The molecular basis of T helper 1 and T helper 2 cell differentiation. *Trends Cell Biol.* 10, 542–550.

Olsen, I., and Sollid, L. M. (2013). Pitfalls in determining the cytokine profile of human T cells. *J. Immunol. Methods* 390, 106–12.

Pala, P., Hussell, T., and Openshaw, P. J. M. (2000). Flow cytometric measurement of intracellular cytokines. *J. Immunol. Methods* 243, 107–124.

Peine, M., Rausch, S., Helmstetter, C., Fröhlich, A., Hegazy, A. N., Kühl, A. A., et al. (2013). Stable T-bet(+)GATA-3(+) Th1/Th2 hybrid cells arise in vivo, can develop directly from naive precursors, and limit immunopathologic inflammation. *PLoS Biol.* 11, e1001633.

Pelchen-Matthews, A., Parsons, I. J., and Marsh, M. (1993). Phorbol ester-induced downregulation of CD4 is a multistep process involving dissociation from p56lck, increased association with clathrin-coated pits, and altered endosomal sorting. *J. Exp. Med.* 178, 1209–22.

Pittet, M. J., Speiser, D. E., Valmori, D., Cerottini, J.-C., and Romero, P. (2000). Cutting Edge: Cytolytic Effector Function in Human Circulating CD8+ T Cells Closely Correlates with CD56 Surface Expression. *J. Immunol.* 164, 1148–1152.

Pollice, A. A., McCoy, J. P., Shackney, S. E., Smith, C. A., Agarwal, J., Burholt, D. R., et al. (1992). Sequential paraformaldehyde and methanol fixation for simultaneous flow cytometric analysis of DNA, cell surface proteins, and intracellular proteins. *Cytometry* 13, 432–44.

Preece, G., Murphy, G., and Ager, A. (1996). Metalloproteinase-mediated regulation of L-selectin levels on leucocytes. *J. Biol. Chem.* 271 , 11634–11640.

Qin, S., Rottman, J. B., Myers, P., Kassam, N., Weinblatt, M., Loetscher, M., et al. (1998). The chemokine receptors CXCR3 and CCR5 mark subsets of T cells associated with certain inflammatory reactions. *J. Clin. Invest.* 101, 746–54.

Raphael, I., Nalawade, S., Eagar, T. N., and Forsthuber, T. G. (2014). T cell subsets and their signature cytokines in autoimmune and inflammatory diseases. *Cytokine* 74, 5–17.

Reinherz, E. L., Hussey, R. E., and Schlossman, S. F. (1980). A monoclonal antibody blocking human T cell function. *Eur. J. Immunol.* 10, 758–62.

Reinherz, E. L., Kung, P. C., Goldstein, G., and Schlossman, S. F. (1979). Separation of functional subsets of human T cells by a monoclonal antibody. *Proc. Natl. Acad. Sci. U. S. A.* 76, 4061–5.

Riordan, N. H., Ichim, T. E., Min, W.-P., Wang, H., Solano, F., Lara, F., et al. (2009). Non-expanded adipose stromal vascular fraction cell therapy for multiple sclerosis. *J. Transl. Med.* 7, 29.

Robins, H. S., Campregher, P. V, Srivastava, S. K., Wacher, A., Turtle, C. J., Kahsai, O., et al. (2009). Comprehensive assessment of T-cell receptor β-chain diversity in αβ T cells. *Immunobiology* 114, 4099–4107.

Rodríguez-Caballero, A., García-Montero, A. C., Bueno, C., Almeida, J., Varro, R., Chen, R., et al. (2004). A new simple whole blood flow cytometry-based method for simultaneous identification of activated cells and quantitative evaluation of cytokines released during activation. *Lab. Invest.* 84, 1387–98.

Roederer, M. (2001). Spectral compensation for flow cytometry: visualization artifacts, limitations, and caveats. *Cytometry* 45, 194–205.

Roederer, M., De Rosa, S., Gerstein, R., Anderson, M., Bigos, M., Stovel, R., et al. (1997). 8 color, 10-parameter flow cytometry to elucidate complex leukocyte heterogeneity. *Cytometry* 29, 328–39.

Romagnani, S. (2000). T-cell subsets (Th1 versus Th2). *Ann. Allergy. Asthma Immunol.* 85, 9–18; quiz 18, 21.

Rooke, R., Waltzinger, C., Benoist, C., and Mathis, D. (1997). Targeted complementation of MHC class II deficiency by intrathymic delivery of recombinant adenoviruses. *Immunity* 7, 123–34.

De Rosa, S. C., Brenchley, J. M., and Roederer, M. (2003). Beyond six colors: A new era in flow cytometry. 9, 112–117.

De Rosa, S. C., Herzenberg, L. A., Herzenberg, L. A., and Roederer, M. (2001). 11-color, 13-parameter flow cytometry: Identification of human naive T cells by phenotype, function, and T-cell receptor diversity. *Nat Med* 7, 245–248.

Rostaing, L., Tkaczuk, J., Durand, M., Peres, C., Durand, D., de Préval, C., et al. (1999). Kinetics of intracytoplasmic Th1 and Th2 cytokine production assessed by flow cytometry following in vitro activation of peripheral blood mononuclear cells. *Cytometry* 35, 318–28.

Sakaguchi, S., Yamaguchi, T., Nomura, T., and Ono, M. (2008). Regulatory T cells and immune tolerance. *Cell* 133, 775–787.

Sallusto, F., Lenig, D., Förster, R., Lipp, M., and Lanzavecchia, A. (1999). Two subsets of memory T lymphocytes with distinct homing potentials and effector functions. *Nature* 401, 708-12.

Salzman, G. C., Crowell, J. M., Goad, C. A., Hansen, K. M., Hiebert, R. D., LaBauve, P. M., et al. (1975). A flow-system multiangle light-scattering instrument for cell characterization. *Clin. Chem.* 21, 1297–304.

Sander, B., Andersson, J., and Andersson, U. (1991). Assessment of cytokines by immunofluorescence and the paraformaldehyde-saponin procedure. *Immunol. Rev.* 119, 65–93.

Seddiki, N., Santner-Nanan, B., Martinson, J., Zaunders, J., Sasson, S., Landay, A., et al. (2006). Expression of interleukin (IL)-2 and IL-7 receptors discriminates between human regulatory and activated T cells. *J. Exp. Med.* 203, 1693–700.

Shapiro, H. (2005). *Practical flow cytometry*. Stefanová, I., Dorfman, J. R., and Germain, R. N. (2002). Self-recognition promotes the

foreign antigen sensitivity of naive T lymphocytes. *Nature* 420, 429–34. Suri-Payer, E., and Cantor, H. (2001). Differential cytokine requirements for regulation of

autoimmune gastritis and colitis by CD4(+)CD25(+) T cells. *J. Autoimmun.* 16, 115–23. Szabo, S. J., Kim, S. T., Costa, G. L., Zhang, X., Fathman, C. G., and Glimcher, L. H. (2000).

A novel transcription factor, T-bet, directs Th1 lineage commitment. *Cell* 100, 655–669. Szuba, A., and Rockson, S. G. (1998). Lymphedema: classification, diagnosis and therapy.

Vasc. Med. 3, 145–56. Tai, T.-S., Pai, S.-Y., and Ho, I.-C. (2013). GATA-3 regulates the homeostasis and activation of CD8+ T cells. *J. Immunol.* 190, 428–37.

Takeda, S., Rodewald, H. R., Arakawa, H., Bluethmann, H., and Shimizu, T. (1996). MHC class II molecules are not required for survival of newly generated CD4+ T cells, but affect their long-term life span. *Immunity* 5, 217–28.

Tanaskovic, S., Fernandez, S., Price, P., Lee, S., and French, M. A. (2010). CD31 (PECAM- 1) is a marker of recent thymic emigrants among CD4+ T-cells, but not CD8+ T-cells or γδ T-cells, in HIV patients responding to ART. *Immunol. Cell Biol.* 88, 321–327.

Tanchot, C., Rosado, M. M., Agenes, F., Freitas, A. A., and Rocha, B. (1997). Lymphocyte homeostasis. *Semin. Immunol.* 9, 331–7.

Thivierge, M., Turcotte, S., Rola-Pleszczynski, M., and Stankova, J. (2015). Enhanced cysteinyl-leukotriene type 1 receptor expression in T cells from house dust mite-allergic individuals following stimulation with der p. *J. Immunol. Res.* 2015, 1–11.

Thornton, A. M., and Shevach, E. M. (1998). CD4+CD25+ immunoregulatory T cells suppress polyclonal T cell activation in vitro by inhibiting interleukin 2 production. *J. Exp. Med.* 188, 287–296.

Tomiyama, H., Matsuda, T., and Takiguchi, M. (2002). Differentiation of human CD8(+) T cells from a memory to memory/effector phenotype. *J. Immunol.* 168, 5538–50.

Tosolini, M., Kirilovsky, A., Mlecnik, B., Fredriksen, T., Mauger, S., Bindea, G., et al. (2011). Clinical impact of different classes of infiltrating T cytotoxic and helper cells (Th1, Th2, Treg, Th17) in patients with colorectal cancer. *Cancer Res.* 71, 1263–1271.

Trickett, A., and Kwan, Y. L. (2003). T cell stimulation and expansion using anti-CD3/CD28 beads. *J. Immunol. Methods* 275, 251–255.

Truneh, A., Albert, F., Golstein, P., and Schmitt-Verhulst, A.-M. (1985). Early steps of lymphocyte activation bypassed by synergy between calcium ionophores and phorbol ester. *Nature* 313, 318–320.

Tsoukas, C. D., Landgraf, B., Bentin, J., Valentine, M., Lotz, M., Vaughan, J. H., et al. (1985). Activation of resting T lymphocytes by anti-CD3 (T3) antibodies in the absence of monocytes. *J. Immunol.* 135, 1719–23.

Tsuchiya, S., Kobayashi, Y., Goto, Y., Okumura, H., Nakae, S., Konno, T., et al. (1982). Induction of maturation in cultured human monocytic leukemia cells by a phorbol diester. *Cancer Res.* 42, 1530–6.

Vieira, P. L., Christensen, J. R., Minaee, S., O'Neill, E. J., Barrat, F. J., Boonstra, A., et al. (2004). IL-10-secreting regulatory T cells do not express Foxp3 but have comparable regulatory function to naturally occurring CD4+CD25+ regulatory T cells. *J. Immunol.* 172, 5986–93.

Viret, C., Wong, F. S., and Janeway, C. A. (1999). Designing and maintaining the mature TCR repertoire. *Immunity* 10, 559–568.

Voo, K. S., Wang, Y.-H., Santori, F. R., Boggiano, C., Wang, Y.-H., Arima, K., et al. (2009). Identification of IL-17-producing FOXP3+ regulatory T cells in humans. *Proc. Natl. Acad. Sci. U. S. A.* 106, 4793–8.

Wan, Y. Y., and Flavell, R. A. (2009). How diverse—CD4 effector T cells and their functions. *J. Mol. Cell Biol.* 1, 20–36.

Warren, R. L., Freeman, J. D., Zeng, T., Choe, G., Munro, S., Moore, R., et al. (2011). Exhaustive T-cell repertoire sequencing of human peripheral blood samples reveals signatures of antigen selection and a directly measured repertoire size of at least 1 million clonotypes. *Genome Res.* 21, 790–797.

Weng, W.-K., Armstrong, R., Arai, S., Desmarais, C., Hoppe, R., and Kim, Y. H. (2013). Minimal residual disease monitoring with high-throughput sequencing of T cell receptors in cutaneous T cell lymphoma. *Sci. Transl. Med.* 5, 214ra171.

Wills, M. R., Carmichael, A. J., Weekes, M. P., Mynard, K., Okecha, G., Hicks, R., et al. (1999).

Human virus-specific CD8+ CTL clones revert from CD45ROhigh to CD45RAhigh in vivo: CD45RAhighCD8+ T cells comprise both naive and memory cells. *J. Immunol.* 162, 7080–7.

Woodsworth, D., Castellarin, M., and Holt, R. (2013). Sequence analysis of T-cell repertoires in health and disease. *Genome Med* 5, 98.

Wu, D., Sherwood, A., Fromm, J. R., Winter, S. S., Dunsmore, K. P., Loh, M. L., et al. (2012). High-throughput sequencing detects minimal residual disease in acute T lymphoblastic leukemia. *Sci. Transl. Med.* 4, 134ra63.

Yssel, H., De Waal Malefyt, R., Roncarolo, M. G., Abrams, J. S., Lahesmaa, R., Spits, H., et al. (1992). IL-10 is produced by subsets of human CD4+ T cell clones and peripheral blood T cells. *J. Immunol.* 149, 2378–2384.

Zheng, W., and Flavell, R. A. (1997). The transcription factor GATA-3 is necessary and sufficient for Th2 cytokine gene expression in CD4 T cells. *Cell* 89, 587–596.

Zhu, J., and Paul, W. E. (2010). Peripheral CD4 T cell differentiation regulated by networks of cytokines and transcription factors. *Immunol. Rev.* 238, 247–262.

Zhu, J., Yamane, H., and Paul, W. E. (2010). Differentiation of effector CD4 T cell populations. *Annu. Rev. Immunol.* 28, 445–489.

Zlotnik, A., and Yoshie, O. (2000). Chemokines. *Immunity* 12, 121–127.

Appendix 1

Excitation and emission spectra of the 12 dyes used in the staining panels. The fluorochromes are grouped according to the excitation laser line used (305, 405, 488, 635 nm). The band pass filters are also indicated. The percentages indicate the estimated efficiency of the primary detector filter (**coloured**) and the spillover by the other fluorochromes.

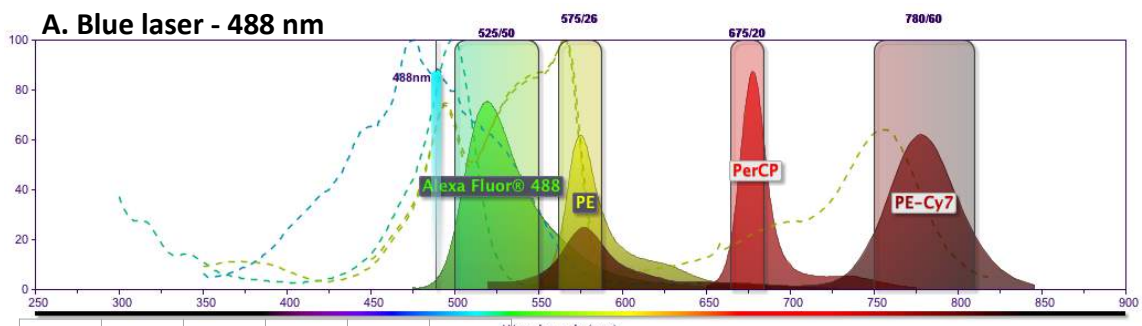

	Filter	AF488	PE	PerCP	PE-Cy7
AF488	525/50	72.7%	1.6%	--	4.0%
PE	575/26	13.5%	55.9%	--	20.8%
PerCP	675/20	0.2%	2.9%	63.8%	1.6%
PE-Cy7	780/60	--	--	3.5%	60.5%

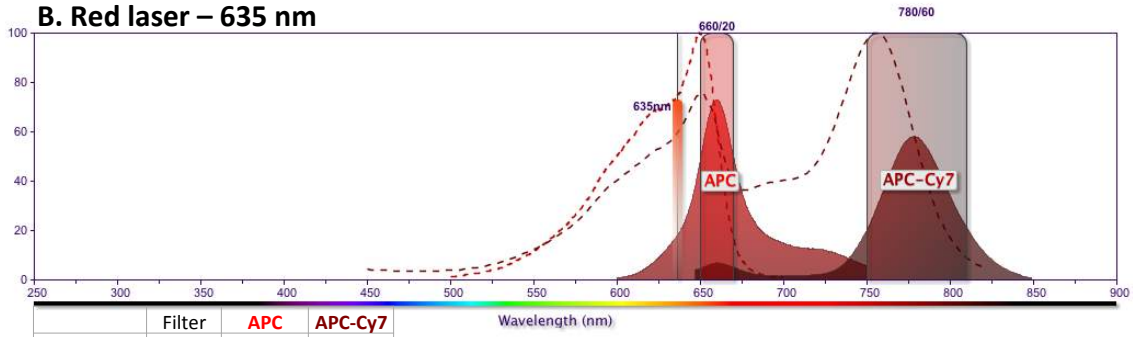

	Filter	APC	APC-Cy7
APC	660/20	40.2%	4.8%
APC-Cy7	780/60	--	77.8%

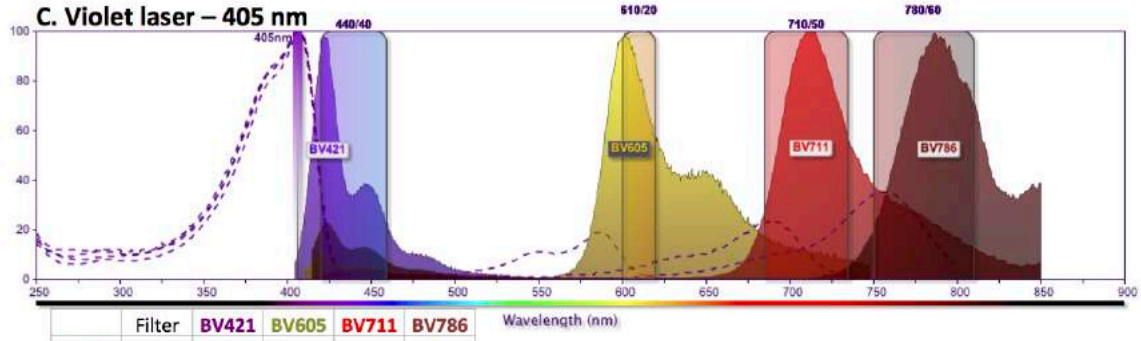

	Filter	BV421	BV605	BV711	BV786
BV421	440/40	56.6%	35.1%	--	1.2%
BV605	610/20	0.1%	25.9%	--	0.0%
BV711	710/50	--	35.1%	56.6%	1.2%
BV786	780/60	--	--	39.0%	61.5%

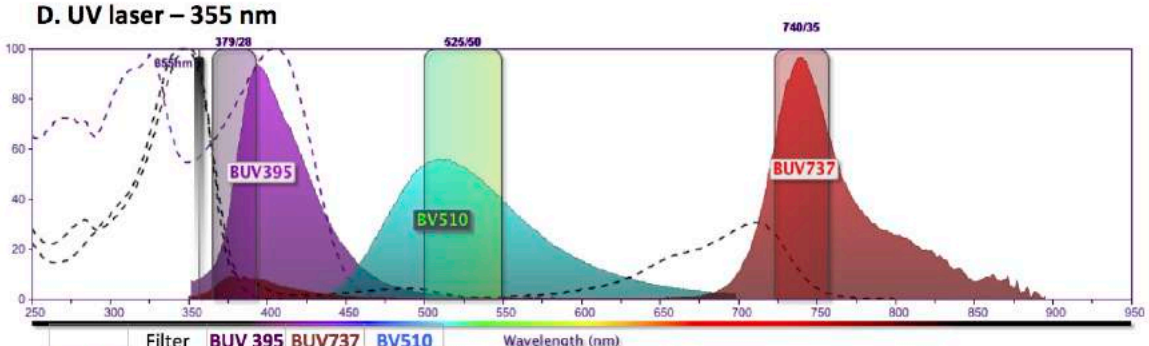

	Filter	BUV 395	BUV737	BV510
BUV 395	379/28	27.6%	7.5%	--
BUV737	740/35	--	42.6%	--
BV510	525/50	3.3%	0.4%	41.9%

Appendix 2

Memory subset classification of transcription factor-positive CD4 T cells.
Based on the staining in normal blood (Figure 10), shown here are the transcription factor-positive CD4 T cells (blue and orange) and their co-expression with CD197 (CCR7), CD27 and CD62L, before stimulation **(A)** and after PMA/ionomycin stimulation **(B)**. For T-bet, the T-bet^{hi} population observed earlier (Figure 10 – Part II, A and B) was backgated (not shown) in orange. Top row shows gating on all CD4 T cells; last row shows unstained controls.

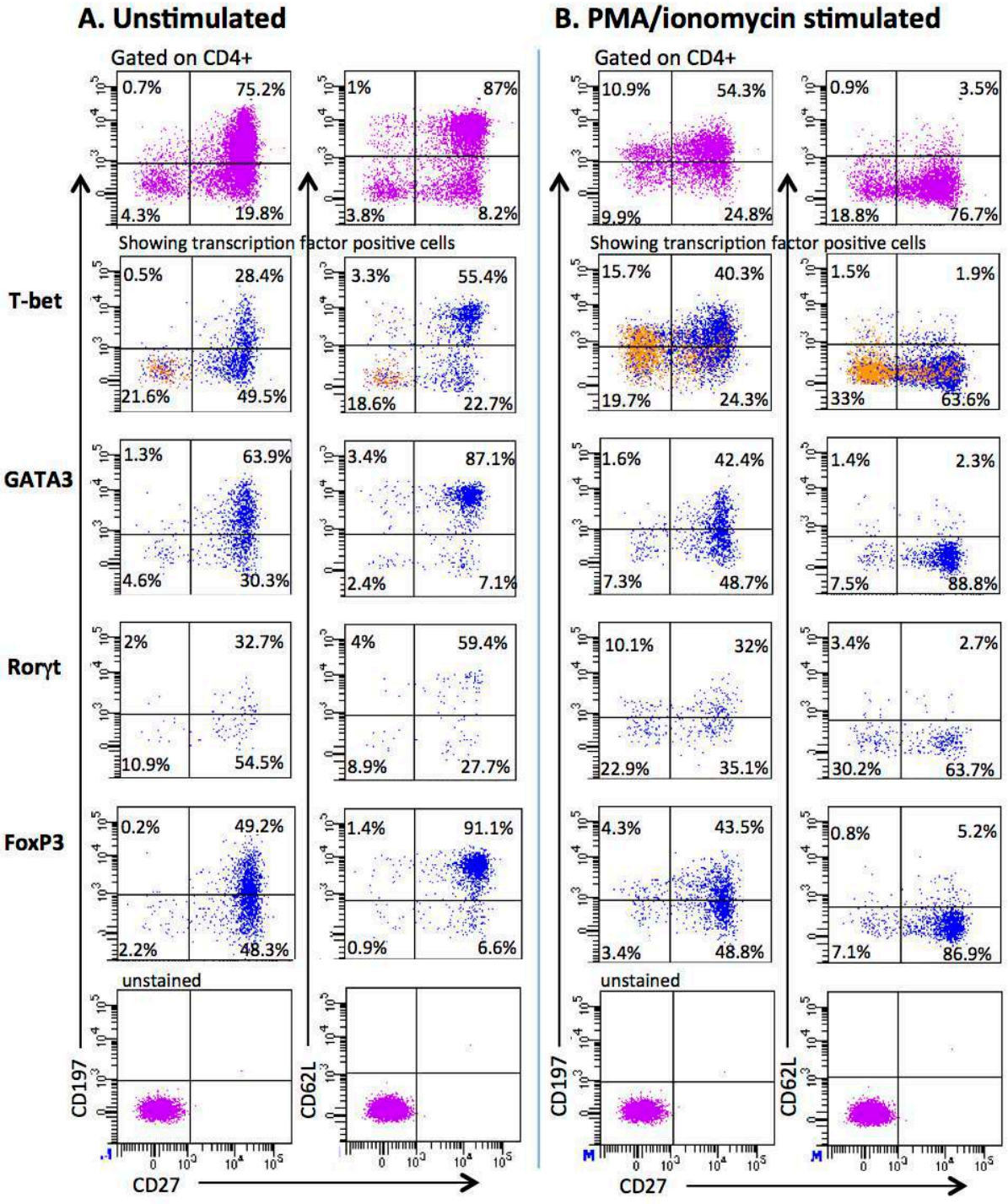

Appendix 3

Memory subset classification of transcription factor-positive CD8 T cells.

Based on the staining in normal blood (Figure 10), shown here are the transcription factor-positive CD8 T cells (orange) and their co-expression with CD197 (CCR7), CD27 and CD62L, before stimulation **(A)** and after PMA/ionomycin stimulation **(B)**. Top row shows gating on all CD4 T cells; last row shows unstained controls.

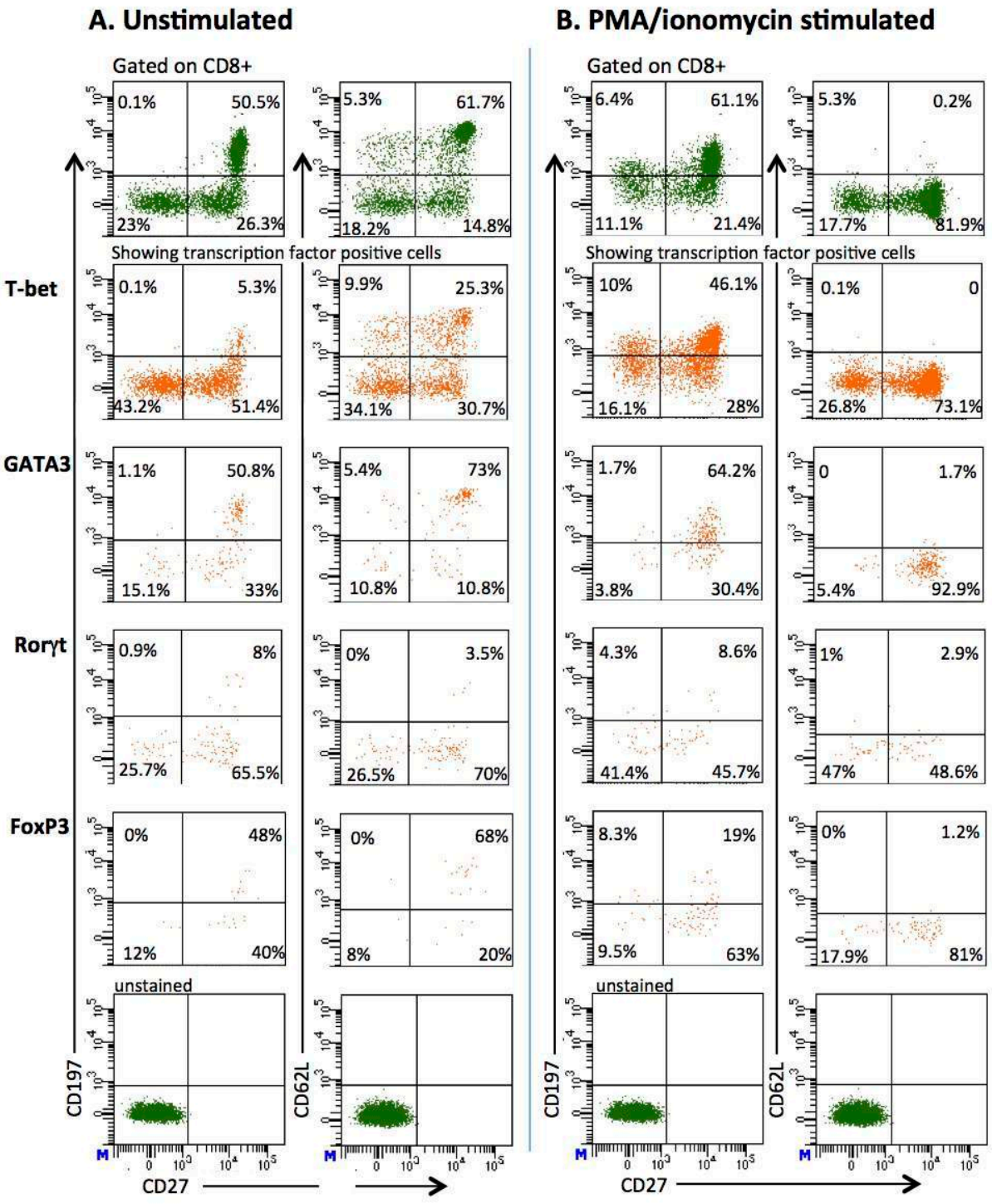

Appendix 4. Representative voltage settings, compensation calculations and single colour controls

Parameters	Type	Voltage	Log
FSC	A, H, W	451	Off
SSC	A, H, W	291	Off
FITC	A	510	On
PE	A	570	On
PerCP	A	590	On
PE-Cy7	A	780	On
BV421	A	385	On
BV605	A	460	On
BV711	A	570	On
APC	A	810	On
APC-Cy7	A	735	On
BUV395	A	550	On
BUV737	A	620	On

Threshold Operator:	OR
Threshold Parameters	**Threshold**
FSC	5,000

Compensation State:	Enabled
Fluorochromes	**Value(%)**
PE - FITC	34.58
PerCP - FITC	2.64
PE-Cy7 - FITC	0.46
BV421 - FITC	0.00
BV605 - FITC	0.10
BV711 - FITC	0.00
APC - FITC	0.00
APC-Cy7 - FITC	0.00
BUV395 - FITC	0.00
BUV737 - FITC	0.00
FITC - PE	0.93
PerCP - PE	14.14
PE-Cy7 - PE	2.53
BV421 - PE	0.00
BV605 - PE	1.81
BV711 - PE	0.82
APC - PE	0.00
APC-Cy7 - PE	0.00
BUV395 - PE	0.00
BUV737 - PE	0.52
FITC - PerCP	0.39
PE - PerCP	0.31
PE-Cy7 - PerCP	21.73
BV421 - PerCP	0.00
BV605 - PerCP	0.04
BV711 - PerCP	27.57
APC - PerCP	72.43
APC-Cy7 - PerCP	8.63
BUV395 - PerCP	0.05
BUV737 - PerCP	25.73
FITC - PE-Cy7	0.02
PE - PE-Cy7	0.82
PerCP - PE-Cy7	0.15
BV421 - PE-Cy7	0.00
BV605 - PE-Cy7	0.00
BV711 - PE-Cy7	0.02
APC - PE-Cy7	0.00
APC-Cy7 - PE-Cy7	14.46
BUV395 - PE-Cy7	0.00

BUV737 - PE-Cy7	0.89
FITC - BV421	0.00
PE - BV421	0.00
PerCP - BV421	0.00
PE-Cy7 - BV421	0.01
BV605 - BV421	0.33
BV711 - BV421	0.20
APC - BV421	0.00
APC-Cy7 - BV421	0.01
BUV395 - BV421	0.14
BUV737 - BV421	0.04
FITC - BV605	0.00
PE - BV605	0.51
PerCP - BV605	14.74
PE-Cy7 - BV605	4.55
BV421 - BV605	16.00
BV711 - BV605	91.21
APC - BV605	0.00
APC-Cy7 - BV605	0.00
BUV395 - BV605	1.42
BUV737 - BV605	31.88
FITC - BV711	1.34
PE - BV711	1.24
PerCP - BV711	4.20
PE-Cy7 - BV711	11.25
BV421 - BV711	19.15
BV605 - BV711	0.48
APC - BV711	4.92
APC-Cy7 - BV711	34.46
BUV395 - BV711	1.07
BUV737 - BV711	56.78
FITC - APC	0.11
PE - APC	0.09
PerCP - APC	0.95
PE-Cy7 - APC	0.22
BV421 - APC	0.02
BV605 - APC	0.04
BV711 - APC	1.98
APC-Cy7 - APC	21.07
BUV395 - APC	0.04
BUV737 - APC	2.60
FITC - APC-Cy7	0.09
PE - APC-Cy7	0.04
PerCP - APC-Cy7	0.03
PE-Cy7 - APC-Cy7	0.98
BV421 - APC-Cy7	0.00
BV605 - APC-Cy7	0.01
BV711 - APC-Cy7	0.10
APC - APC-Cy7	2.83
BUV395 - APC-Cy7	0.03
BUV737 - APC-Cy7	0.54
FITC - BUV395	1.14
PE - BUV395	0.71
PerCP - BUV395	0.33
PE-Cy7 - BUV395	0.38
BV421 - BUV395	20.14
BV605 - BUV395	0.53
BV711 - BUV395	0.96
APC - BUV395	0.97
APC-Cy7 - BUV395	0.37
BUV737 - BUV395	1.16
FITC - BUV737	0.16
PE - BUV737	0.11
PerCP - BUV737	0.35
PE-Cy7 - BUV737	10.20
BV421 - BUV737	0.90
BV605 - BUV737	0.03
BV711 - BUV737	2.92
APC - BUV737	0.57
APC-Cy7 - BUV737	32.51
BUV395 - BUV737	2.21

Appendix 4

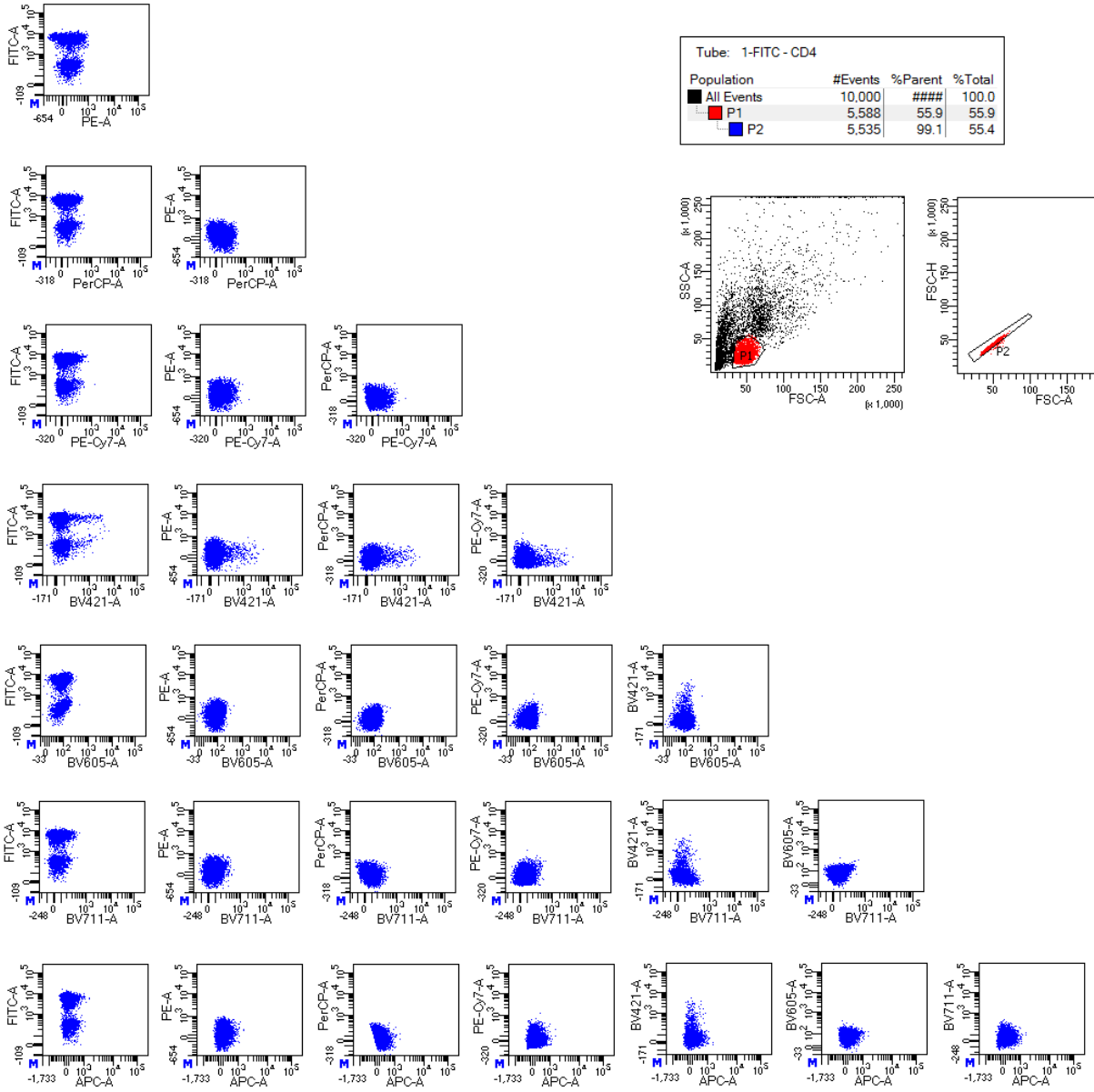
Tube: 1-FITC - CD4
Population #Events %Parent %Total
All Events 10,000 #### 100.0
P1 5,588 55.9 55.9
P2 5,535 99.1 55.4
SSC-A
FSC-A
FSC-H
FSC-A
FITC-A
PE-A
PerCP-A
PE-Cy7-A
BV421-A
BV605-A
BV711-A
APC-A

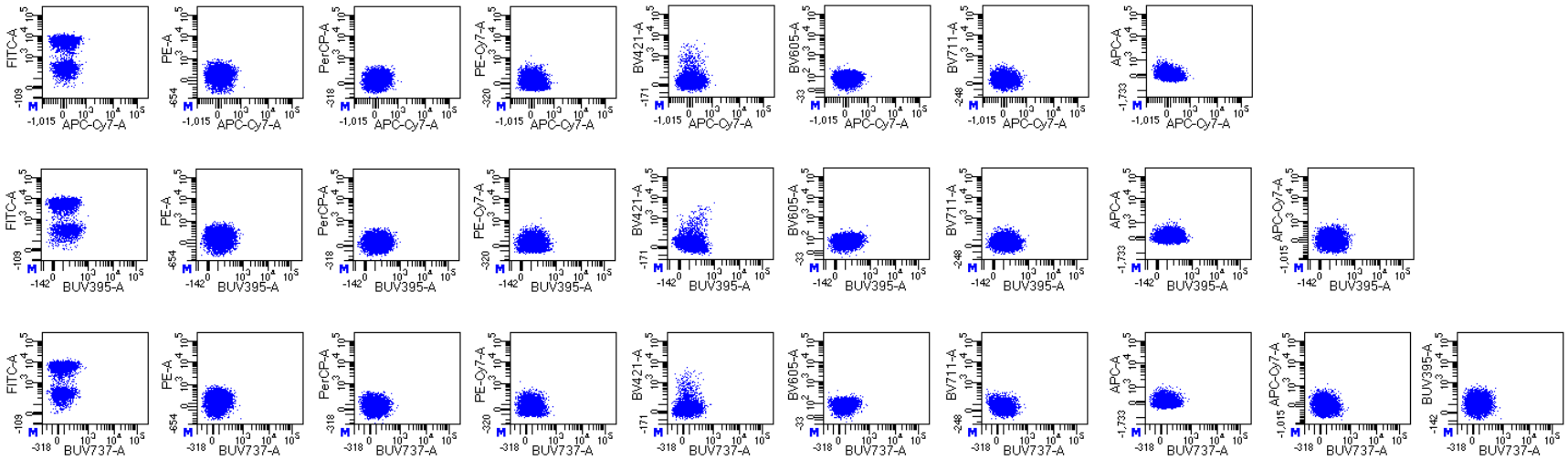
FITC-A
PE-A
PerCP-A
PE-Cy7-A
BV421-A
BV605-A
BV711-A
APC-A
APC-Cy7-A
BUV395-A
BUV737-A

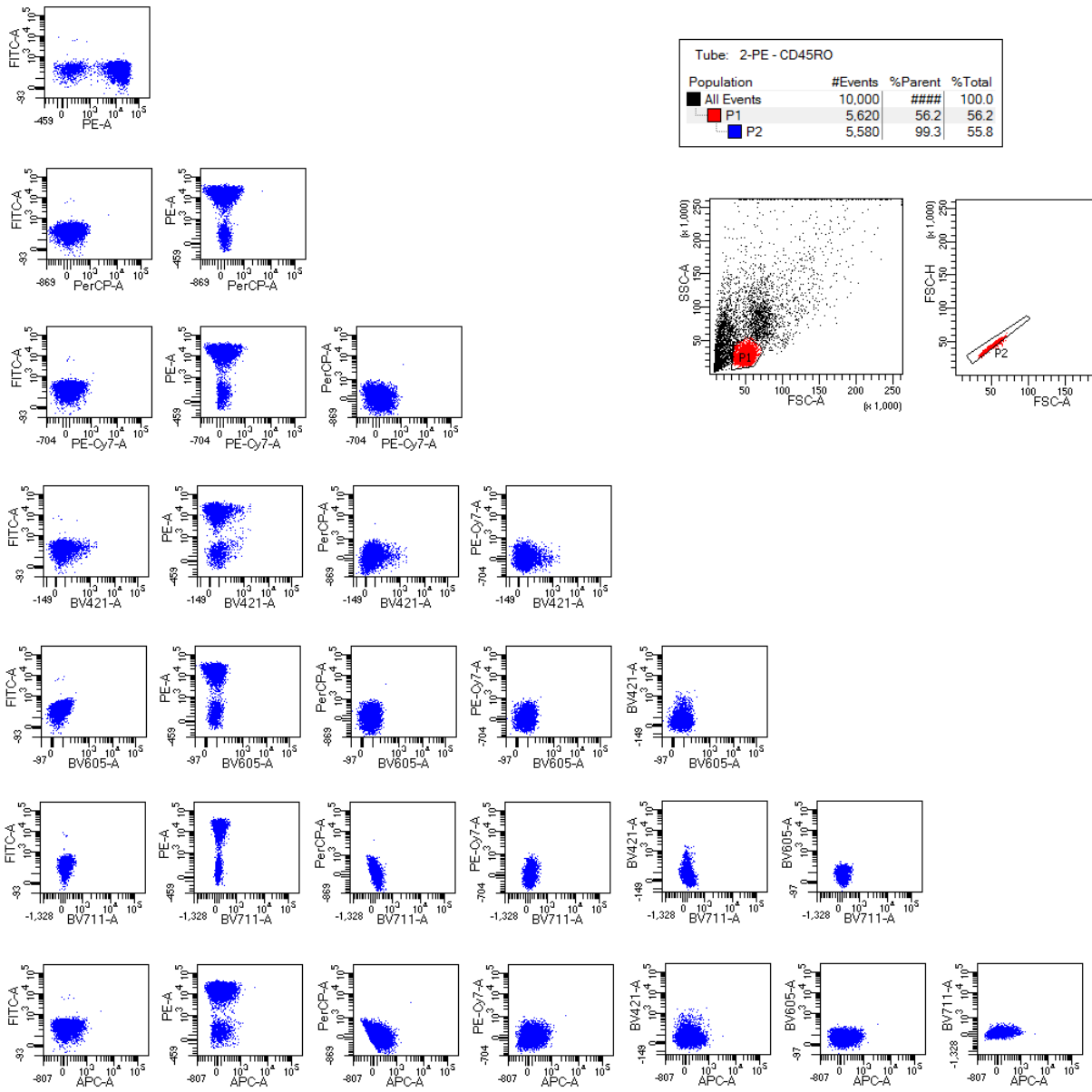
Tube: 2-PE - CD45RO
Population #Events %Parent %Total
All Events 10,000 #### 100.0
P1 5,620 56.2 56.2
P2 5,580 99.3 55.8
SSC-A
FSC-A
FSC-H
P1
P2
FITC-A
PE-A
PerCP-A
PE-Cy7-A
BV421-A
BV605-A
BV711-A
APC-A

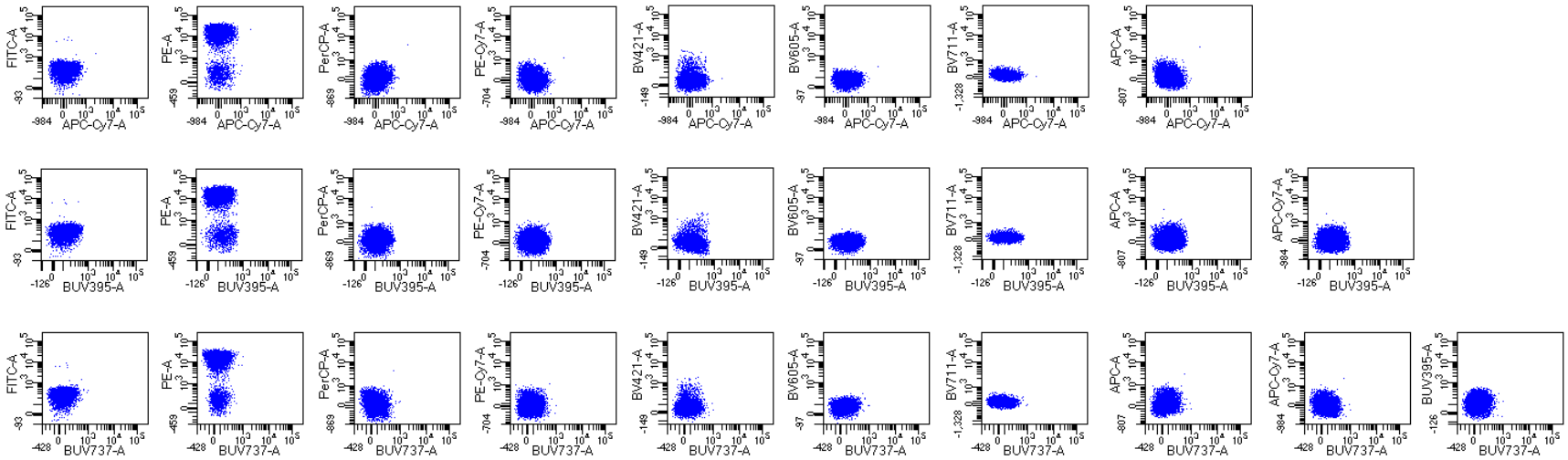
FITC-A
PE-A
PerCP-A
PE-Cy7-A
BV421-A
BV605-A
BV711-A
APC-A
APC-Cy7-A
BUV395-A
BUV737-A

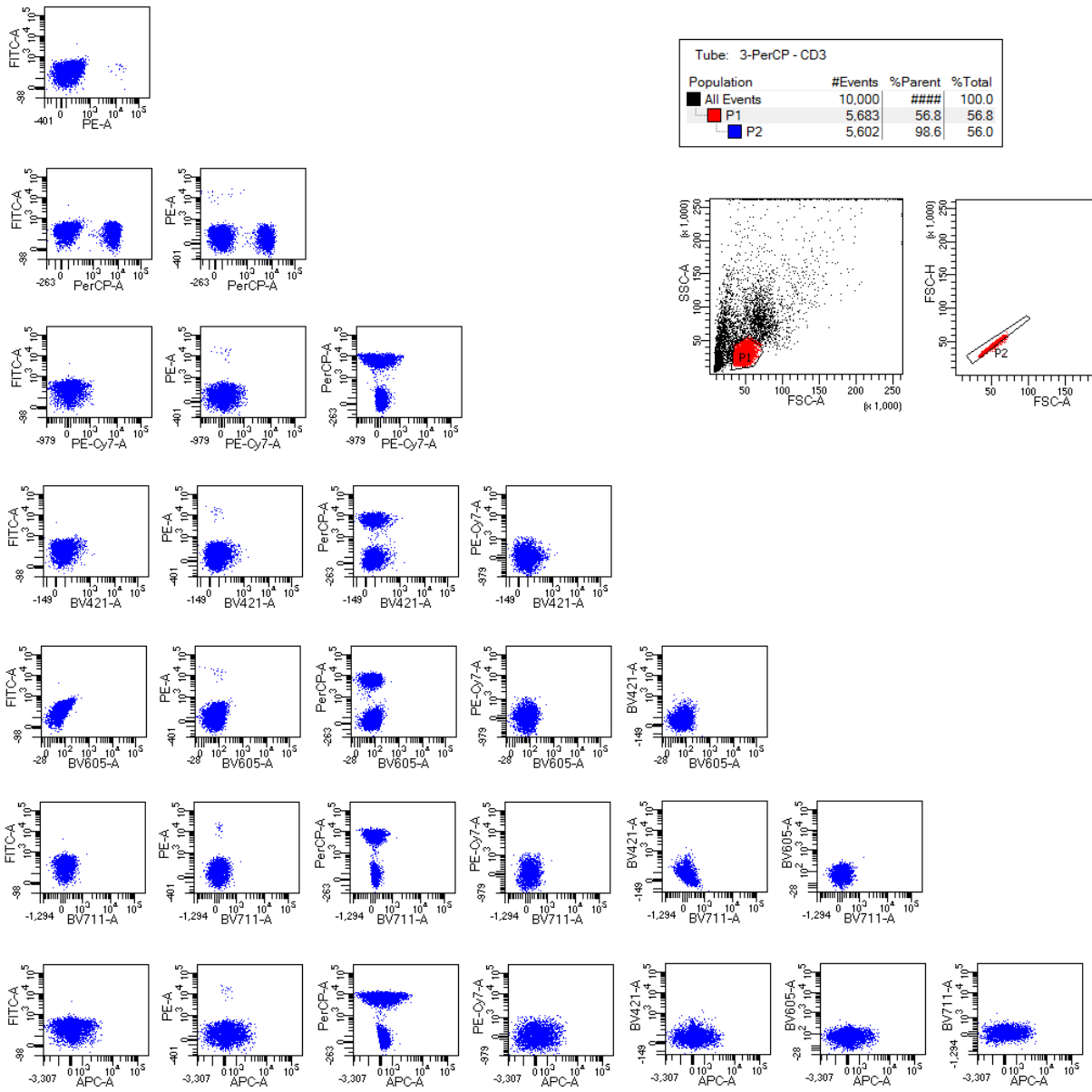
Tube: 3-PerCP - CD3
Population #Events %Parent %Total
All Events 10,000 #### 100.0
P1 5,683 56.8 56.8
P2 5,602 98.6 56.0
SSC-A
FSC-A
FSC-H
P1
P2
FITC-A
PE-A
PerCP-A
PE-Cy7-A
BV421-A
BV605-A
BV711-A
APC-A

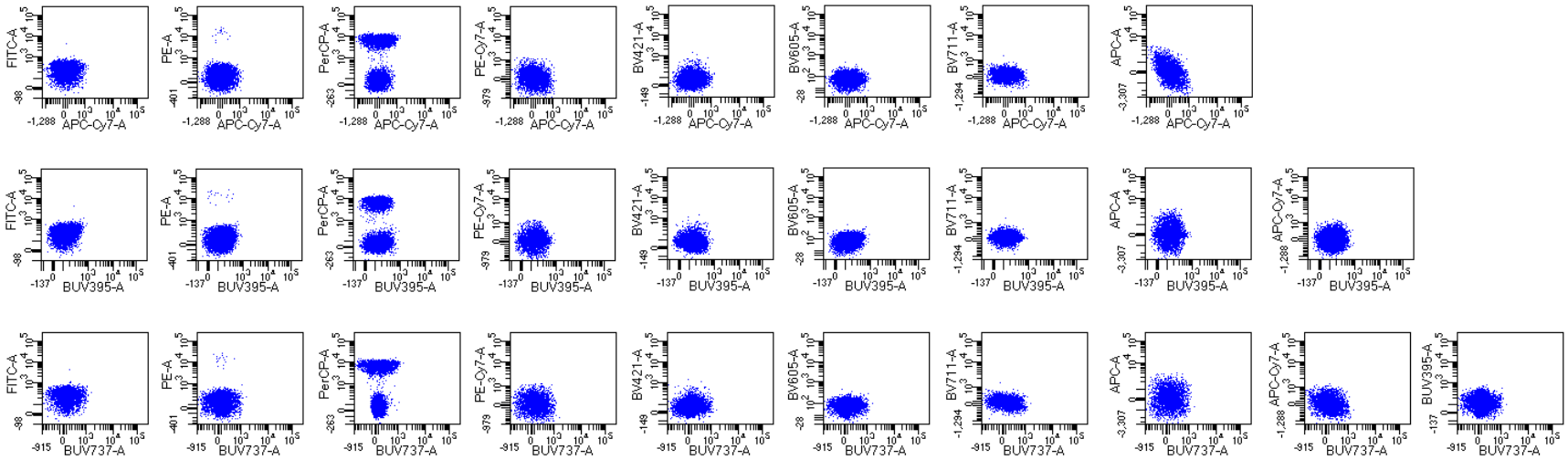
FITC-A
PE-A
PerCP-A
PE-Cy7-A
BV421-A
BV605-A
BV711-A
APC-A
APC-Cy7-A
BUV395-A
BUV737-A

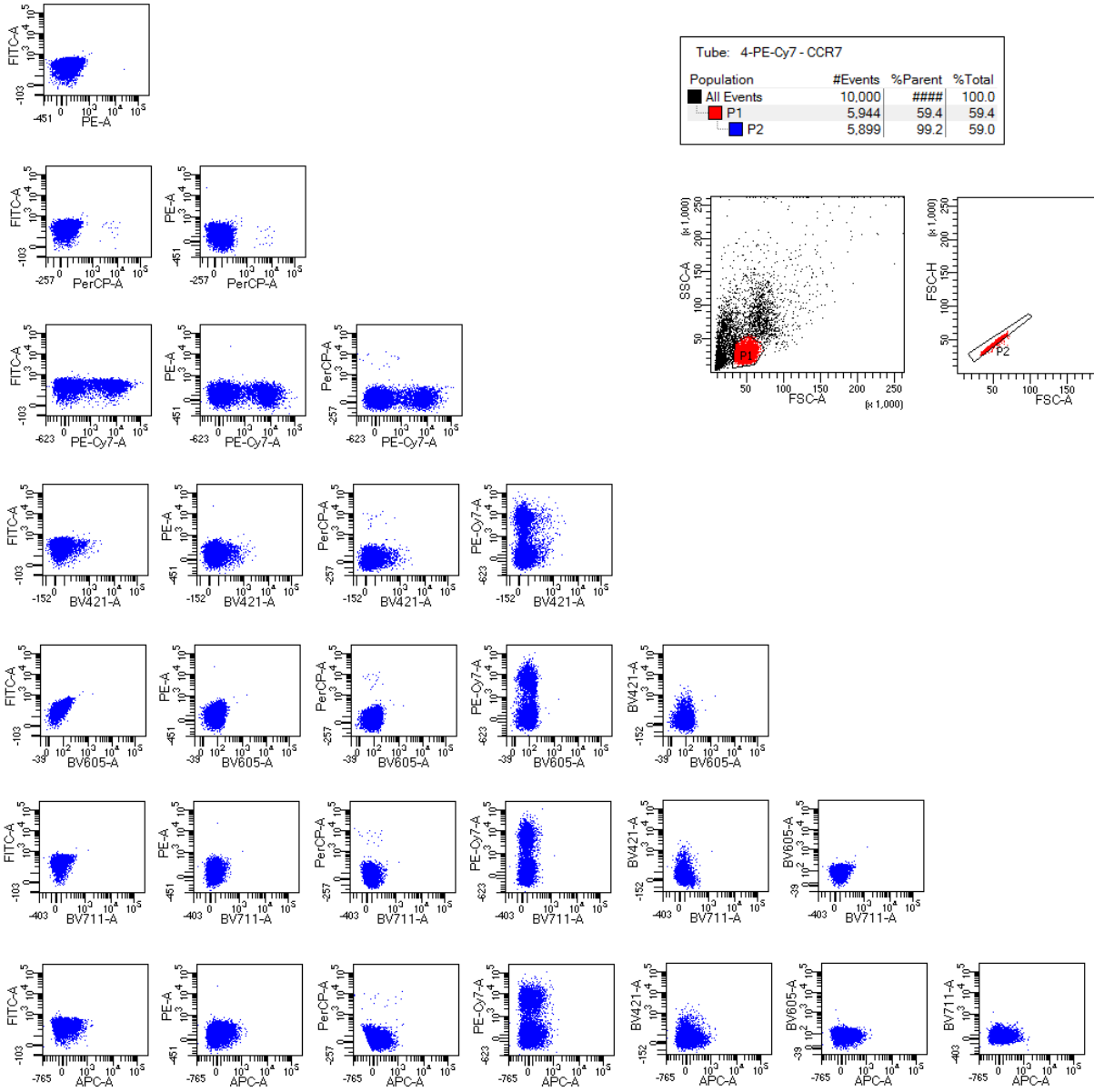
Tube: 4-PE-Cy7 - CCR7
Population #Events %Parent %Total
All Events 10,000 #### 100.0
P1 5,944 59.4 59.4
P2 5,899 99.2 59.0
SSC-A
FSC-A
FSC-H
P1
P2
FITC-A
PE-A
PerCP-A
PE-Cy7-A
BV421-A
BV605-A
BV711-A
APC-A

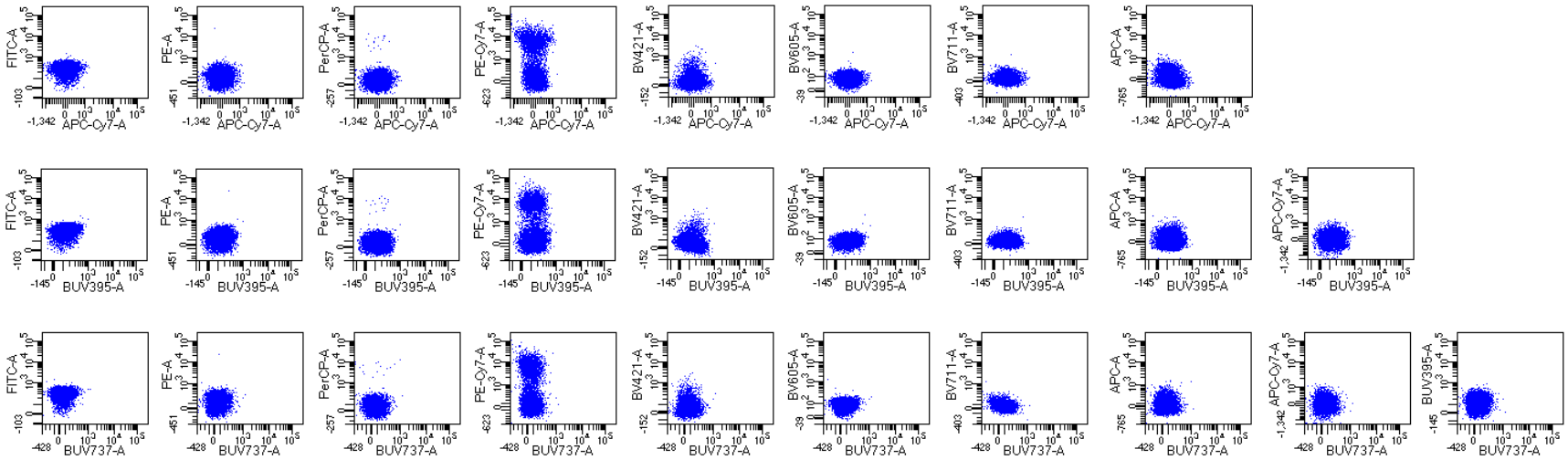
FITC-A
PE-A
PerCP-A
PE-Cy7-A
BV421-A
BV605-A
BV711-A
APC-A
APC-Cy7-A
BUV395-A
BUV737-A

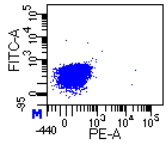

Tube: 5-BV421 - CD45RA

Population	#Events	%Parent	%Total
All Events	10,000	####	100.0
P1	5,358	53.6	53.6
P2	5,259	98.2	52.6

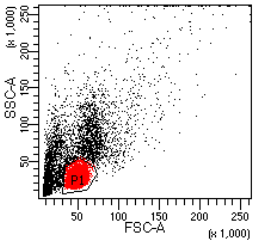

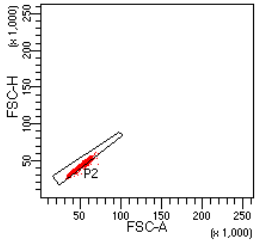

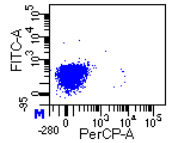

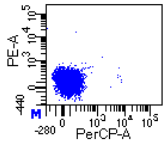

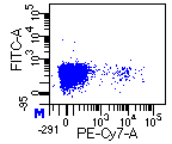

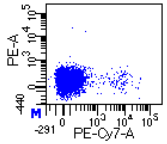

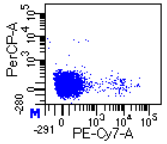

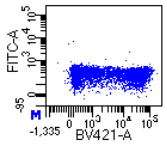

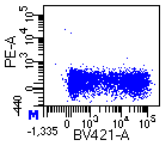

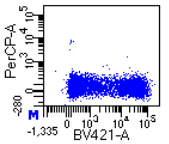

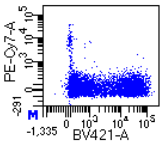

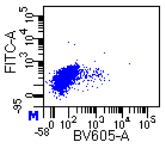

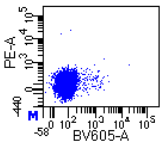

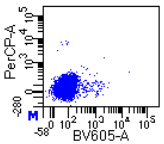

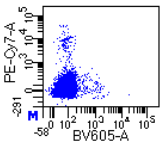

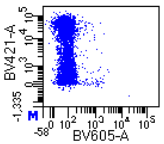

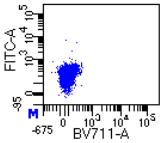

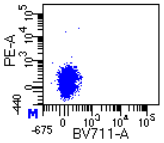

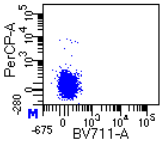

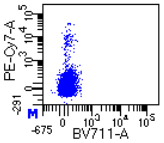

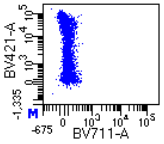

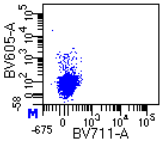

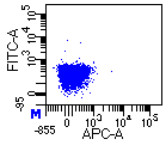

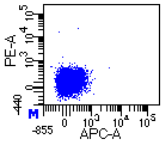

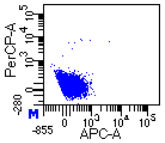

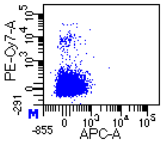

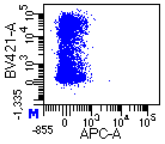

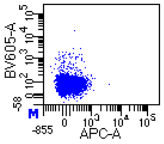

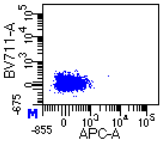

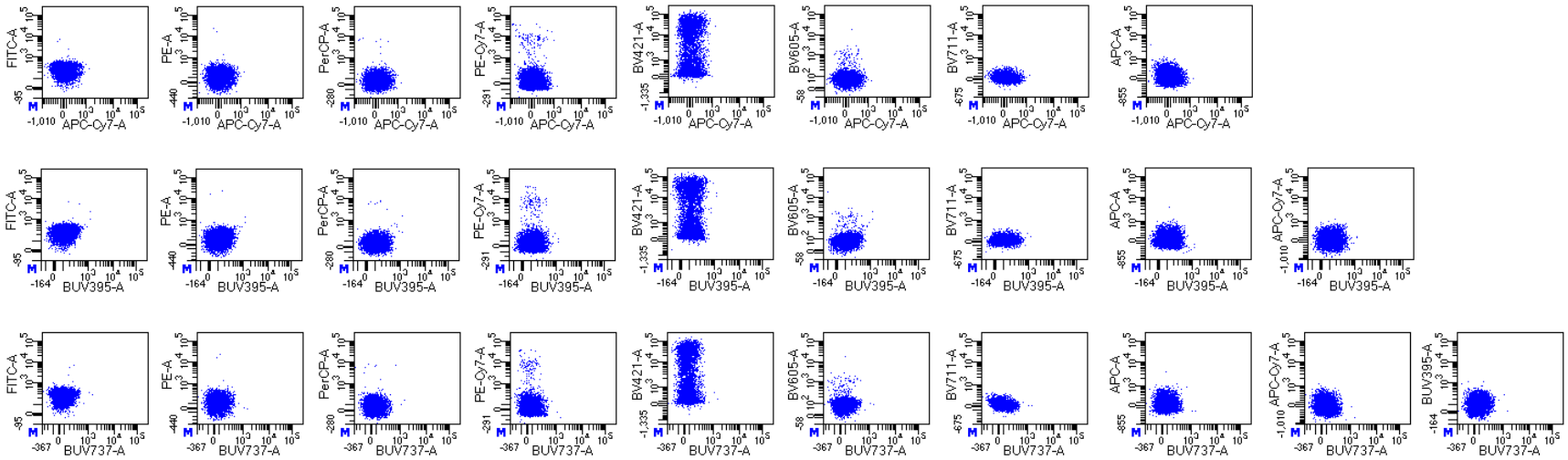
FITC-A
PE-A
PerCP-A
PE-Cy7-A
BV421-A
BV605-A
BV711-A
APC-A
APC-Cy7-A
BUV395-A
BUV737-A

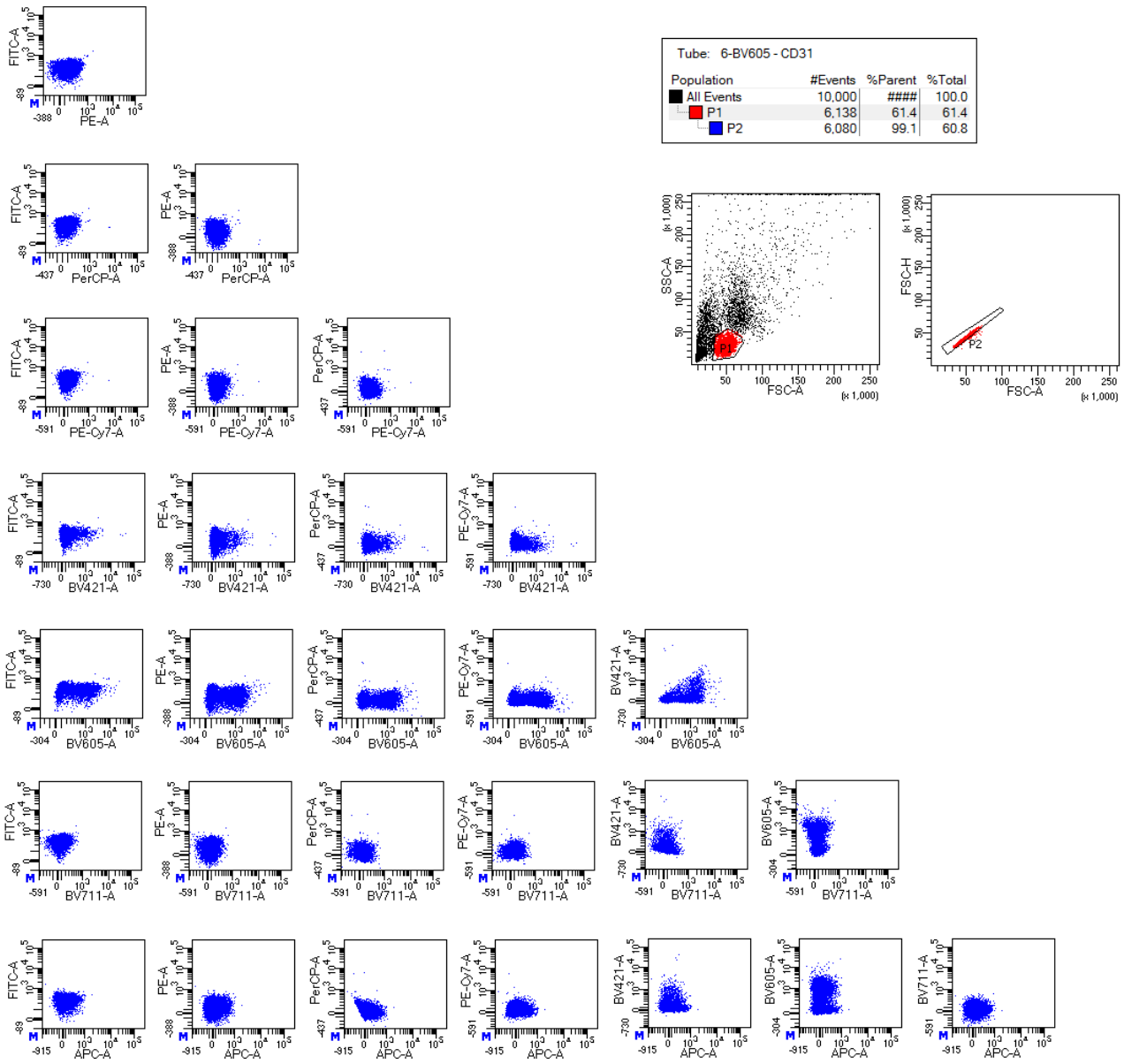
Tube: 6-BV605 - CD31
Population #Events %Parent %Total
All Events 10,000 #### 100.0
P1 6,138 61.4 61.4
P2 6,080 99.1 60.8
SSC-A
FSC-A
FSC-H
P1
P2
FITC-A
PE-A
PerCP-A
PE-Cy7-A
BV421-A
BV605-A
BV711-A
APC-A

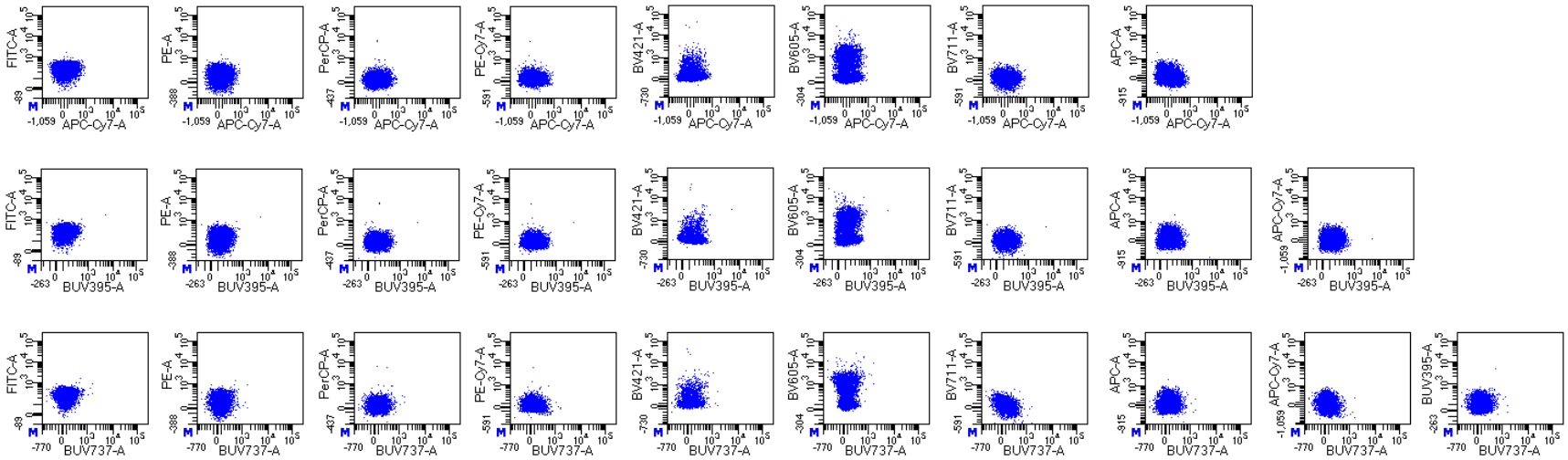
FITC-A
PE-A
PerCP-A
PE-Cy7-A
BV421-A
BV605-A
BV711-A
APC-A
APC-Cy7-A
BUV395-A
BUV737-A

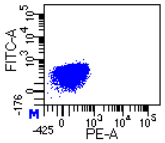

Tube: 7-BV711 - CD25

Population	#Events	%Parent	%Total
All Events	10,062	####	100.0
P1	5,684	56.5	56.5
P2	5,620	98.9	55.9

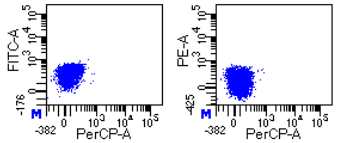

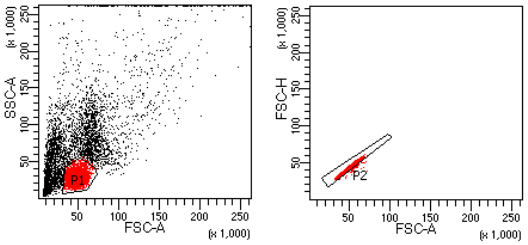

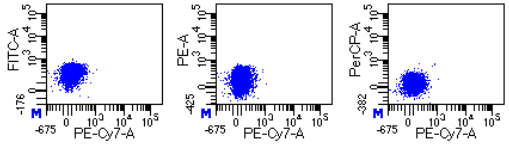

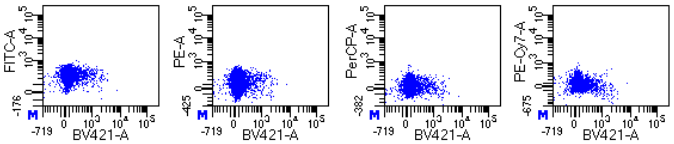

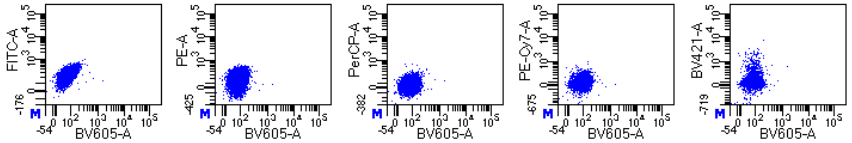

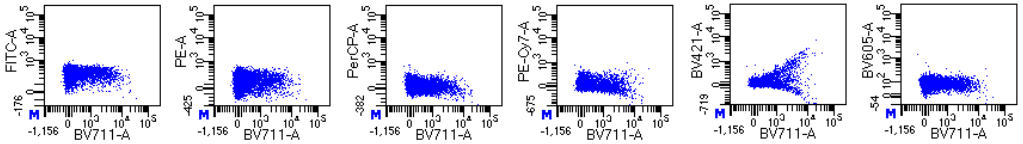

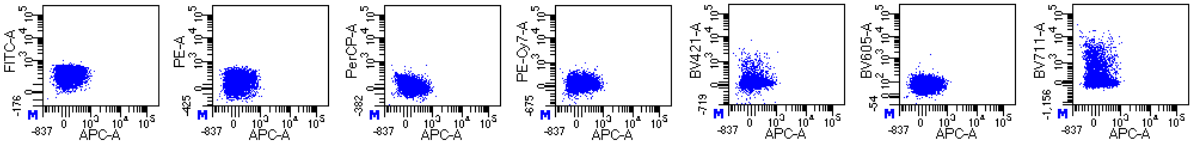

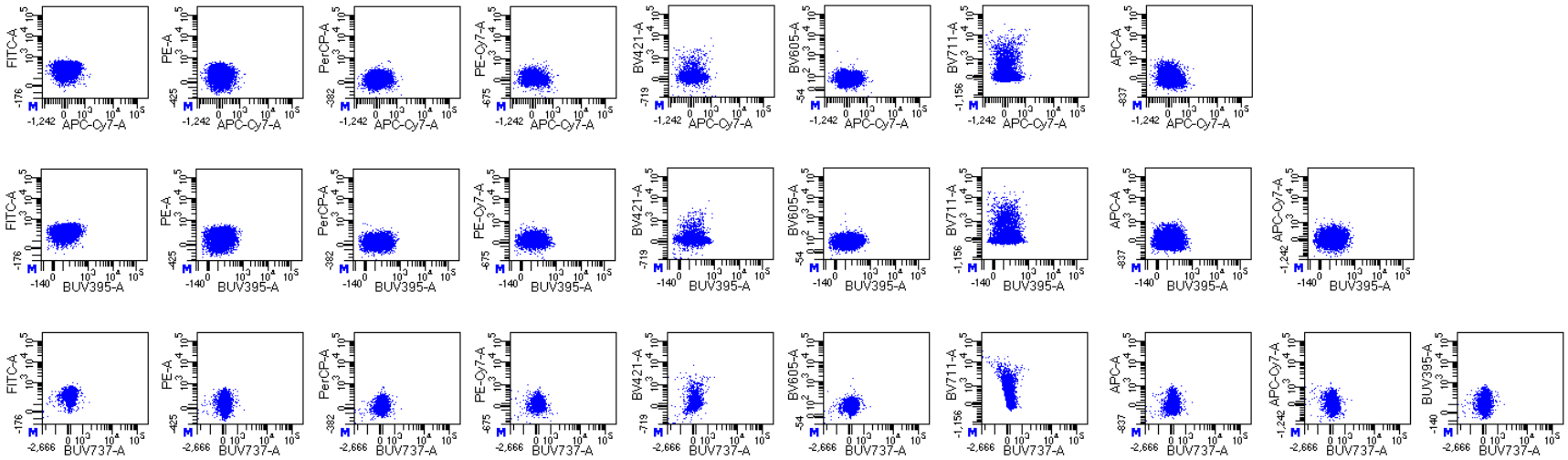
FITC-A
PE-A
PerCP-A
PE-Cy7-A
BV421-A
BV605-A
BV711-A
APC-A
APC-Cy7-A
BUV395-A
BUV737-A

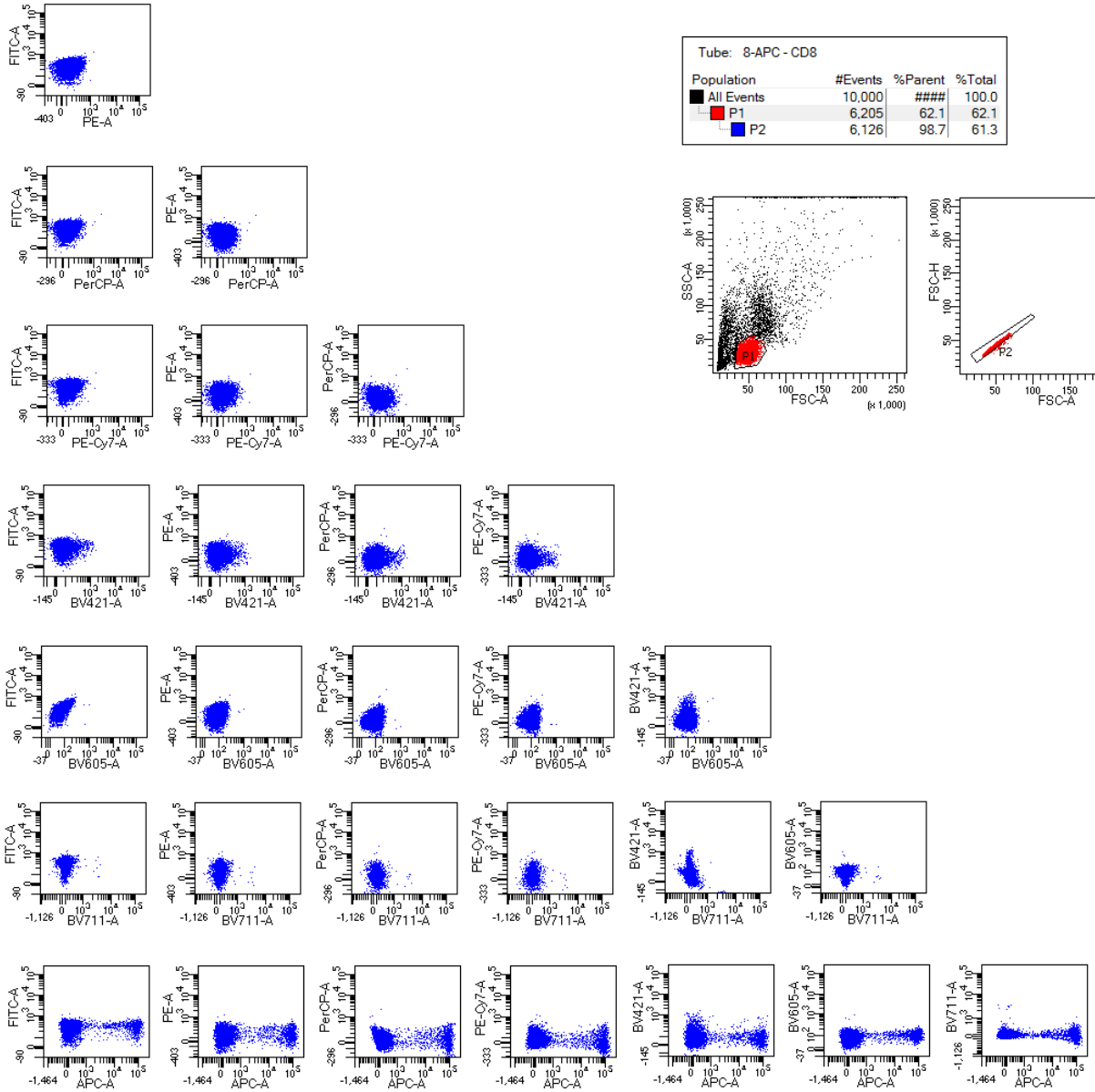
Tube: 8-APC - CD8
Population #Events %Parent %Total
All Events 10,000 #### 100.0
P1 6,205 62.1 62.1
P2 6,126 98.7 61.3
SSC-A
FSC-A
FSC-H
P1
P2
FITC-A
PE-A
PerCP-A
PE-Cy7-A
BV421-A
BV605-A
BV711-A
APC-A

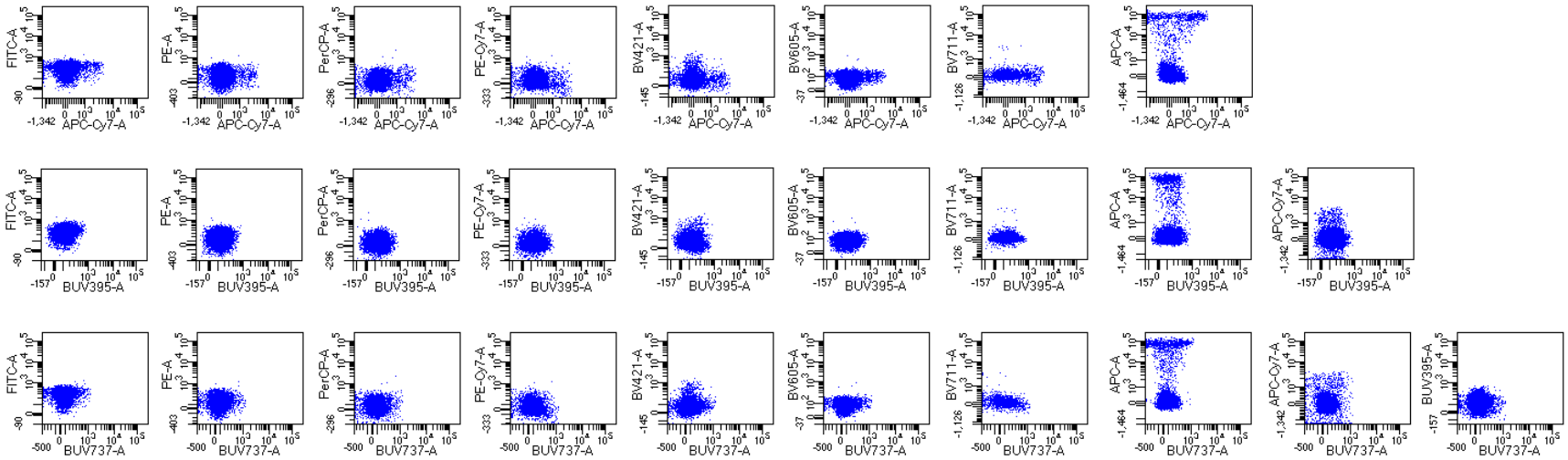
FITC-A
PE-A
PerCP-A
PE-Cy7-A
BV421-A
BV605-A
BV711-A
APC-A
APC-Cy7-A
BUV395-A
BUV737-A
APC-Cy7-A

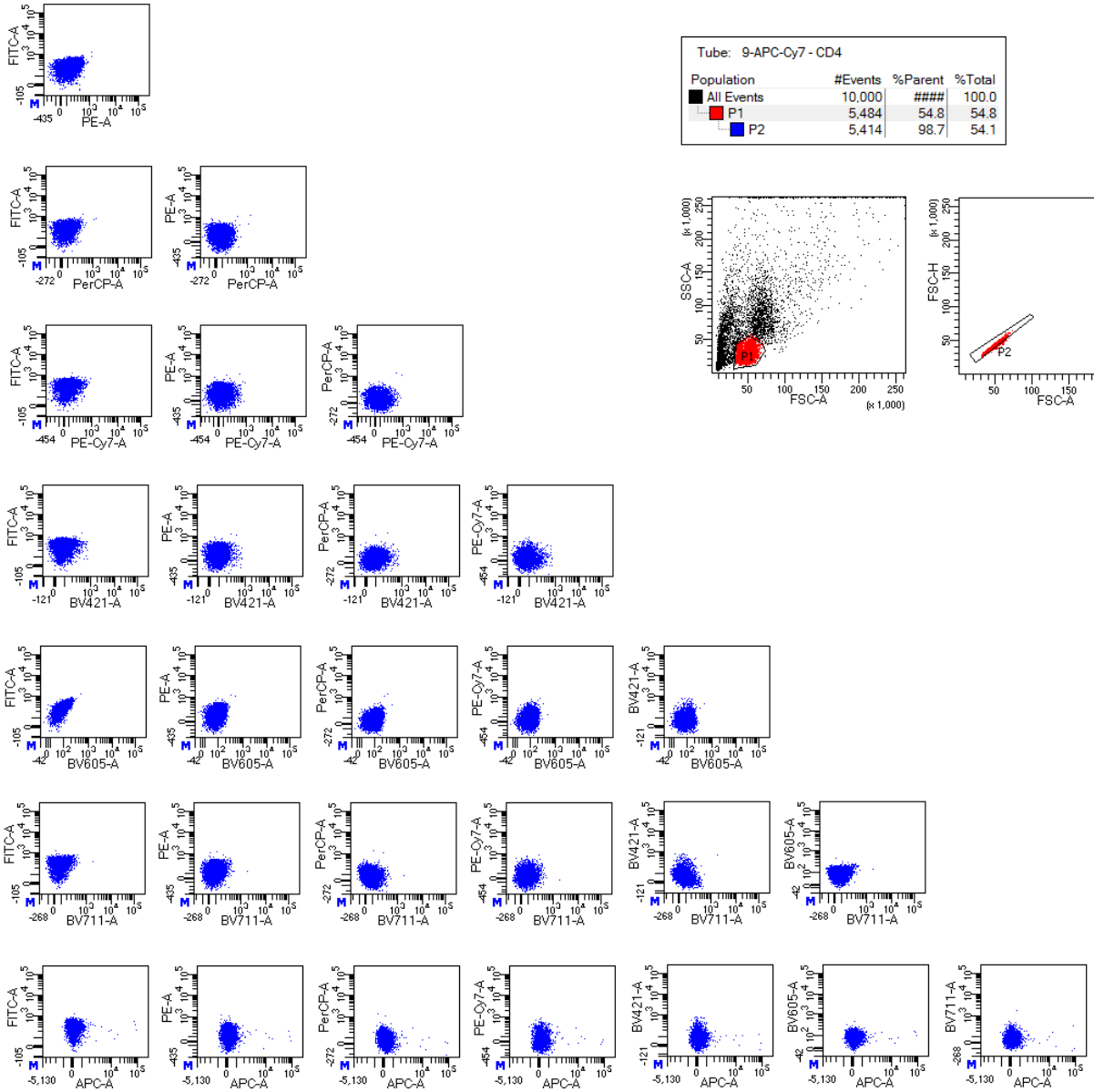
Tube: 9-APC-Cy7 - CD4
Population #Events %Parent %Total
All Events 10,000 #### 100.0
P1 5,484 54.8 54.8
P2 5,414 98.7 54.1
SSC-A
FSC-A
FSC-H
P1
P2
FITC-A
PE-A
PerCP-A
PE-Cy7-A
BV421-A
BV605-A
BV711-A
APC-A

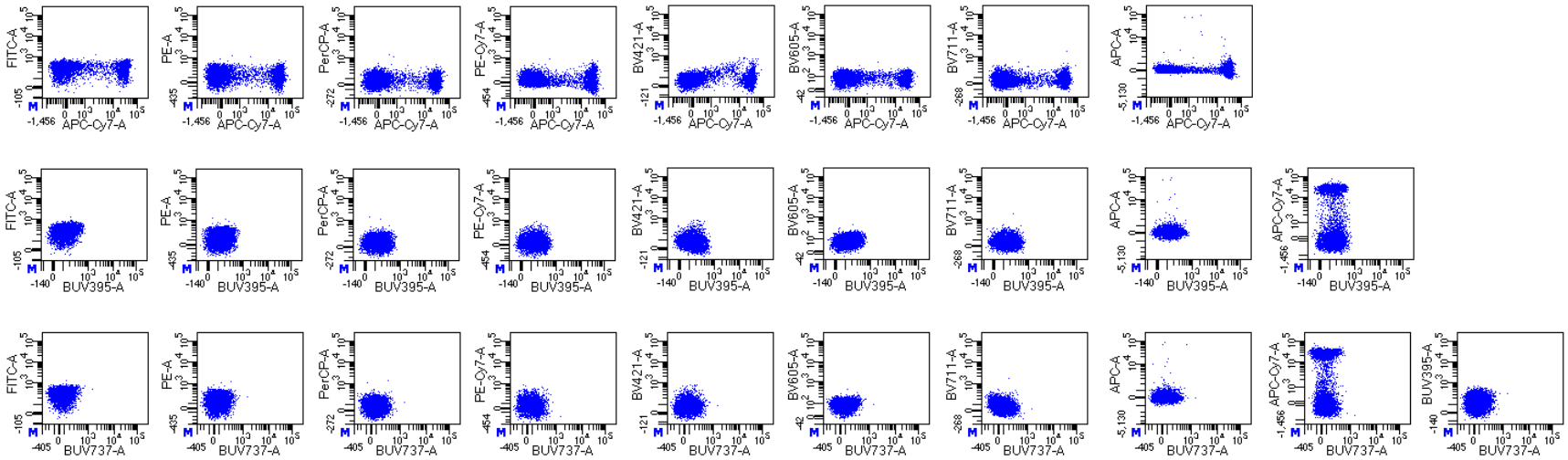
FITC-A
PE-A
PerCP-A
PE-Cy7-A
BV421-A
BV605-A
BV711-A
APC-A
APC-Cy7-A
BUV395-A
BUV737-A

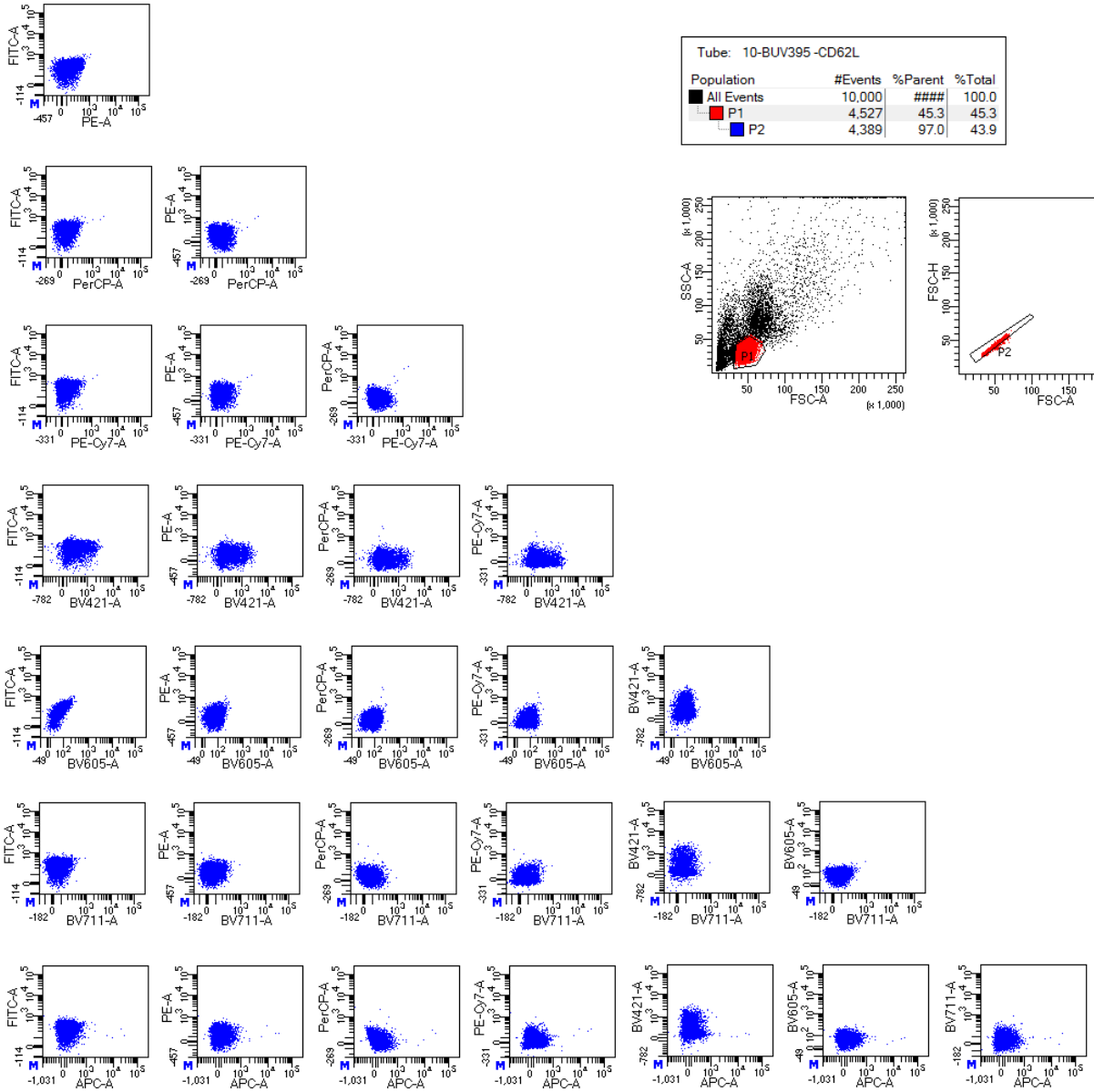
Tube: 10-BUV395 -CD62L
Population #Events %Parent %Total
All Events 10,000 #### 100.0
P1 4,527 45.3 45.3
P2 4,389 97.0 43.9
SSC-A
FSC-A
FSC-H
P1
P2
FITC-A
PE-A
PerCP-A
PE-Cy7-A
BV421-A
BV605-A
BV711-A
APC-A

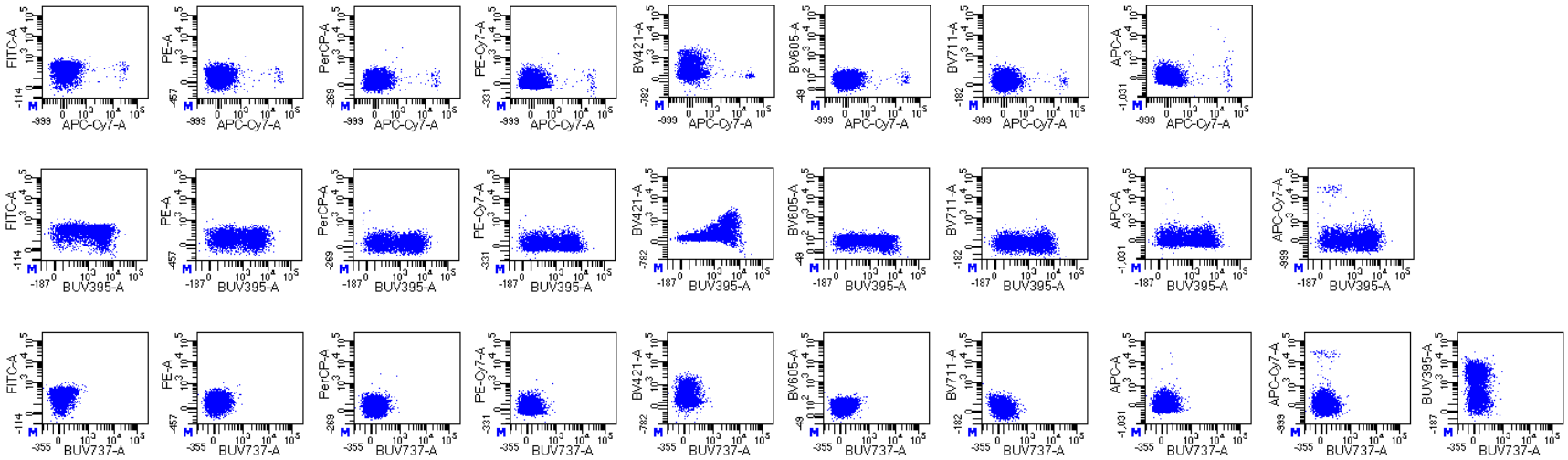
FITC-A
PE-A
PerCP-A
PE-Cy7-A
BV421-A
BV605-A
BV711-A
APC-A
APC-Cy7-A
BUV395-A
BUV737-A

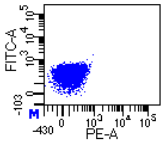

Tube: 11-BUV737 - CD27

Population	#Events	%Parent	%Total
All Events	10,000	####	100.0
P1	5,394	53.9	53.9
P2	5,275	97.8	52.8

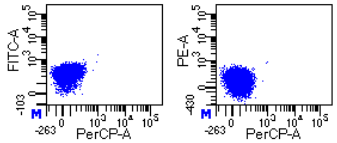

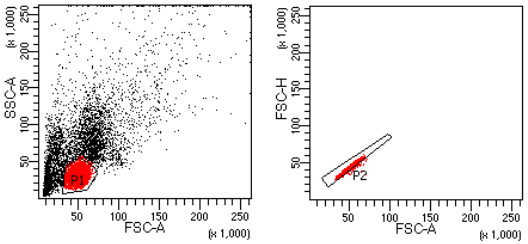

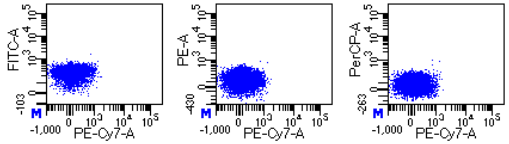

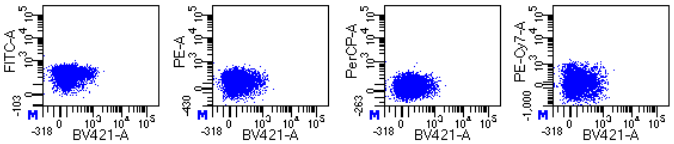

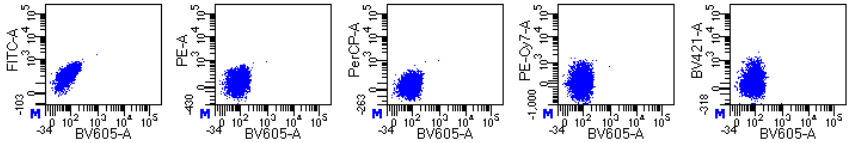

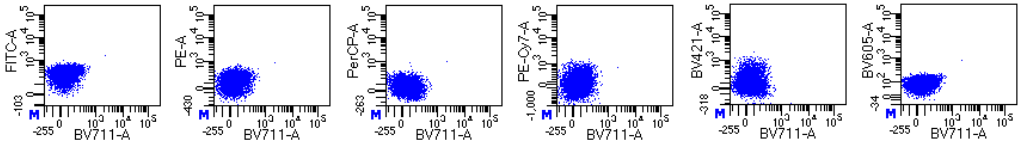

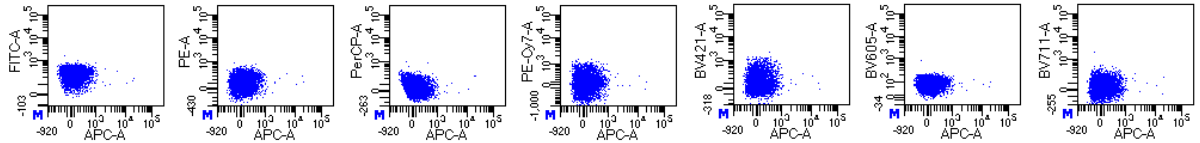

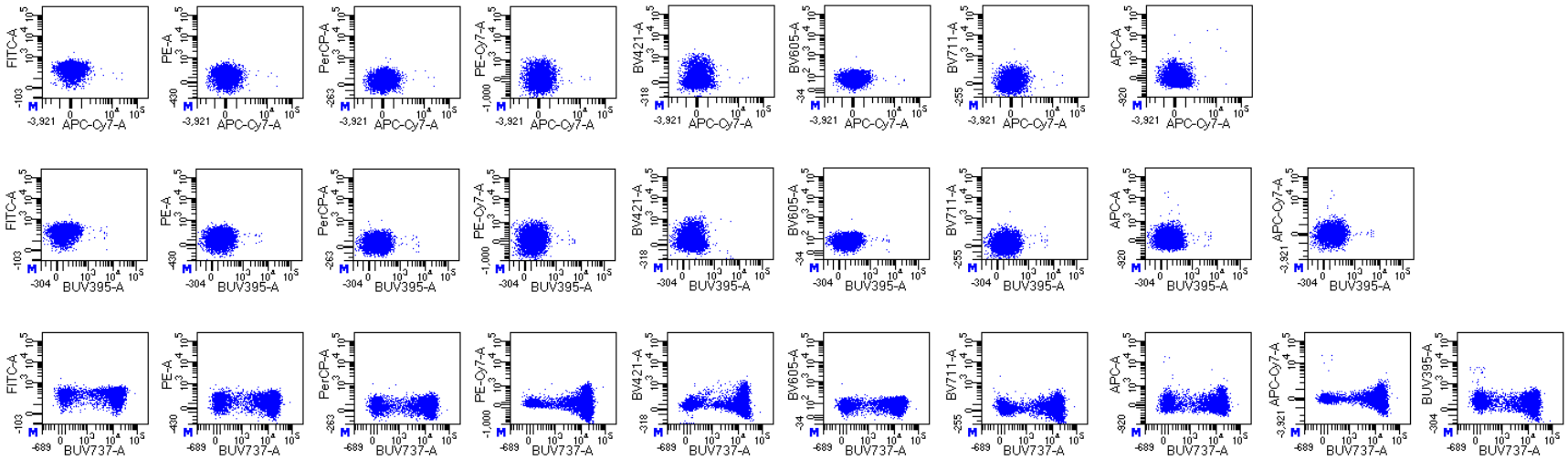
FITC-A
PE-A
PerCP-A
PE-Cy7-A
BV421-A
BV605-A
BV711-A
APC-A
APC-Cy7-A
BUV395-A
BUV737-A

Appendix 5

HREC Approval Letter

On 6/06/2013 5:30 pm, "Ethics Secretariat" <ethics.secretariat@mq.edu.au wrote:

Dear Dr Boyages

RE: "Lymphoedema Medical Research" (REF: 5201300315)

Thank you for submitting the above application to the Macquarie University Human Research Ethics Committee (Medical Sciences) (HREC (Medical Sciences)) for ethical and scientific review. Your application has been reviewed by the HREC (Medical Sciences) at its meeting held on 2 May 2013 and the Scientific Sub Committee out of session.

The HREC (Medical Sciences) is fully constituted and operates in accordance with the National Health and Medical Research Council's National Statement on Ethical Conduct in Human Research (2007) (the National Statement) and the CPMP/ICH Note for Guidance on Good Clinical Practice.

I am pleased to advise that the above project has been ethically and scientifically approved. This research meets the requirements of the National Statement which is available at the following website: http://www.nhmrc.gov.au/_files_nhmrc/publications/attachments/e72.pdf

This letter constitutes ethical and scientific approval only. In order to ensure that your research conforms to the governance requirements of MQ/MUH you must contact the Research Administration Coordinator on 9812 3516 before commencing research at this site.

In addition to this letter of approval, the following amendment to the above study has also been approved:

1. To access and analyse clinical records/data from patients who have previously attended the Advanced Lymphoedema Assessment Clinic at Macquarie University Hospital. Consent to access these records will be obtained from participants.

2. Participants will be recruited as they attend the clinic, by email or by mail. Consent will be obtained by a research assistant or others from the clinic who are not directly involved in patient treatments.

The following documentation has been reviewed and approved by the HREC (Medical Sciences):

1. National Ethics Application Form (2008, v 2.0)
2. Macquarie University Participant Information and Consent Form (PICF) - Genetic Tests (v 3, 03/06/2013)

3. Macquarie University PICF - Lymphoedema Medical Research (v 3, 03/06/2013)
4. Macquarie University PICF - Lymphoedema Medical Research - Generic (v 1, 06/06/2013)
5. Macquarie University PICF - Lymphoedema Medical Research - Clinical Data (v 1, 26/05/2013)

Please note the following standard requirements of approval:

1. The approval of this project is conditional upon your continuing compliance with the National Statement. It is the responsibility of the Principal Investigator to ensure that the protocol complies with the
HREC-approval and that a copy of this letter is forwarded to all project personnel.

2. The National Statement sets out that researchers have a "significant responsibility in monitoring, as they are in the best position to observe any adverse events or unexpected outcomes. They should report such events or outcomes promptly to the relevant institution/s and ethical review body/ies, and take prompt steps to deal with any unexpected risks" (5.5.3).

Please notify the Committee within 72 hours of any serious adverse events or Suspected Unexpected Serious Adverse Reactions or of any unforeseen events that affect the continued ethical acceptability of the project.

3. Approval will be for a period of five (5) years subject to the provision of annual reports. NB. If you complete the work earlier than you had planned you must submit a Final Report as soon as the work is completed. If the project has been discontinued or not commenced for any reason, you are also required to
submit a Final Report for the project.

Progress reports and Final Reports are available at the following website:
http://www.research.mq.edu.au/for/researchers/how_to_obtain_ethics_approval/human_research_ethics/forms

4. If the project has run for more than five (5) years you cannot renew approval for the project. You will need to complete and submit a Final Report and submit a new application for the project. (The five year limit on renewal of approvals allows the Committee to fully re-review research in an environment where legislation, guidelines and requirements are continually changing, for example, new child protection and privacy laws).

5. All amendments to the project must be reviewed and approved by the Committee before implementation. Please complete and submit a Request for Amendment Form available at the following website:
http://www.research.mq.edu.au/for/researchers/how_to_obtain_ethics_approval/human_research_ethics/forms

6. At all times you are responsible for the ethical conduct of your
research in accordance with the guidelines established by the Hospital and

University. This information is available at the following websites:

http://www.mq.edu.au/policy/
http://www.research.mq.edu.au/for/researchers/how_to_obtain_ethics_approval/human_research_ethics/policy

If you will be applying for or have applied for internal or external funding for the above project it is your responsibility to provide the Macquarie University's Research Grants Management Assistant with a copy of
this email as soon as possible. Internal and External funding agencies will not be informed that you have ethics approval for your project and funds will not be released until the Research Grants Management Assistant has received a copy of this email.

If you need to provide a hard copy letter of ethics approval to an external organisation as evidence that you have approval please do not hesitate to contact the Ethics Secretariat at the address below.

Please retain a copy of this email as this is your official notification of ethics approval.

The HREC (Medical Sciences) wishes you every success in your research.

Yours sincerely
Dr Karolyn White
Director of Research Ethics
Chair, Human Research Ethics Committee (Medical Sciences)

Ethics Secretariat
Research Office
Level 3, Research Hub, Building C5C East
Macquarie University
NSW 2109 Australia